Development of Design Method for Straight Compound Channels

Volume 2

Hydraulics Research Ltd
Project Report 252/1/T

NRA

National Rivers Authority

Development of Design Method for Straight Compound Channels

Volume 2 -   Detailed Development of Design Method - Part 2
             Appendices

Hydraulics Research Ltd

Project Report 252/1/T

National Rivers Authority
Rivers House, Waterside Drive
Almondsbury Bristol BS12 4UD

Tel: 0454 624400
Fax: 0454 624409

Dissemination status
Internal: Restricted
External: Restricted

Research contractor
This document was produced under R & D Contract 252 by:

Hydraulics Research Ltd.
Wallingford
Oxfordshire
OX10 8BA

Tel: 0491 35381
Fax: 0491 32233

NRA Project Leader
The NRA's Project Leader for R & D Contract 252 was:

P Johnson

Additional Copies
Further copies of this document may be obtained from the R&D Coordinator, Thames
Region.

Project Report 252/1/T

This report describes the development of new and improved design procedures for two-stage (compound) flood channels. This work was carried out by Peter Ackers as consultant to HR Wallingford, with funding made available by the Regional Water Authorities in 1988, prior to their demise when their responsibilities in this context were passed to the National Rivers Authority. Funding was provided in order that such research results are better disseminated within engineering practice.

The report consists of two volumes. Volume 1 begins with a Summary and Design Method which effectively provides a Manual for the hydraulic design of two-stage channels. The detailed review supporting these new procedures follows, continuing into volume 2, which also contains several Appendices.

Hydraulic engineers will find essential information in the first section, Summary and Design Method, but will probably wish to refer to some of the details given in the main body of the report and in the Appendices in order to extend their understanding of the complex behaviour of two-stage flood channels.

Appendix 7 provides a design example of the computation procedures, and includes tables which indicate how observed stage-discharge data might be used to extend the stage-discharge function. These tables also provide a cross-check for any computer program developed to solve the recommended hydraulic equations and logic procedures.

It is stressed that the equations given in this Manual are for the hydraulic design of straight parallel two-stage conveyances, although information will be found which extends the application to small angles of skew (not exceeding 10°). Information given on meandering channels in Chapter 8 of the main text (see volume 2) shows that they behave quite differently. Improvements in the hydraulic calculations for meandered and irregular channels must await further work.

NB.   The design method is disseminated internally within the NRA as R & D Note 44.

DETAILED DEVELOPMENT OF DESIGN METHOD

CONTENTS

CONTENTS   (CONT'd)

CONTENTS (CONT'd)

CONTENTS   (CONT'd)

7. ANCILLARY TOPICS

7.1 Application to more complex sections.

7.1.1 Natural river cross-sections and also many artificial or "engineered" two-stage channels differ in shape from the classic compound trapezoid for which most of the research evidence is available. Their berms, or flood plains, are likely to have a cross fall and the main channels of natural rivers are seldom of simple trapezoidal shape. Their beds may irregular, deeper on one side than the other; and their banks may not be trimmed to an even gradient. Despite these complexities of form, the hydraulic engineer has traditionally handled real cross-sections using the basic parameters of cross-sectional area and wetted periemter, which jointly provide a measure of hydraulic mean depth, $R = A/P$. What is required is an extension of the basic methods of handling complex cross-sections so that the methods derived from research on "classic" sections can be applied in practice.

7.1.2 As the recommended method starts from the basic computation of flows in the lower-stage main channel and the upper-stage flood plain separated by vertical divisions, using conventinal friction formulae, there is no problem in terms of the basic computation: the "real" cross section can be used, with appropriate areas, wetted perimeters and hydraulic mean depths of the zones of flow. The problem arises solely from the need to simplify the section geometry to deduce the values of several of the independent variables contained in the adjustment equations, particularly for Region 1 flow, the shallower range of depths of flood plain inundation. The relevant geometric variables to be defined are:

h   - main channel mean depth
H   - depth of flow relative to mean bed level, hence $H_* = (H-h)/h$
w_c - half top width of channel
B   - effective half width of valley floor at flood plain level
s_c - bank slope
N_r - number of flood plains

7.1.3 Reasoning that the interaction effect is mainly dependent on condition adjacent to the bank line of river, H_* has to be defined so that

1

(H-h) is the flow depth on the flood plain at the river edge, not an average depth assuming the flood plain to have a cross fall. w_C is probably the most obvious of these geometric variables: the tops of the river banks define the vertical divisions between main channel and berm flows, and the distance between is obviously $2w_C$. The bank slope is less readily defined as the bank itself may be formed of a compound slope or curve. From the engineering point of view, what is required is a representative value and it is suggested that the way to achieve this is to plot the actual cross-section and "eye-in" an average bank slope at each side matching the upper two thirds, say, of the actual bank profile. This is illustrated on Figure 7.1. s_C is then the average value of the left and right bank figures. Having identified w_C and s_C, the mean bed level is also fixed, by the requirement that the area of the trapezoid so defined is the same as the true channel cross-section.

7.1.4 The number of flood plains or berms will usually be self-evident, and so this leaves only B to be defined. For horizontal flood plains, for the analysis of the experimental data, B was half the total width between the outer limits of the berms. Where they are sloped, this is clearly the most appropriate definition when the flood plains are inundated over their full width. However, with partial inundation of the flood plains, the flow "knows nothing" of the dry part of the cross-section, so that for partial inundation the value of B is half the effective width of the above berm flow, i.e. half the actual water surface width. This can be defined from the "real" geometry at any flow stage. These procedures for defining the geometric parameters are illustrated in Figure 7.1. (The use of b as the semi-channel bed width and B as the semi above-berm width stems from the terminology adopted as standard by the teams of researchers using the FCF at Wallingford. It was considered preferable to retain these definitions in the present publication, whilst stressing their special nature in the engineering context. w_C is also a semi-dimension.)

7.1.5 The discharge adjustments in flow Regions 2, 3 and 4 are based on the channel coherence, COH, which is explained and defined in Chapter 3, paras 3.3.4 to 3.3.6. These definitions and the formulations of equations 3.1, 3.2 and 3.3 are general and can be applied to the real section, however complex, or to a simplified section following the derivation of the previous paragraphs. The value of coherence derived will not be very

sensitive to the method used, which can therefore be chosen for convenience of calculation.

7.2   Shear Stress

7.2.1 The variation of shear stress around the boundary of a compound channel was illustrated in a qualitative way in Figure 2.9. Shiono and Knight,(1990b), provided a valuable picture of the various processes at work, including the boundary shear stress distribution, reproduced as Figure 7.2. In the absence of lateral shear and secondary flows, the distribution of horizontal shear in the vertical is linear, varying from zero at the water surface to $\rho g y S$ at the bed. However, Figure 7.2 shows that momentum transfer at the interface and also secondary circulations may modify the basic depth-related distribution of stress on the solid boundary by bringing to it some higher – or indeed lower - velocities. Hence the shear stress distribution is complicated by several processes arising from the interaction between main channel and flood plain zones.

7.2.2 Knight, Samuels and Shiono (1990) analysed some early results from the research on the FCF showing the vertical distributions of shear stress at positions across the channel, for a particular flow depth, see Figure 7.3. There is reasonable approximation to the "normal" linear variation with depth at the centre line (Y = 0, where Y is the distance from the centre line), and towards the edge of the flood plain (Y = 1.5), but there are major departures over much of the width, especially in the region of the sloping banks. Clearly the conventional formula for the shear stress on any horizontal surface, $\tau_H = \rho g(y - z)S$ does not apply (y = flow depth, z = vertical distance from bed of point of interest). Shiono and Knight (1990b) continuing analysis of the same source of data plotted the boundary shear stress, τ_B, in the form of the difference from what might be considered a standard value, $\tau_o = \rho g y S$:

Relative change in shear stress, $\delta\tau_* = (\tau_o - \tau_B\sigma)/\tau_o$ ... 7.1

where $\sigma = \sqrt{(1 + 1/s^2)}$ ... 7.2

s being the local cross-slope of the bed. σ is thus an allowance for the fact that where the boundary has a cross slope its horizontal component of length defines the shear action on the column of water above. Shiono and Knight's results are illustrated in Figure 7.4, for three flood plain widths

3

and a range of relative depths, H_*.

7.2.3 Although these plots are at too small a scale to be used directly in design, the information therein is very significant. Within the main channel, $\delta\tau_*$ is positive indicating a reduction of shear stress from its "normal" value, and with $\delta\tau_* =$ approx 0.15 to 0.35, the reduction is important, for example in the context of sediment movement. Over the flood plains, $\delta\tau_*$ is negative and so indicates an increase in shear stress over the normal value, ρgyS, again by a significant proportion even remote from the channel bank line with relative wide flood plains.

7.2.4 For the particular geometry upon which Figure 7.4 is based, the channel bed extends to Y = 0.75m, and the bank top is at Y = 0.9m. The bank top shows a considerable increase of stress over the normal value, with $\delta\tau_*$ ranging up to and even beyond 4. This signifies that the shear stress locally at the edge of the channel bank with shallow flood plain depths, H_* = 0.1 approx, is five times its normal depth-based value. This arises because the high velocity within the main channel spills on to the berm, and this spillage effect extends some distance across the flood plain, perhaps to Y = 1.3m, i.e. up to 3 times the channel depth of 0.15m beyond the bank line. At the base of the sloping channel bank, Y = 0.75m, the positive value of $\delta\tau_*$ is rather above that at the centre line, indicating a rather lower actual shear stress. This is characteristic of shear stress distribution in trapezoidal channels, it diminishes towards the re-entrant corner, and in theory would drop to zero if the corner was truly sharp and there were no secondary currents. So over the depth of the sloping main channel bank, the shear stress distribution passes from a "below normal" value to an "above normal" value, very much above normal at shallow overbank flows.

7.2.5 In broad engineering terms, the reason for the significant reduction in bed shear stress in the main channel below the value given by ρgyS is that the component of weight down the stream gradient is only partly balanced by the boundary shear stress. With a two-stage channel, the interaction between the flow zones gives additional stress on the interface between main channel and flood plain, and also the secondary circulations and the turbulence arising from momentum exchange change the flow structure from that in a simple channel. As a first attempt to quantify the magnitude

4

of the effect, it might be reasoned that the mean bed shear stress will approximate to that which would occur with the same mean velocity. The discharge, as we have already seen, is reduced below the basic calculated figure for the main channel considered separately by a factor, $DISADF_C$, that depends on the flow geometry and roughnesses of the zones, but which is calculable. The mean velocity reduces by the same factor, of course, and with a square law of boundary drag, as in the Manning and rough-turbulent equations, the resultant mean boundary shear stress is proportional to V^2. Hence, to a first order of approximation, one might expect that the mean shear stress on the main channel bed would be given to a sufficient approximation for engineering purposes by:

$$\tau_{BAV} = \rho \, gHS \, (DISADF_C)^2 \qquad \qquad \ldots 7.3$$

or by:

$$\tau_{BAV} = \rho \, gR_CS \, (DISADF_C)^2 \qquad \qquad \ldots 7.4$$

depending upon whether the channel may be considered wide or not.

7.2.6 From the detailed measurements of shear stress (using a Preston tube) in the FCF program of research, the average bed shear stresses were established for the range of test conditions, though here only the results for varying flood plain width are considered, with channel bank slope, $s_C = 1$, and smooth channel and flood plains. For these smooth conditions, the square law of rough turbulence does not strictly apply, but in Appendix 2, eq.3.6, it was shown that a power law of 1.8 would be appropriate. The two equations above can therefore be modified by providing $DISADF_C$ with the exponent 1.8 as an alternative. Thus, using the procedures for calculating the discharge adjustment factor, with the logic of selecting regions and the approach to the separation of the zonal adjustments for Regions other than 1 as explained in Chapter 3, para 3.5.10, theoretical values of τ_{BAV} can be calculated for comparison with experiment. Figure 7.5 shows this, with the upper diagram for test series 02 (see Table 3.1 for the geometry). Both methods of calculation, using the hydraulic mean depth of the main channel, R_C, and the water depth, H, were used, coupled both with the square law exponent of 2 and the smooth law value of 1.8. One would expect the data to lie between the two theoretical graphs for exponent 1.8 (shown as full

lines) and indeed they do. The observed data τ_{BAV} lie fairly close to but above the plot based on h.m.d., R_C, and as the plotted function is really an indication of mean shear stress around the whole solid perimeter, it is to be expected that the mean value on the bed will exceed this. Test series 01 and 03 at different B/b ratios are shown in the lower part of Figures 7.5, and the picture remains much the same, the observed mean bed shear stress lies between the values calculated on the basis of flow depth and on the basis of h.m.d., lying nearer to the latter. It appears that the simple procedure incorporated in equations 7.3 and 7.4 above straddle the true value of mean bed shear stress, whilst explaining the bulk of the departure from the "normal" value, $\rho g y S$. This calculated adjustment, $DISADF_C^{1.8}$, accounts for a reduction of up to 30% in this particular test series.

7.3 Critical flow, energy and water levels

7.3.1 Critical flow is usually defined in standard hydraulics textbooks as the flow condition in an open channel when the specific energy for a given discharge is at a minimum, and for which maximum discharge occurs for a given energy level. It also indicates a change in flow state, in that small surface disturbances will travel upstream with sub-critical conditions but cannot do so with super-critical conditions. It is this latter criterion that makes the concept of critical flow of particular significance in numerical calculations of non-uniform or non-steady flows. The theory of critical flow is dealt with at some length by Jaeger (1956) including the proof that whether energy or momentum is considered the same conventional definition of critical flow in an open channel of general cross-sectional shape applies *provided* it may be assumed that the velocity distribution is uniform. This leads to the conventional definition of Froude number, $Fr = V/(gA/W)$, where V is the mean velocity of flow, A the cross-section area, W the water surface width and g the gravitational acceleration. Critical flow is when $Fr = 1$.

7.3.2 The assumption of uniform velocity distribution may not be an unreasonable approximation for simple cross-sections but it is clearly inadmissable with compound channels. The velocity variation across the section can be described by α or β, depending on whether one is concerned with energy or momentum, and the incorporation of these factors into the energy and momentum equations then gives differing formulations for the Froude Number, Fr:

Energy basis:

$$Fr = \sqrt{\left[\left(\frac{\alpha W}{A} - \frac{d\alpha}{dd}\right)\frac{Q^2}{2gA^2}\right]}$$ ... 7.5

Momentum basis:

$$Fr = \sqrt{\left[\left(\frac{\beta W}{A} - \frac{d\beta}{dd}\right)\frac{Q^2}{2gA^2}\right]}$$ ... 7.6

which revert of course to the conventional definition for $\alpha = \beta = 1$. The appearance of the water surface width, W, in the above functions indicates that in a channel with horizontal berms, there will be a discontinuity in the calculated Froude number/stage function for a given channel gradient, and there could be duality in the critical condition in more general cases.

7.3.3 Knight and Yuen (1990) carried out experiments to examine and compare aspects of critical depth in a compound channel with b = h = 75mm, B = 225mm and $s_C = s_F = 1$, with variable slope, and for a range of relative depths, $0.05 < H_* < 0.5$. They were concerned not only with the concept of an overall value for the Froude Number but also with its local variation across the channel. With depths and velocities being measured at many verticals across the width, they were able to assess the local values of Froude number, $U/\sqrt{(gy)}$, and specific energy, $E = y + U^2/2g$ where U is the depth mean velocity at any vertical. It is worth mentioning at this stage that the water level is the same at each point across the section, no doubt because with an aligned system of flow there is hydrostatic pressure throughout. The lateral variation of Froude number when the overall flow is critical is illustrated in Figure 7.6. This confirms that there can be local zones of super-critical velocity on the berms near the channel bank line, induced by the increase of discharge intensity due to lateral shear, although on the berms away from the bank line the flow is sub-critical, as it is within the central deep section.

7.3.4 Petryk and Grant (1978) examined methods of calculating the Froude number in compound channels, referring to field observations of surface disturbances that clearly indicated a variation of Froude number across the section. They were seeking explanation for the observation of a pattern of

7

surface waves in the main channels of flooded rivers, when overall the flow might be expected to be sub-critical. With cross-sections more typical of natural rivers than those tested by Knight and Yuen, there can obviously be conditions where the high velocity in the main channel can yield locally high Froude numbers when the shallow depth and roughness of the flood plain render the flow there sub-critical. There is also the condition already mentioned when the penetration of fast main channel flow on to the edge of the flood plain can generate a pattern of surface waves on the berm itself because there the depth is shallow, so increasing the Froude number above the main channel value. Viewed in the context of surface wave patterns, there are clearly different possible combinations according to the local values of Froude number across the channel width.

7.3.5 Samuels (1989) includes a review of the influence of Froude number on numerical modelling, and how it might properly be calculated incorporating values of the momentum coefficient, β. The subject is a complex one and further research is required for a full understanding. For hydraulic engineering purposes, the important point is perhaps that the simple "text book" definition of Froude number no longer applies to compound channels, and that with a knowledge of the separate flows as calculated by the method given earlier in the Manual, approximate values for the main channel and for the flood plain zones could be calculated. They will not be the same as the overall section value but are probably more relevant for engineering purposes.

7.4   Sources of basic information on roughness

General

7.4.1 The main resistance functions used in open channel design are the Manning equation and the Colebrook-White equation. The former is for rough turbulent flow and so should not be used for relatively smooth construction materials, such as good quality concrete lining; the latter is for turbulent conditions embracing all surface conditions from smooth to rough, so is more general. However, the choice of equation can not be separated from the data base available on the roughness coefficient. The Manning equation has been so widely used in engineering practice that extensive listings of the coefficient value, Manning's n, are available in the literature, based on

8

the body of experience in the use of that equation in hydraulic design.
Ven Te Chow (1959) gives such information for a whole range of construction
materials, through metal, wood, brick, masonry and concrete, to channels
excavated in earth, gravel and even rock; natural streams in the mountains
or plains, weedy reaches and also variously described flood plains. These
values are listed in Appendix 5, Table A5.1.

7.4.2 The roughness coefficient in the Colebrook-White function is less
empirical in that it has a physical basis, namely the textural roughness of
the surface referred to as an "equivalent sand roughness, k_s", the diameter
of grains, forming a plane granular surface that would provide the same
resistance. This fundamental concept has been extended over the years to
incorporate empirical information from a wide range of surfaces and
construction materials, including typical values for rivers and gravel bed
streams etc. Table A5.2 in Appendix 5 gives values for concrete and some
other materials.

7.4.3 The Manning equation will normally be used for natural channels, and
for rivers in an "engineered" condition. The methods given above apply only
to straight, or very gently skewed or curved channels (limiting deflections
say 10°), and wherever possible the roughness coefficient used should be
based on actual measurement of the river under study. It is usually found
that the Manning's n value varies in a systematic way with stage and
Figure 7.7 illustrates the results of field measurements in five Scottish
rivers, by Sargent (1979). The coefficient value reduces with increase of
stage, possibly because there are typically features in the bed, such as
bars, shoals and scour holes, that have a greater influence at shallow
depths than at stages approaching bank full. The value of main channel n to
use for above-bank flows would be the value obtained when flow is just below
bank-full. However a coefficient variation of the form shown in Figure 7.7.
can also arise where the relative roughness is somewhat over-severe for the
Manning equation to apply, when the Colebrook-White equation might prove
more robust.

7.4.4 A conversion between the Manning coefficient and the value of k_s (in
metres) is available through the formula:

$$n = k_s^{1/6}/26 \qquad \qquad \dots 7.7$$

but the Manning equation is only theoretically correct where $7 < R/k_s < 130$, so Manning might not be expected to provide a good fit to measured data when:

$$n \gg 0.03 \, R^{1/6} \qquad \qquad \ldots \ 7.8$$

This suggests restrictions at shallow flow depths in typical rivers.

Gravel bed rivers

7.4.5 The dominant size of sediment found in the beds of alluvial rivers is related to their gradient, so that steep rivers in mountainous terrain have beds of boulders and coarse gravel, those in the sub-montane region will have gravel beds with some sand, and in the plains beyond will have sand and silt beds. A particular feature of coarse bed streams is the wide range of sediment sizes found in them – and being transported through them. Considerable sorting is observed between different parts of the stream bed as well as in depth. Armouring frequently occurs, where a one or two grain thick layer of coarse material overlies the bulk of the bed with its mix of a wide range of sizes. This armour layer is left by decreasing flows after a flood event, by the winnowing out of finer material when the flow is no longer competent to move the coarsest fraction. This layer then protects the underlying material with smaller D_{50} size, until a flow large enough to initiate motion in the armour layer occurs, so triggering rapid transport of the sediment forming the bulk of the bed.

7.4.6 The resistance of boulder and gravel bed rivers is associated with the texture of the bed arising from the coarser fractions of material there, and so current methods use various modifications of the rough turbulent equation, (which is one of the limiting regions of the Colebrook-White function), relating the linear roughness of that equation, k_s, to the bed material size. A variant of that is to use the Strickler form of the Manning equation, with its linear measure of roughness determined from bed grading (Strickler, (1924)). The Limerinos (1970) equation was based on Californian data, and effectively incorporates the conversion into Manning's n of the k_s value that would be used in the rough turbulent function:

$$n_m = 0.113 \, R^{1/6}/[1.16 + 2 \, \log(R/D_{84})] \qquad \qquad \ldots \ 7.9$$

D_{84} is the grain size for which 84 percent of the bed material is finer.

7.4.7   Bray (1982) reviewed the resistance of gravel bed rivers, generally confirming the Limerinos function. Hey (1979) effectively used a modified form of this rough turbulent equation which included a cross-section shape parameter. There have been two international conferences dealing specifically with gravel bed rivers, from the morphological, sedimentological and hydraulic points of view, and the proceedings of these conferences provide an excellent state-of-the-art summary: Hey, Bathurst and Thorne (eds) (1982); Thorne, Bathurst and Hey (eds) (1987).

Sand bed channels

7.4.8   In laboratory experiments starting with a plain sand bed, once the flow conditions are able to generate sediment movement, ripples or dunes will form. The normal condition in nature is also for similar features to form on the bed: a plane bed is an unusual condition and is more likely to occur at high transport rates when the stream velocity is high enough to wash out the pre-existing features. The presence of bed features means that the overall resistance of the bed will comprise both the drag due to the obstruction of ripples or dunes (form drag) and the resistance of the - granular texture itself (grain resistance).

$$\tau_o = \tau_{form} + \tau_{grain} \qquad \qquad \text{... 7.10}$$

where

$$\tau_o = \rho\, gyS \qquad \qquad \text{... 7.11}$$
y = flow depth
S = hydraulic gradient

7.4.9   The grain resistance for coarse material can be estimated from the rough-turbulent equation, as was noted for gravel bed rivers, but for sand bed rivers the subject is considerably complicated by the existence of bed features. Ripples and dunes and combinations of them are known as "lower regime" and the high transport plane-bed region of rapid flow, together with the anti-dune condition that can arise in steep channels at high Froude numbers, forms the "upper regime". The distinction between lower and upper

regime is not clear cut: there is a transition between them as velocities increase and it is possible for different parts of the bed to be in one regime or the other, or to be somewhere between, when flow conditions are not clearly one side or the other of the dividing criterion. Features are dependent also on sediment size: gravel bed rivers do not have ripples and have shoals rather than dunes.

7.4.10 White, Paris and Bettess (1980) used the same parameters as appear in the Ackers and White (1973) sediment transport calculation method, for assessing the resistance of rippled and duned sand bed rivers, and it is possible to combine these functions in given circumstances to assess suitable values of Manning's n, as illustrated by Ackers (1980) for irrigation canals. Although the method has been shown to be reliable and forms the basis of modern design procedures for sand bed irrigation canals, it is too complex to cover in detail here. Bettess and Wang Shiqiang (1987) also used the same sediment parameters to study upper regime bed form resistance, and the transition between upper and lower bed forms, but again it would be inappropriate to detail their procedures here. Suffice it to say that typical Manning's n values for straight sand bed channels are in the range 0.022 to 0.040 depending on size of channel and size of sediment, but major sand bed rivers can show considerable variation in times of severe flood if the bed of main channel goes through the transition from ripples and dunes to plane bed. This was illustrated from the river Indus by Hogg, Gugenasherajah, Gunn and Ackers (1988)), using flood data for 1976 and 1986, showing a reduction in n_m to about 0.011 as the dunes are washed out and the bed becomes plane, later reverting to a duned bed with n about 0.03. The different bed forms possible in sand bed rivers are thus of significance to hydraulicians, though within UK few rivers would come into this category, many having effectively rigid beds.

Vegetation

7.4.11 River vegetation falls into three categories: mid-channel aquatic weed; channel edge growth (grass, reeds, willows etc); and bankside/flood berm vegetation (pasture, growing crops, orchards, trees, shrubs, hedges etc). This rich variety is environmentally desirable but it inevitably has an influence on the hydraulic performance of the system. Moreover it varies seasonally, and so assessment of the roughness coefficient can not be

12

considered an accurate science. Clearly, past experience based on measurements at the site of interest will provide the best guide, though of course any seasonal changes must be borne in mind. Research has also provided important sources of information, though again caution is required in transferring results from one geographic zone to another, which may support different flora.

7.4.12 The most extensive work on grass comes from America, and is described by Kouwen, Li and Simons (1981). The method is to identify a retardance class based on a US Dept of Agriculture classification, as shown in Table 7.1, and then to use a simple formula involving the product of mean velocity and hydraulic mean depth to assess the Manning's n value. There are dual functions depending on VR: at very low values long grasses will remain erect and increasing depth and velocity will increase the n value due to greater depth of immersion. Above a limiting value, they will deflect so that Manning's n reduces with increasing depth and velocity. For shorter stands of grass, n diminishes progressively with increasing VR, though not very strongly. The governing equations are given in Table 7.2.

TABLE 7.1. GRASS COVER RETARDANCE CLASSIFICATION.

Average length	Stand:	GOOD Class	FAIR Class
Longer than 0.76m		A	B
0.28 - 0.60m		B	C
0.15 - 0.28m		C	D
0.05 - 0.15m		D	D
Less than 0.05m		E	E

TABLE 7.2. MANNING'S N VALUES FOR GRASS SURFACES.

The coefficients p and q apply to the equation

$$n = p + q/(VR) \qquad \qquad \dots 7.12$$

Retardance class:	Coefficients in equation		Limits of VR m²/s
	p	q	
A	0.440	-1.617	< 0.154
	0.046	+0.022	> 0.154
B	0.403	-3.336	< 0.053
	0.046	+0.010	0.053 - 0.179
	0.035	+0.012	> 0.179
C	0.034	+0.046	< 0.083
	0.028	+0.005	> 0.083
D	0.038	+0.002	< 0.100
	0.030	+0.003	> 0.100
E	0.029	+0.001	< 0.123
	0.0225	+0.002	> 0.123

7.4.13 Regarding channels with aquatic weeds, research by HR Wallingford led to the following formula, depending on the extent of weed coverage:

$$n_C = n_{basic} + 0.02 K_W/Fr \qquad \qquad \dots 7.13$$

where n_{basic} is the Manning's n value for the channel without weeds
          K_W is the fractional surface area coverage of weed growth
          Fr is the channel Froude number, $V/\sqrt{(gA/W_C)}$

Larsen, Frier and Vestergaard (1990) describe both field work in a weed affected reach of river and flume tests, and develop a similar type of function as those given for grasses in Table 7.2 above. They relate Manning's n to VR, with the dry weight of growth in g/m^2 forming a further parameter. They suggest that there is a basic winter function for n in terms of VR, and that the summer function will depart from this for VR < 0.4 m^2/s, the presumption being that above this value the weeds will lay flat or be scoured away. One field measurement may then characterise the trend of the summer roughness function. The influence of weed growth on an East Anglian river was investigated by Powell (1978) clearly demonstrating the strong seasonality of the roughness coefficient, also indicating large tolerances on its assessment.

7.4.14 Regarding flood plain roughness, Klaasen and Van der Zwaard (1973) carried out laboratory research on modelled vegetation, including such features as orchards and hedges, which may be a helpful source of information. So far as orchards and forests and forests are concerned, provided there is no undergrowth and the water surface is below the top growth, the method of analysis used for the rod roughness in the FCF can also be applied, utilising a knowledge of the typical diameter and spacing of tree trunks. There is also the information in Appendix 5. However, in the absence of actual measurements under above bank conditions, there will probably be greater tolerances on estimating the conveyance due to uncertainty in the roughness coefficient than will arise from the computation of the recommended adjustment to these basic values to allow for the flood plain/channel interaction.

7.5 Need for and utilisation of field data

7.5.1 If river engineers are to make best use of existing knowledge of the behaviour of compound channels when assessing the flood conveyance of their river system, it is important that they not only acquire the best quality field data over as wide a range of depths as feasible, but also that they interpret them correctly in the framework of what is now known about the complexity of two-stage channels. Understanding of the processes at work has been deficient in the past, and so conventional methods of treating field data under over-bank conditions has probably led to serious errors. It has been demonstrated quite positively that the main result of interaction between main channel and flood plain flows is the reduction of the main channel flow, yet the conventional treatment of above-bank stage discharge data has, in effect, been to allow for any interaction by adjusting the flood plain roughness coefficient, the basic resistance function for the main channel being assumed to correctly represent its component discharge at above-bank flow. This has perhaps been inevitable, given the previous state of knowledge, but the net result may have been the use of inflated values of flood plain roughness. The combination of this with inaccurate methods of treating the compound section must have led to many errors - and in some cases large errors - in assessing the flood conveyance of rivers. Thus it is firmly recommended that all future analyses of stage- discharge data under above-bank conditions should make full use of the new methodology.

7.5.2 The problem is illustrated by some sample calculations for a small river, bed width 15m, channel depth 1.5m, side slopes 1/1, Manning's n = 0.03, two flood plains of width 20m, Manning's n = 0.06, channel gradient 0.3/1000, (this is the same cross-section as later used to typify a small sand bed river in Chapter 9). The stage discharge function for depths up to 3m is shown in Figure 7.8a on a log- log basis for a range of assumptions. The basic calculation before making allowance for interaction is shown in the upper part of Figure 7.8 as a broken line, and shows the full depth flow as 80.34 m³/s. With allowance for interaction, this reduces to 61.81 m³/s as at the terminal point of the full line. The chain dotted line illustrates the assumption that would have to be made about the flood plain roughness in order to achieve close agreement at the highest stages if no allowance is made in the analysis for interaction effects: this is with n = 0.60, TEN times the true

value assumed in this example. This unrealistic value comes about because what is being attempted is to get the correct discharge by adjusting the flood plain roughness coefficient when in reality the "loss" of conveyance under above-bank conditions occurs in the main channel, and not on the flood plains.

7.5.3 It may be noted that the predicted stage discharge curve shown by the full line in the upper Figure 7.8 has a change in gradient at bank full, with a humped character over the lower range of flood plain depths. This is very similar to many field observations of real rivers (see for example Chapter 5, section 5.5.). Even with a false increase in flood plain roughness there is no way that this characteristic hump can be produced without taking account of interaction. The line drawn for $n_F = 0.60$ forecasts significantly higher discharges in this range, even though it can give approximately correct discharges at high stages. Note also that the stage-discharge function with allowance for interaction does not give a straight line on this log-log plot and so methods of interpreting and extrapolating from observed stage/discharge data that presume the existence of a power law i.e. a straight line on a log-log plot, for above-bank flows are likely to be inaccurate and could be somewhat misleading.

7.5.4 The false picture of the division of flow that emerges if one tries to compensate for interaction effects in this way is shown in the lower Figure 7.8. There are two sets of curves corresponding to the assumptions explained above, for both Q_C/Q_T and Q_F/Q_C. The full predictive method shows Q_C/Q_T reducing from unity at bank full to 0.624 at depth 3m ($H_* = 0.5$). The figure with no allowance for interference would be 0.719, but using the increase of n_F to achieve the correct maximum flow suggests that the main channel component of the total is 0.962. Turning to Q_F/Q_C, with Q_F being for both flood plains, the correct prediction at maximum depth is 0.602, the basic calculation with the true n values gives 0.390, whilst the falsely assessed n_F value would yield 0.040. This is a gross distortion of the reality of the flow division and the consequent potential for serious error using the traditional methods of analysis must cause considerable concern.

7.5.5 It is not the purpose here to explain in detail the field procedures for the measurement of stage and discharge. There are British and

17

International Standards on the subject as well as codes of practice. The subject is well described in the book Hydrometry, edited by Herschy (1978).

7.6 Incorporation into numerical models.

7.6.1 One of the mathematical procedures used for assessing flood wave propagation down a river system is channel routing of the Muskingum-Cunge type, see for example Cunge (1969). This takes account of the speed of movement of the flood wave and also its dissipation, utilizing the flow parameters section by section along the river valley. Garbrecht and Brunner (1991) have recently published a development of the method which specifically aims to take account of two-stage channel effects. They do this by separately computing for main channel and flood plains in a given reach, and then joining the outflows from these zones together before progressing to the next reach. However, they neglect the interaction effect between the zones so that the velocities used are the basic values which we have seen may be 15% or so different from the true values under over-bank conditions. Clearly the methods of allowing for interaction developed in this Manual could be incorporated into such a routing model, thereby improving its ability to simulate real rivers. In their recent paper, Garbrech and Brunner compare their hydrologic routing method with the U S National Weather Services fully dynamic DAMBRK model (Fread, 1984), using the latter as a bench mark. However, the bench mark method itself also has the shortcoming of not making allowance for the interaction effects of compound cross-sections.

7.6.2 One dimensional dynamic computational models typically solve the St Venant equations of energy (or more strictly momentum) and continuity in a time and space framework, utilising geometric information at many cross-sections defining the fluvial system. Some models may use the cross-section data to define a unitary channel: this is no longer to be recommended because by so doing the roughness coefficient is also required to take account of spurious changes due to the geometric anomalies introduced by flow over the flood plains, as well as real changes in roughness with stage as the flood plains are inundated, and the extra resistance due to interference effects. However, if the model requires the sections to be treated as units, not divided into main channel and flood plain zones, the predictive methods given above could be used as a

roughness/cross-section pre-processor, to deduce overall equivalent
conveyance functions in terms of flow depth, which could be incorporated
into the model data store as "look up" tables.

7.6.3 Other models will use cross-section information in its more rational
form, with separate data for flood plain and main channel. In this case
also it would seem appropriate to use the predictive methods given here in
the form of a pre-processor to provide the conveyance/depth function at each
section in the model. Conveyance, K, is usually defined by:

$$K = Q/\sqrt{S} \qquad\qquad\qquad ... 7.14$$

where S is the hydraulic gradient, so can readily be assessed from the
predictive equations over the required range of depths. From a knowledge of
the distribution of flow between the main channel and flood plain zones, it
is also possible to assess the momentum coefficient, to be associated with
the conveyance as a function of stage. Both are required for use in
one-dimensional models.

7.6.4 The question of Froude Number, Fr, was dealt with in Section 7.3.
and it was explained that in a two-stage channel the Froude Numbers in the
main channel and on the berms will be different, and also different from a
whole cross- section value. These differences are real, of course, and as
the Froude Number is a measure of the speed of propagation of a small
surface disturbance, it is significant in assessing the stability of
numerical schemes and their associated time steps. It is therefore
conceivable that the flood plain component could be computationally stable
whilst the main channel component would be unstable - and that the stability
status could not be obtained from the whole-channel parameters. Clearly
care has to be exercised, with recent improvements in the understanding of
compound channel flow providing scope for a significant step forward, both
in the reliability of simulating real rivers in 1-D models and in assessing
the stability of computational schemes.

7.6.5 This report deals essentially with straight rivers in their flood
plains, and so, in a modelling context, it provides a one-dimensional
treatment of a one-dimensional system. It will be clear from Chapter 8 that
the methods developed here are not applicable to systems with irregular plan

form, where the processes at work are significantly different. The methods of allowing for interaction effects with straight aligned systems are not adequate, therefore, for 1-D models of highly irregular rivers, nor are they appropriate for models incorporating two dimensions on plan. It will be apparent from Chapter 8 that there is much to be learned about how to incorporate the exchanges of flow and momentum into numerical models of meandering or very irregular rivers. Such models, even if two-dimensional, are currently over-simplified. Improvements corresponding to those that are now possible in dealing with 1-D systems will have to await the outcome of detailed analysis and review of the findings from later phases of research in the FCF at Wallingford.
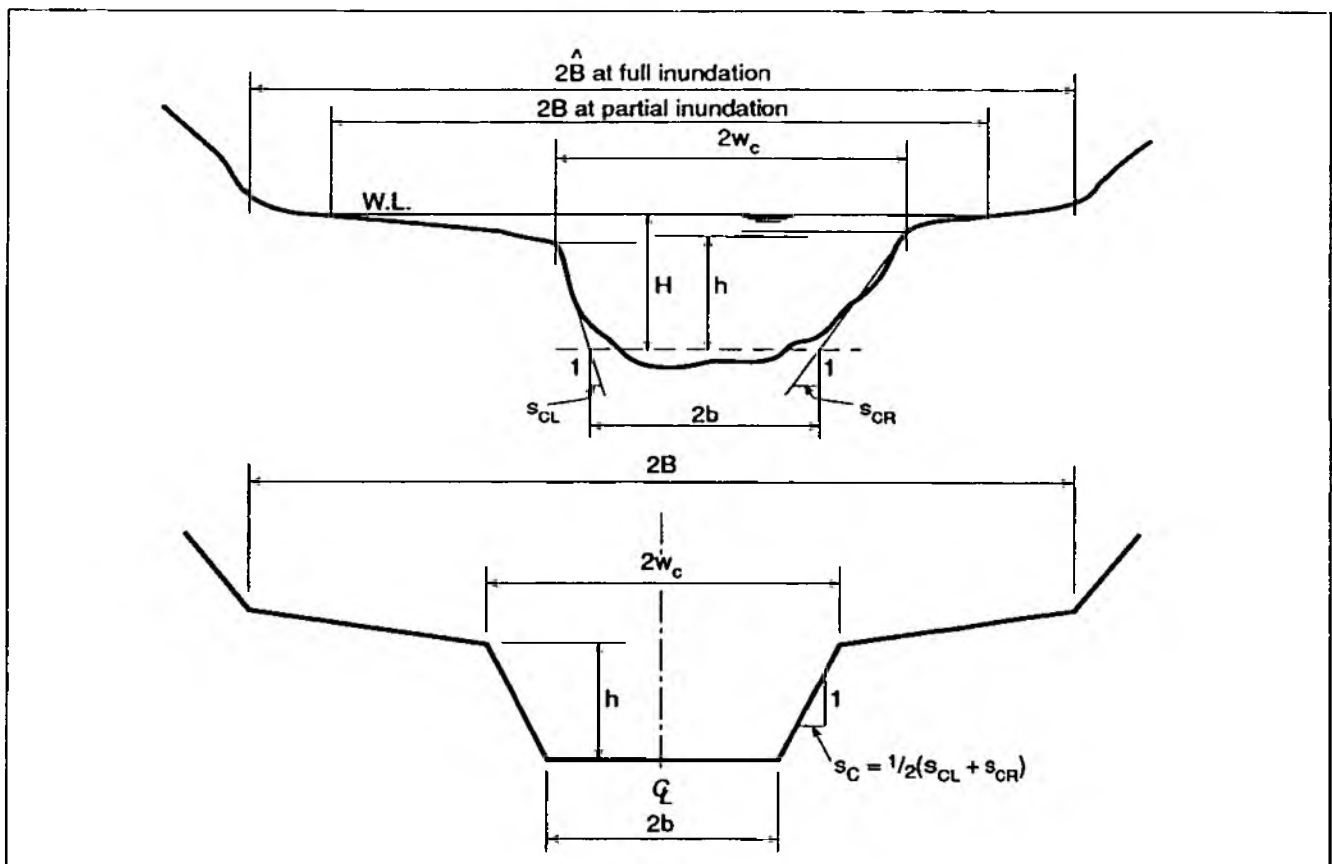
Fig 7.1   Illustration of method of assessing the sectional goemetry parameters for a natural river cross-section
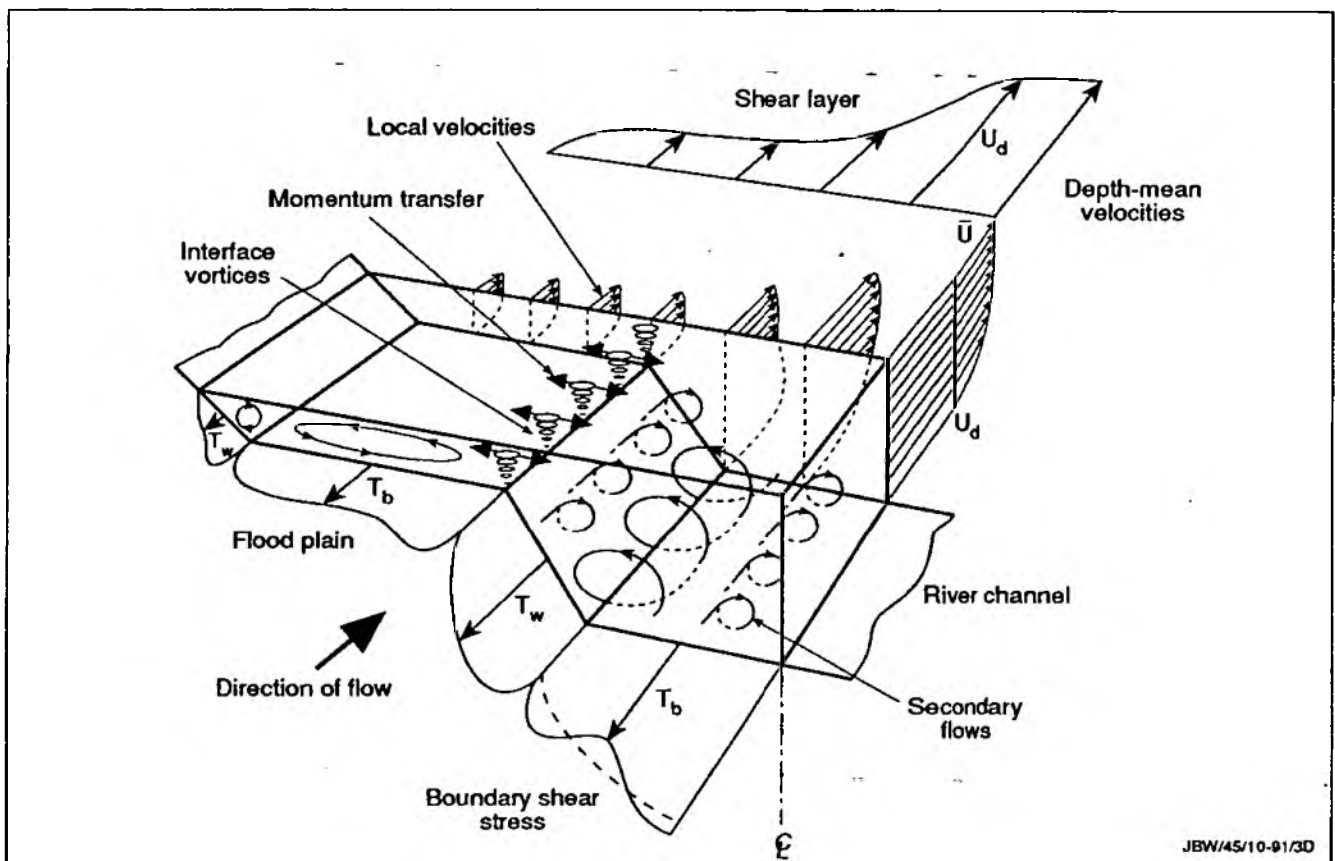
Fig 7.2   Some of the flow processes in two-stage channels, with their influence on boundary shear stress (Shiono and Knight, 1991)
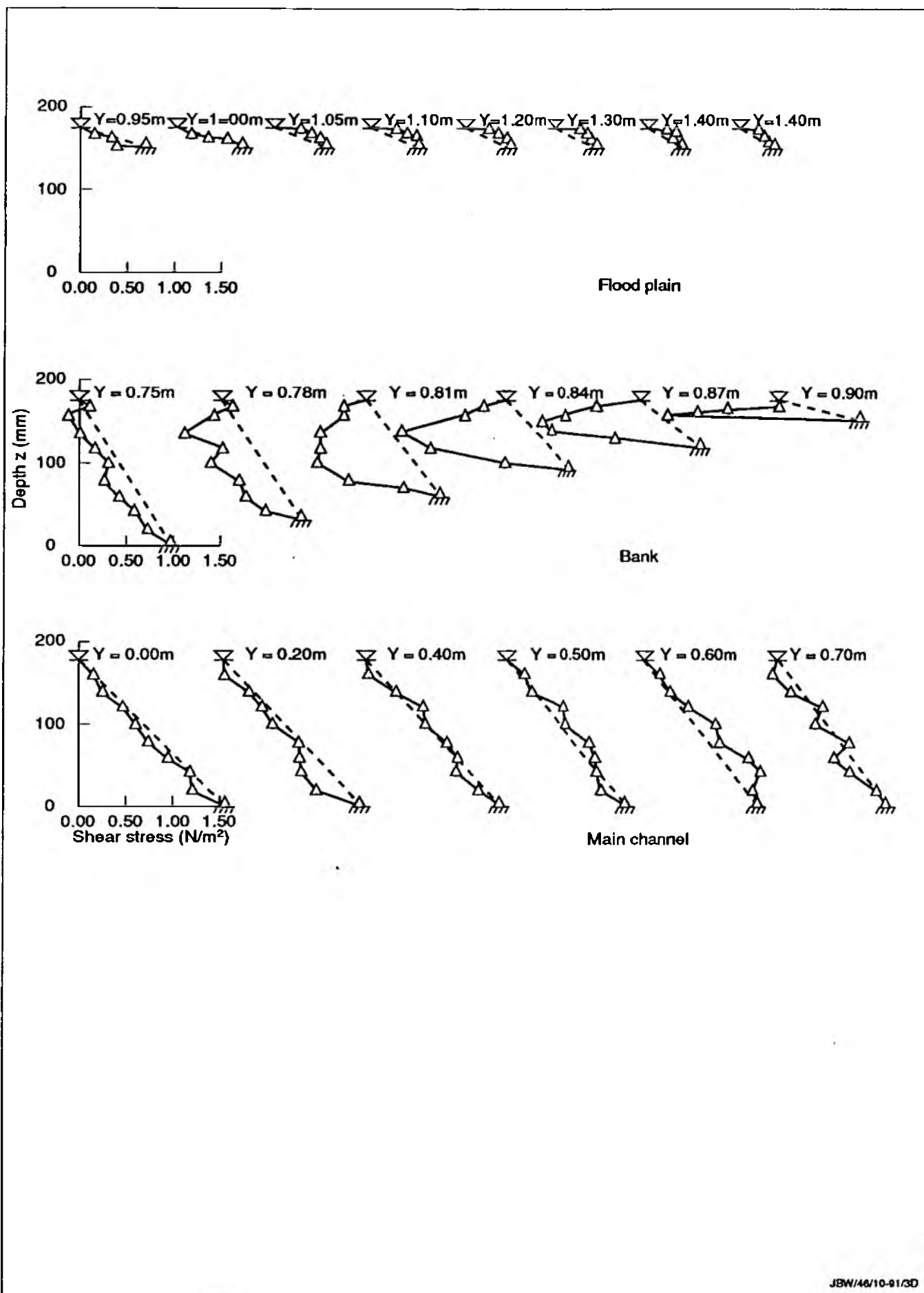
Fig 7.3 Vertical distributions of shear stress, τ_H: bed values based on Preston tube measurements, others using laser doppler anemometry. Y denote lateral distance from centre-line. $H_* = 0.152$. (Knight, Samuels and Shiono, 1990)
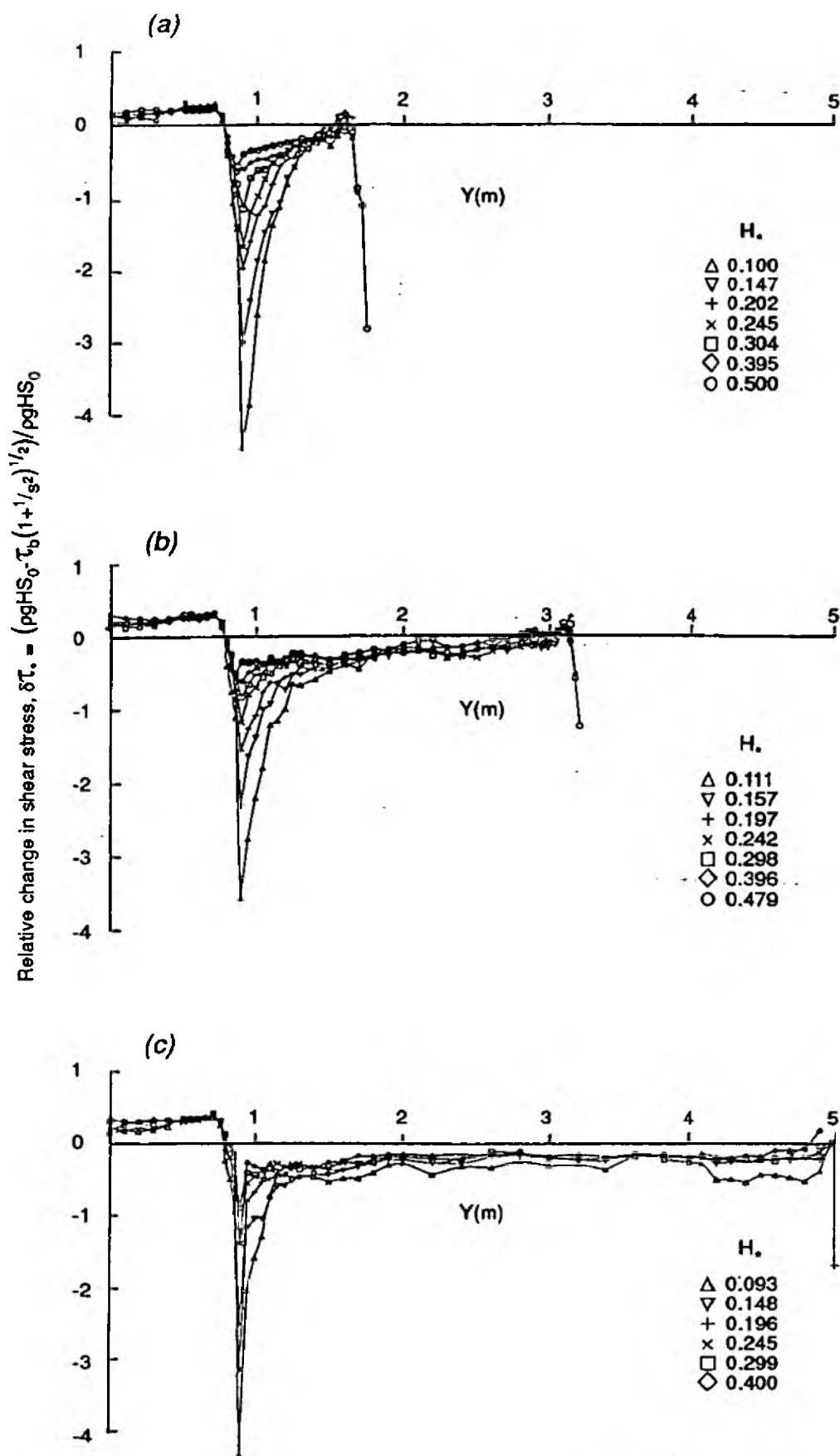
Fig 7.4   Lateral variation of boundary shear stress for different relative
depths, H∗, for B/b = 2.2, 4.2 and 6.67, (series 01, 02, 03)
(Shiono and Knight, 1991)
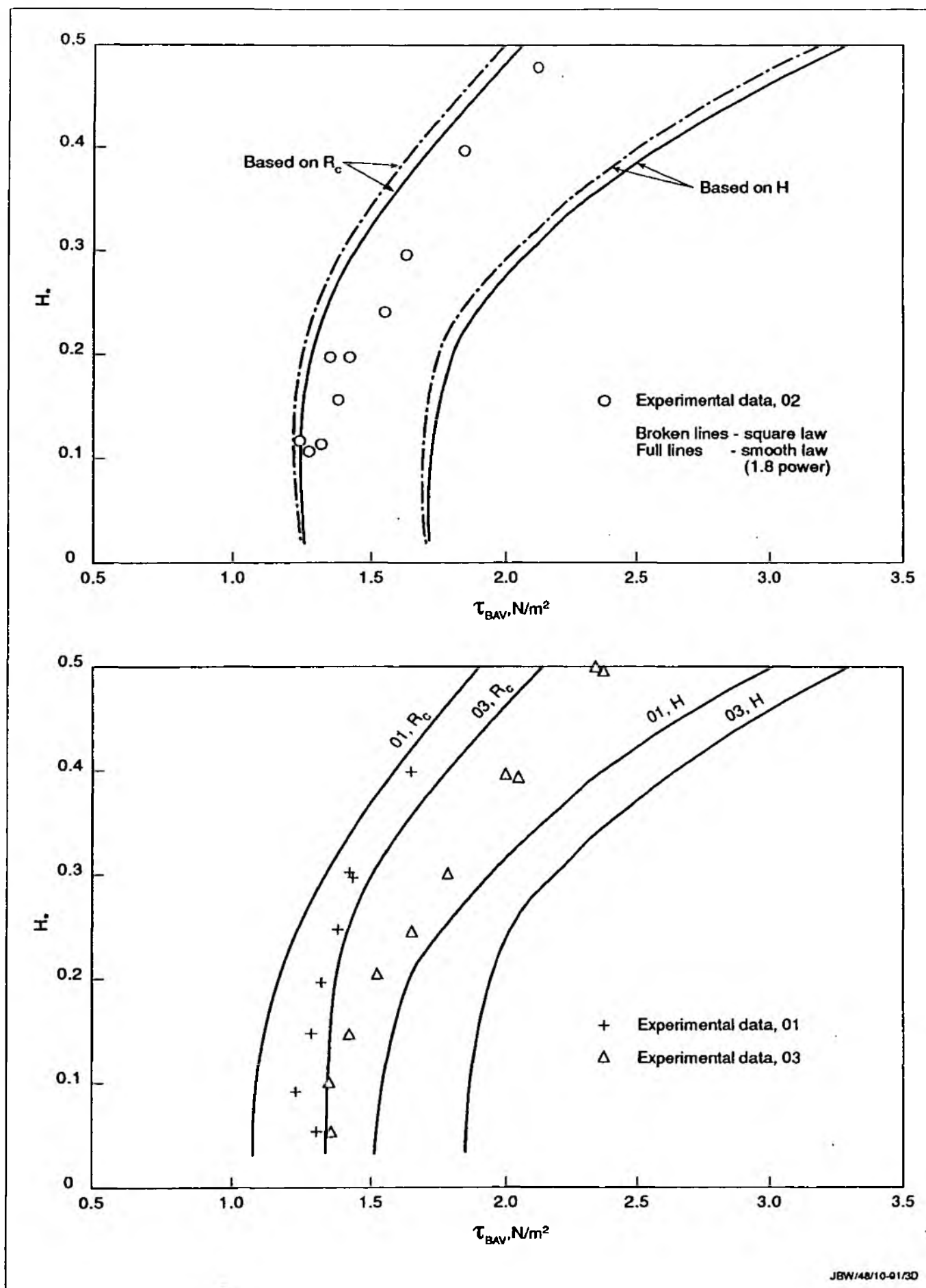
Fig 7.5 Comparison of observed average shear stress on bed of main channel with calculated values based on flow depth, H, and hydraulic mean depth, Rc, series 01, 02 and 03 (see table 3.1 for details of geometry).
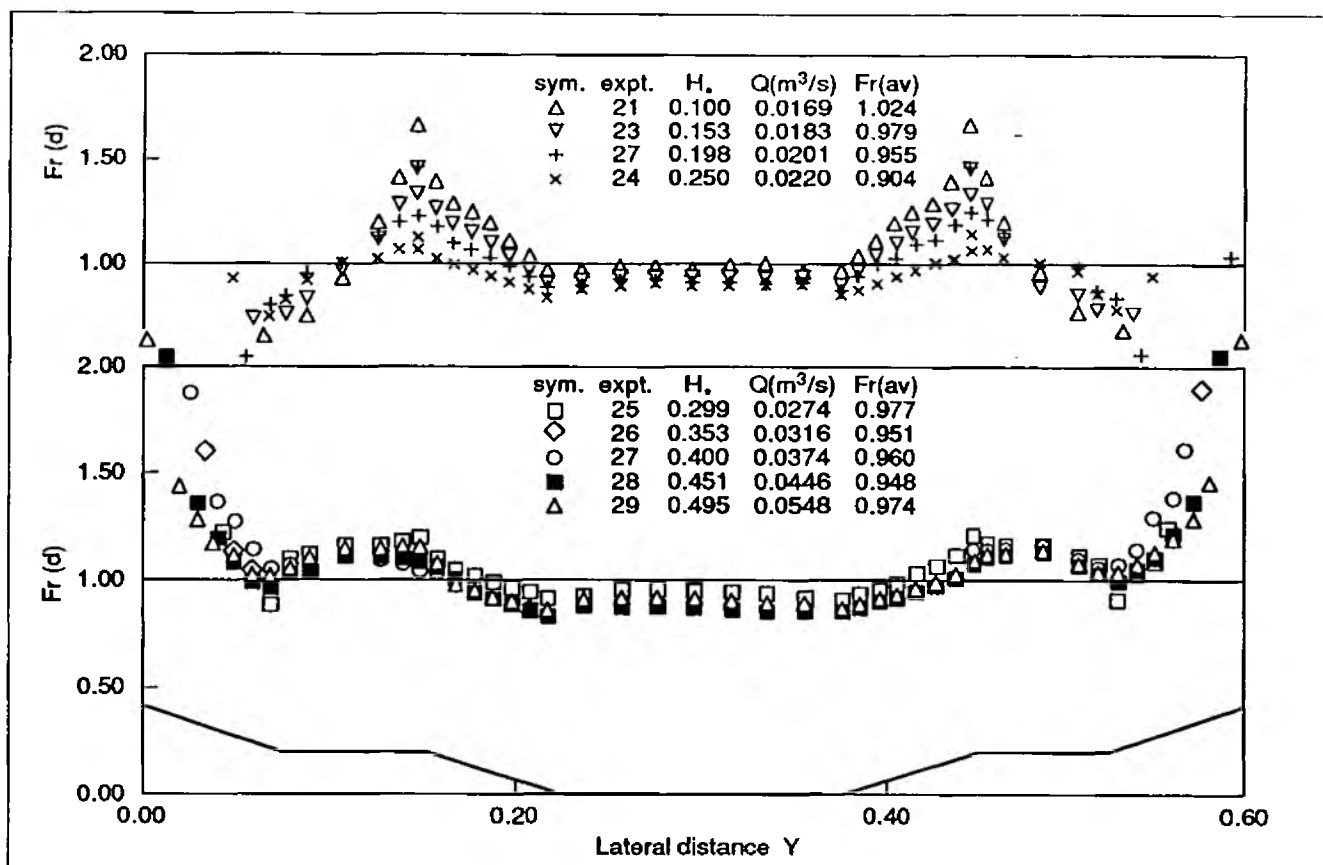
Fig 7.6   Lateral distribution of local Froude number when overall flow condition is critical (Knight and Yuen, 1990)
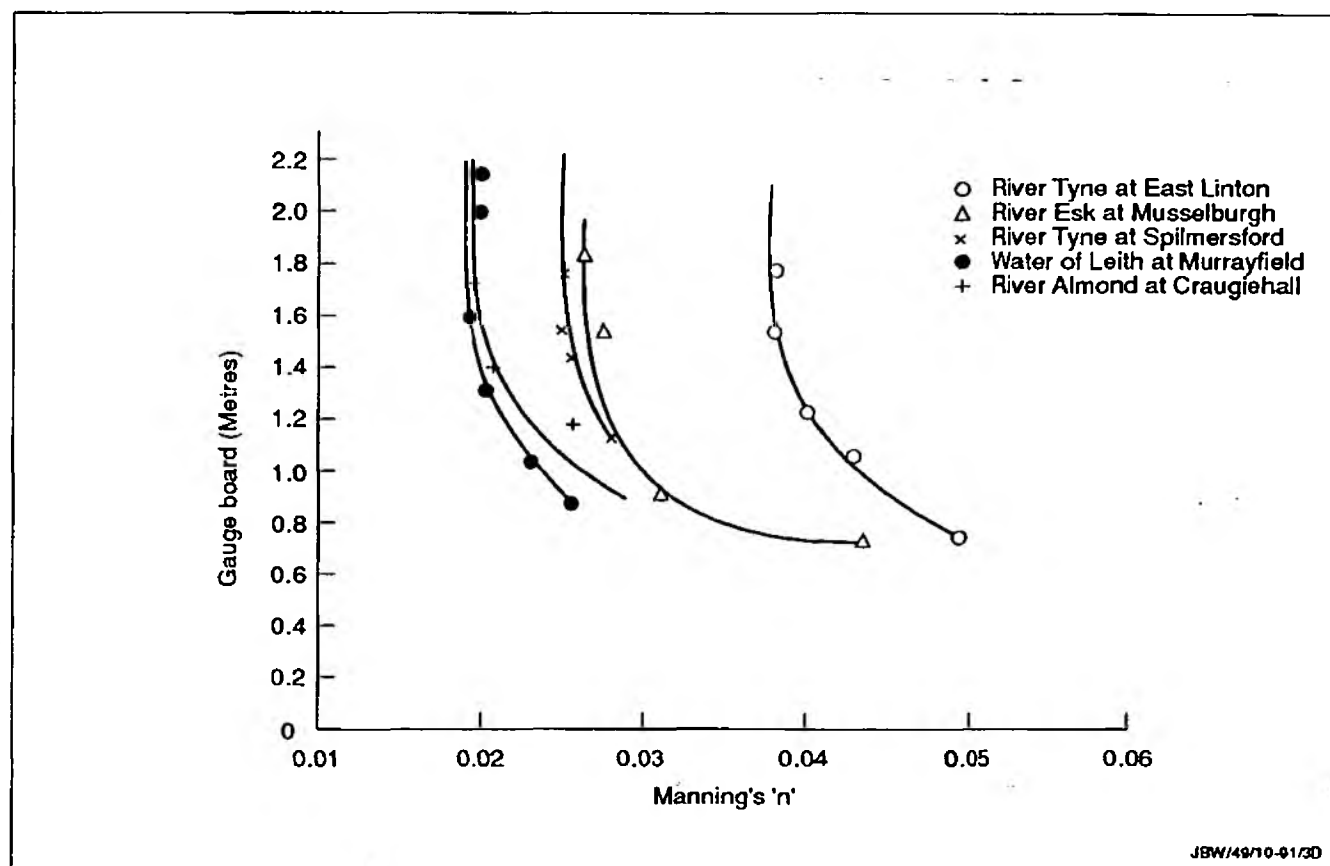
Fig 7.7   Manning's n values for within bank flows in five Scottish rivers, (Sargent, 1979)
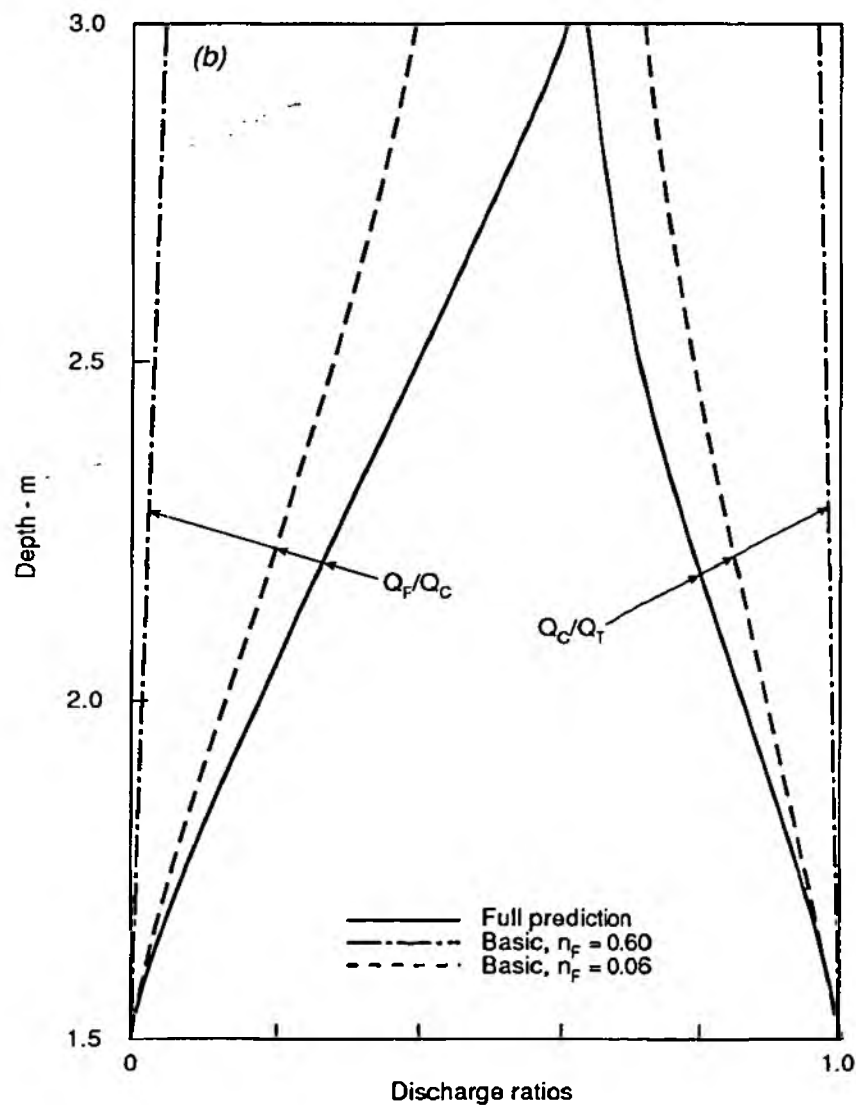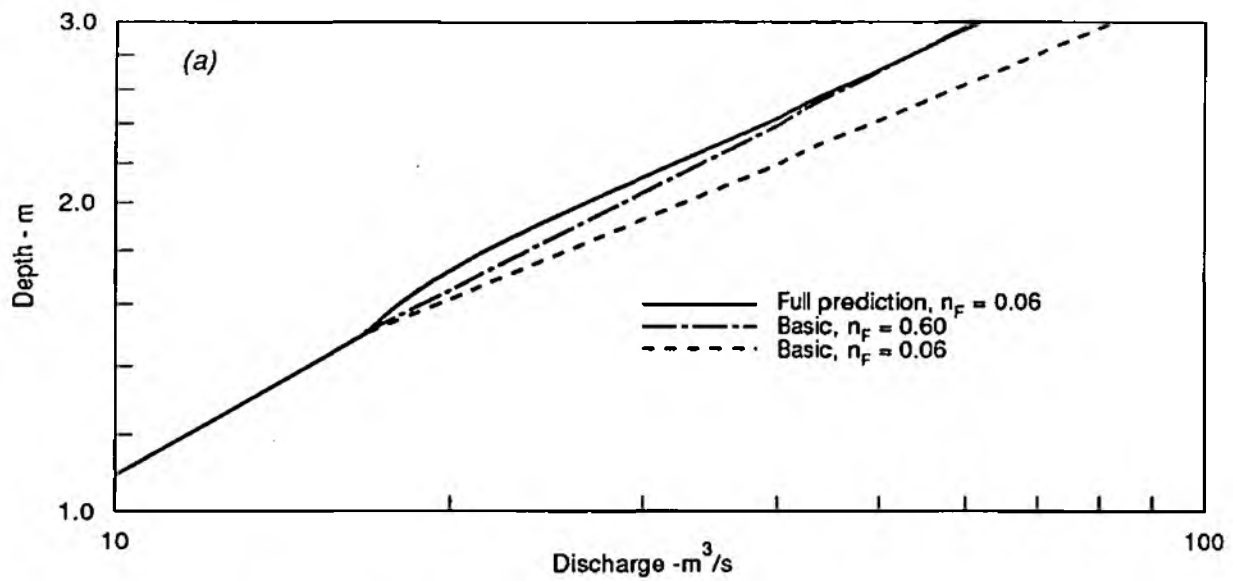
Fig 7.8   (a) Stage discharge function for a hypothetical small river, comparing full
            prediction allowing for interaction with traditional calculations.
            (b) Ratios of discharges; channel/total, and flood plain/channel, with and
            without allowance for interaction effects

8. IRREGULAR PLAN FORM

8.1 Features of meandering flows in-bank

8.1.1   Even when flowing below bank-full, a curved or meandered channel shows distinctive flow features that make its hydraulic performance significantly different from straight channels. When a fluid flows round an open channel bend, secondary currents are generated because the radial pressure arising from the horizontal curvature is not in balance at all points in the depth with the centripetal acceleration imposed by the mean curvature in plan. The faster moving upper layers tend to move outwards; the slow near bed layers move towards the inner bank. This sets up a secondary circulation which develops as flow proceeds round the bend. In a meandering system, the secondary current cell set up in one bend decays as flow passes through the cross-over and is replaced by one of opposite hand as flow passes through the subsequent bend.

8.1.2   In a meandering system, the length of stream is greater than the straight line distance along the valley, of course, and thus the available hydraulic gradient along the stream is less than the valley slope. The bank full capacity is therefore reduced by two effects, this loss of available gradient as a result of channel sinuosity and also-the-additional head losses arising from the succession of bends. This "bend loss" occurs in the secondary circulations, their development, decay and reversal in quick succession, from redistributions of flow across the channel width and from flow separation from the convex bank.

8.1.3   The system of secondary currents, and the special form of those currents in meandered channels, also affects the morphology of those channels. There is a familiar deepening of mobile bed channels on the outsides of bends, accompanied by shoaling on the insides of bends. The hydraulic engineer often makes good use of these secondary currents in siting intakes to avoid blockage by bed material and to minimise the intake of suspended sediments. In the context of hydraulic capacity, however, these natural channel forms with almost triangular cross sections, switching regularly from deep on the left to deep on the right and vice versa in a meandered system, would be expected to perform somewhat differently from an artificial meandered channel with trapezoidal cross-section. The hydraulics

21

of channels with irregular plan form is clearly very complex, even without the interactions with flood plain flow when above bank.

8.1.4   There have been many research studies into the flow round open channel bends, and several into meandering channels, see for example the recent text by Chang (1988). It is not the purpose here to provide a comprehensive review of previous work but rather to point out some salient features. Ervine and Ellis (1987) included in-bank meandering in their review of flow in rivers with flood plains, and they provided the following summary of some of the typical geometric features, with the terminology defined also in figure 8.1.

TABLE 8.1   Typical geometric details for meandered rivers.

Sinuosity (Sy) = channel length along curved "thalweg"
straight line "valley" length

Description: Straight, Sy = 1.00 to 1.05
                   Sinuous, Sy = 1.05 to 1.5
                   Meandered, Sy > 1.5

Meander wavelength (between bends of same hand), L_M = 10 tw_C approx.
Average radius of curvature in bends, R_M = 2.7 tw_C "
Double amplitude of meanders, for Sy = 1.5, a_M = 0.5 L_M "
                              for Sy = 2, a_M = 0.8 L_M "
                              for Sy = 3, a_M = 1.4 L_M "
                              for Sy = 4, a_M = 2.0 L_M "
Meander belt width, W_M = a_M + tw_C by definition

The reader is referred to Leopold and Wolman (1957) and Jansen et al (1979) for a more comprehensive treatment of fluvial morphology. However, according to the above classification, many of the research projects on meandered channels have actually concerned sinuous channels, as the sinuosity was below 1.5. A meandering channel with the cross-over sections at 60° to the valley axis would typically have a sinuosity of 1.4 or so. Such a channel is illustrated in plate 4 (Volume 1, following summary report).

8.1.5   The balance between the various components of overall channel resistance when within bank can be broadly assessed from the large scale

research at the US WES Station reported in 1956. The main series of tests on meandering channels was with overbank flow, with a channel of bed width 0.6m. They were, however, preceded by within bank calibration runs, with a straight channel of the same cross-section and also with bank full conditions at each of three sinuosities. Knowing the sinuosity in each case, the loss of bank full capacity because the gradient has been reduced by the factor $1/Sy$ is readily computed. In fact, the observed bank full flows are lower again, and this is because a proportion of the gradient along the thalweg is taken up by the form drag of the succession of bends on plan, with the balance overcoming the basic boundary friction. In the straight channel, of course, the boundary friction accounts for the whole of the energy dissipation. The following table summarises those results:

TABLE 8.2   Allocation of energy dissipation in US WES experiments.

Sinuosity, Sy	Bankfull discharge allowing for the reducted gradient along thyalweg	Observed bankfull discharge	Reduction factor for planform losses	Proportion of thalwed slope used in planform form losses
	1/s	1/s		
1.00	62.89	62.89	1.00	0
1.20	57.41	43.91	0.765	0.415
1.40	53.15	39.09	0.736	0.459
1.57	50.19	34.56	0.6886	0.526

8.1.6 The above tests were made with a trapezoidal channel cross-section rather than a naturally shaped channel, and although artificial it does provide a basic comparison. With the greatest sinuosity of 1.57 tested, the main channel bankfull capacity was reduced by an overall factor of 0.55. 0.80 of this ($1/\sqrt{Sy}$) comes from the greater path length of the channel, and a further 0.69 ($\sqrt{(1-0.526)}$) from planform losses, giving $0.80 \times 0.69 = 0.55$. Thus depending on the sinuosity, up to half the total energy dissipation can be ascribed to planform losses in these particular tests.

8.1.7 Similar information is available from a preliminary analysis of information from the early within bank tests in the FCF at Wallingford with

a meandered channel of 60° cross-over angle and sinuosity 1.37 (see Plate 4). The section geometry differed from any of the straight channels tested (as described in Chapter 3) but from the initial calibration of those straight channels the basic resistance function for the cement mortar construction was known (see Appendix 2). Hence the equivalent straight channel capacity could be calculated with confidence. There was no attempt to obtain a discharge measurement at precisely bankfull but a whole series of stage discharge tests were carried out over a range of depths up to about 96% of bank full. There were 18 such groups of data, and the running averages of threes were taken, as explained in connection with the straight channel tests, to minimise experimental scatter. It was then possible to assess the reduction factor for planform losses for these within-bank flows, the loss of gradient due to sinuosity being fixed by the plan geometry of course. The planform reduction factor varied from 0.95 at shallow flows (when the boundary drag would be more significant) to 0.86 at 88% of bank full. Extrapolating to bankfull, the form drag reduction factor would become about 0.82, implying that about one-third of the thalweg gradient was used up in planform losses and two-thirds in boundary drag. The bankfull capacity of the corresponding straight channel would have been 0.120 m³/s, reduced to 0.101 m³/s by the greater channel length, and further to 0.082 m³/s by the planform losses. In these FCF tests, the planform losses were rather less than in the nearest comparable US WES tests, though the reason for this is not yet established. Perhaps the width to depth ratio of the channel has a significant effect, as might the details of plan geometry.

8.1.8 If a resistance formula with an empirical coefficient e.g. the Manning equation, is used to determine conditions in an irregular, sinuous or meandering channel, the use of stage discharge observations to establish the coefficient value will automatically take account of the form losses due to plan irregularity as well as the boundary drag arising from the composition of its bed and banks. It is to be anticipated that the coefficient values in such cases will be much in excess of those for straight channels with otherwise similar boundary compositions and roughness texture. Sources of information on channel roughness are mentioned in Chapter 7, section 7.4, and some details are given in Appendix 5. Cowan (1956) proposed a system of building up Manning's n for a channel from various elements of resistance and then applying a factor to allow for meandering. For sinuosities below 1.2 he suggested no specific addition to

the n value; for Sy = 1.2 to 1.5, factor n by 1.15; for Sy above 1.5 factor n by 1.30. These last two n factors are equivalent to allowing 25% and 40% of the thalweg gradient to be used up by planform losses.

8.1.9   The above refers to within bank flows, and demonstrates the compexity of the flow in channels of irregular or meandering planform compared with straight channels. What effect the combination of a meandered main channel with a reasonably straight flood plain will have on the channel processes is considered next.

8.2   Above-bank flows in meandering channels

8.2.1   Ervine and Ellis (1987) reviewed conditions where a deep channel meanders through a relatively straight flood plain, commenting that there had been little attention paid to the mechanics of overbank flow under such conditions. It will be obvious that with the main channel flow no longer confined within its banks, there will be exchanges of flow (with its accompanying momentum) between the main channel and the flood plains. With fairly gentle meanders of modest sinuosity, the expectation is that flow would leave the tapering flood plain to enter the main channel, at the same time squeezing flow out from the opposite bank of the channel on to the opposite flood plain. In more tortuous systems, one might anticipate that major flood flows along the valley floor would almost ignore the main river channel, except for its obstructing influence as the dominant flood flood plain flows crossed and recrossed it as a transverse trough in the valley floor.

8.2.2   There has been much recent detailed work, both in the FCF and elsewhere, in which the details of this three-dimensional flow structure have been examined. Willetts (1991) provides early pointers to the results of that research, with figure 8.2. Showing how the secondary current that occurs with within-bank flows reverses with overbank flow. This also changes the direction of bed movement, and there have been many cases of field observations following major floods that confirm this picture, bed sediments having been lifted out of the deep channel on to the flood plain beyond. So far as the water flow is concerned, with a reasonable depth of flow over the flood plains, the continuity of flow within the main channel is broken: no longer is it basically the same body of water proceeding down

25

the river channel; it is being exchanged continuously with the flood plain waters, at least within the meander belt width. This exchange involves additional head loss, because of differences in the momentum vectors between these continually mixing flows. Figure 8.3 (Ervine and Ellis, 1987) illustrates these flow complexities.

8.2.3   There are very many geometric and roughness conditions involved in any comprehensive study of even the simplest aspect of meandering river flood flows, i.e. their stage discharge function. The research in the FCF at Wallingford is not yet complete (Summer, 1991) and it would be premature to attempt an appraisal in sufficient detail to provide a full design method for irregular channels. However, some preliminary indications of the order of magnitude of the influence of channel irregularities on the hydraulics compound channels will not be amiss.

8.2.4   The early work at the US WES published in 1956 has been referred to already in the context of straight compound channels. The main thrust of that research was into meandered channels, concentrating on the influence of a meandering main channel on the flood capacity. The tests were at large scale and covered three sinuosities, as well as three roughness conditions on the flood plains, created by laying down sheets of expanded metal. In terms of the detail in the published results and the accuracy with which the basic roughnessses were determined, the test series was not ideal. For example only three flow depths were tested the shallowest of which was of the same order of depth as the expanded mesh roughening, which photographs in the original publication show to have been somewhat irregular (expanded metal is difficult to keep flat and uncurled at the edges). However, the scale of the tests and their scope make them a useful reference source.

8.2.5   Perhaps the most useful of the presentations of information in the original publication is that reproduced as figure 8.4. It is in non-dimensional form, showing the reduction in main channel discharge compared with a straight aligned channel system. (The main channel section is defined by vertical divisions at the banks.) This reduction is based on the premise that the flood plain flows themselves may be assumed unchanged, compared with their "straight channel" values, so that any deficit is ascribed solely to the main channel component. When flow first submerges

26

the flood plain, there is already a 30 - 45% reduction in main channel conveyance, depending on the sinuosity. This was explained earlier in this Chapter as being due to the extra stream length due to sinuosity plus the component of energy dissipation arising from planform losses. When overbank depth reaches 0.6 x channel depth ($H_* = 0.375$) this reduction in apparent main channel conveyance has increased to between 45 and 77% when the flood plains have the same roughness as the main channel, yet with very rough flood plains (n_F/n_C = 3 approx) the increase with depth is more modest.

8.2.6   The assumption that the loss of conveyance should all be allocated to the main channel whilst the theoretical flood plain flows are unchanged is hardly a realistic model in terms of flow details, although with straight channels it was found in the FCF work that the main channel discharge deficits were much greater than any compensating addition to flood plain flow. However, it is quite likely bearing in mind what is now known about the detail of the flow exchanges that the main channel component of discharge must suffer considerably from the periodic influxes of flood plain flows and compensating effluxes of main channel flows, so the concept of loss of main channel conveyance was a far-sighted contribution.

8.2.7   Table 8.3 shows the US WES results in two different ways: F1 is the factor by which the measured straight channel discharge at the given depth would have to be multiplied to yield the measured discharge under meandering conditions; F2 is the factor by which the discharge estimated by adding together the main channel flow extrapolated from the observed meandering bank full condition and the estimated flood plain flow, neglecting interference effects, would have to be multiplied. This provides a matrix, albeit sparse, of results for a range of sinuosities, range of relative depths and range of roughness ratios.

27

TABLE 8.3: Discharge and conveyance reduction factors for meandering channels flowing above bank-full.

F1: Factor by which the experimentally observed aligned channel discharge would have to be modified to account for meandering of main channel.
F2: Ratio of observed total discharge to that obtained by summing the main channel discharge, as extrapolated from the observed bank-full meandered flow, and the experimental flood plain discharge, proportioned down to the actual flood plain width.

Ratio of Manning's n on F P to main channel value	H_m	Sy = 1.20		Sy = 1.40		Sy = 1.57	
		F1	F2	F1	F2	F1	F1
1.0	0.167	0.804	0.960	0.729	0.937	0.617	0.854
	0.286	0.819	0.974	0.713	0.891	0.651	0.854
	0.375	0.783	0.944	0.686	0.860	0.630	0.821
2.0	0.167	0.698	0.741	0.616	0.718	0.541	0.696
	0.286	0.867	0.816	0.784	0.790	0.696	0.751
	0.375	0.830	0.854	0.775	0.843	0.714	0.820
3.0	0.167	0.624	0.691	0.576	0.693	0.511	0.695
	0.286	0.713	0.735	0.687	0.747	0.605	0.731
	0.375	0.802	0.802	0.767	0.819	0.717	0.817

8.2.8   The above refer to a particular flood plain width, corresponding to B/b = 4, which in these tests was a varying amount in excess of the meander belt width.   It would be reasonable to assume, perhaps, that if the flood plains were wider those reduction factors might still apply to the zone within 2B = 4 x 2b whilst the sections outside might be relatively unaffected.   This question also illustrates how difficult it is to generalise from a limited range of experiments when so many geometric parameters can be involved - and why a sound co-ordinating theory is required to generalise any design procedures for irregular channels.   It can not be assumed that the above empirical adjustment factors apply to geometries differing from those tested by US WES.

8.2.9   Turning next to recently acquired data, only the FCF work with a 60° cross-over angle and sinuosity 1.37 has been analysed for the treatment that follows. Other cases studied in the FCF and elsewhere include a "naturalised" main channel cross-section with outer bank deep zones and inner bank shoals, and also various distributions of flood plain roughening. Work with a 110° cross-over has also been carried out at Wallingford, and in this geometry the direction of the deep channel partially reverses to simulate high sinuosity. The simple case of equal roughnesses on flood plain and in main channel with a trapezoidal main channel cross-section forms the first progression from the aligned and skewed channels considered in earlier Chapters, so provides a first tentative picture of broad effects.

8.2.10   The geometry selected for this meandering system was not a direct development of one of the cross-sections used in the main series of straight channel tests: the constraints of the flume width and typical meander geometries dictated otherwise. Whereas all the straight channels had a bed width of 1.5m, the meandering channel had a bed width of 0.9m, so that its aspect ratio (width to depth ratio) was 0.9/0.15 = 6, rather than 10. It had 1:1 side slopes and was installed in a total flood plain width, 2B, of 10m, so that B/b = 5.556. Thus there were no actual measured discharges either within bank or over bank for an exact straight channel equivalent. Instead, any comparisons with the corresponding aligned system had to rely on computations for the latter, using the well established basic resistance function for this method of construction. These calculations could either be the basic flows obtained as the sum of the calculated zonal flows, or could include the allowance for interference effects deduced from the comprehensive data analysis of aligned systems reported in Chapters 3 and 5.

8.2.11   Figure 8.5 shows four plots:

I. The predicted flows for an equivalent aligned system, with the main channel calculated basic discharge allowing for both the sinuosity and the allocation of 1/3rd of the available gradient along the thalweg to planform losses, and also for main channel/flood plain interaction effects using the straight channel procedures developed in Chapters 3 and 5; ARF = 0.6. These results are shown as the ratio of the predicted flows to the basic zonal calculation, (i.e. DISADF).

II. The predicted flows for an equivalent straight system, no allowances being made for sinuosity, but including the interaction effects worked out using the methods of Chapter 3 and 5 (ARF = 0.6 = width/depth ratio/10), shown as DISADF.

III. The observed stage discharge data for the meandered channel, in comparison with the basic zonal calculation, with the main channel component allowing for both the sinuosity and planform losses assessed on the basis of in-bank performance, but not for interaction effects.

IV. The ratio of observed discharge to that predicted under I above.

8.2.12   Some features of figure 8.5. require explanation. In computing graph I, the main channel is effectively much rougher than the flood plain, because of sinuosity and planform losses. In consequence the interference effects calculated from the methods deduced from the analysis of straight aligned channels are somewhat reduced, and at the upper limit the velocity difference calculated from the basic resistance of main channel and flood plain has been reversed: the main channel flow is theoretically moving slower than the flood plain flow. This is not a condition ever covered with aligned channels: there the presumption is always that the flood plain offers greater resistance than the main channel. This diminution of velocity difference as depth increases, until they become equal and even reverse, causes the "standard" aligned channel interference equations to show quite small effects, reaching zero (DISADF = 1) when H_* = 0.43 approx. Thus any attempt to allow for meandering as an extension of the computation procedures for straight channels must fail, as the extra resistance of the main channel diminishes rather then enhances the calculated interference effect. The exchanges of flow between flood plain and main channel, with radically different flow structures and discontuity of fluid fluxes in both the deep and shallow sections, rule out any extension of the methods for straight aligned or mildly skewed systems to fully meandered or irregular channels.

8.2.13   With the type of flow structure illustrated in figure 8.3, it is to be expected that the observations of stage discharge plotted as DISADF against H_* on figure 8.5 (points shown by circles, III) will show much more

interference than either of the above computations. The gross exchanges of flow and momentum between the flood plain flow and main channel flow over the meander belt width induce much more powerful mechanisms for energy dissipation than the dispersion across the shear zone at the bank line in straight aligned systems: there are large secondary circulation cells with secondary velocities perhaps an order of magnitude greater than in straight channels, and something akin to expansion and contraction losses as flows move from flood plain to main channel and vice versa. The crosses of plot IV on figure 8.4 show this excess in effect. The values of DISADF for plot IV are the ratios of observed discharge to predicted discharge using scheme I above.

8.2.14   At shallow overbank depths, the conveyance of this system with sinuosity 1.37 is about 70% of the sum of the zonal flows, calculated as if there was no interference or added energy loss due to flow and momentum exchange. This drop in conveyance is additional to that which comes from the extra resistance of the main channel itself. We saw in paragraph 8.1.8 that the bank full capacity reduces from 0.120 m³/s to 0.082m³/s due to sinuosity; a factor of 0.68. As depth increases, the ratio to the basic sum of meandered main channel flow plus flood plain flow increases and steadies at about 0.80. Thus the exchange of momentum for this particular geometry reduces the conveyance compared with a basic calculation, such as might be extrapolated from a knowledge of the meandered channel's resistance coefficient plus a calculation for the flood plain, by 20%, for H_* from 0.25 to 0.50, but can be as much as 30% at lower depths. This is a somewhat greater influence than shown by the comparable F2 factors in Table 8.3, for Sy = 1.4 and Manning's n ratio 1, obtained from the US WES tests.

8.2.15   These few examples of the influence of meandering on the stage discharge function for overbank flow clearly demonstrate that the effect is important in an engineering context and should be allowed for in hydraulic computations. The best method for doing this must await the completion of the current research programmes, especially the large scale work in the FCF at Wallingford, including the complex analyses that will no doubt be required in order to quantify the results in a general form to provide a reliable design method. Although systems with a small angle of skew were shown in Chapter 4 to be amenable to a simple extension of straight aligned channel methodology, the evidence for meandered channels is that the

interference effects with overbank flow are of a radically different character, rendering any extension of straight channel procedures inappropriate: a quite different co-ordinating theory is required.

8.2.16   Table 8.3 above provides a matrix of plausible adjustment factors for discharge and conveyance in comparison with equivalent straight aligned systems: the F1 values. However, for engineering purposes the concept of an equivalent aligned system is less useful than an extrapolation from observed or estimated conditions at bank full flow in the actual meandered river: F2 is then the appropriate adjustment for interference effects. These were based on limited data from 1956. Figure 8.5 provides a first example using more recent and more detailed research results of the influence of flow and momentum exchange under overbank conditions on the extrapolation of stage discharge functions beyond bank full. However, neither Table 8.3 nor figure 8.5 is put forward as an established design procedure for irregular channels. Some indications of the way forward to such a method are suggested in the following section.

8.3   Flow models for sinuous, meandering and irregular channels

8.3.1   Flow in meandering channels with over-bank flow is a complex three-dimensional system, with reversals of secondary currents and major exchanges of discharge and momentum between the main channel and flood plain. These interactions between the different flow regions differ radically in their mechanisms of energy loss from those found in straight channels aligned with their flood plains. There have, however, been several attempts at developing theoretical models of the complex flow structure.

8.3.2   Ervine and Ellis (1987) offered a hydromechanics approach to the problem, considering the flow over the meander belt width (see figure 8.1 for illustration) as if it repeatedly expanded and contracted as it passed from the flood plain to angle across the main channel and then on to the opposite flood plain. They considered four main sources of energy loss in the main channel and three in the flood plain.

Main channel

1. Frictional resistance of the wetted perimeter of the channel itself, which could be assessed from a knowledge of bed material size or other information on its surface condition, using the Colebrook- White equation (or Manning with n related to the surface texture).

2. Meander bends with their secondary currents akin to large scale turbulent eddies occupying most of the cross-section. Energy loss would arise from internal shear and also transverse shear at the boundaries.

3. Turbulent shear stress on the horizontal surface at bank top level due to the overflowing flood plain flow. The velocities of the two streams will differ in magnitude and direction, with the effect that an apparent shear stress will be generated on the interfacial plane, with an influence on the main channel that might be positive or negative depending on the direction of momentum exchange.

4. There may also be pool-riffle sequences in the meandered channel, and indeed the characteristic deepening on the outside of the bend and shoaling on the inside with cross-overs between bends -induces the flow along the thalweg to follow a sequence of deeps and shallows as with a pool-riffle sequence. This source of energy loss is likely to be more significant at shallow flows than with over-bank flows.

Flood plain

1. Friction losses over the wetted perimeter, as determined from a conventional resistance equation.

2. The expansion loss where the flood plain flow encounters the deep main channel.

3. Contraction losses where the flow leaves the main channel to re-enter the flood plain from the opposite bank.

8.3.3. These assumptions simplified the flow situation to permit conventional hydraulic assessments to be made of the various sources of

33

energy dissipation. Ervine and Ellis proceeded on these lines, treating the flood plain flow within the meander belt width separately from that outside the belt width, as the latter would not suffer the expansion and contraction losses mentioned above. The values for expansion and contraction losses came from work by Yen and Yen (1983): the losses due to secondary currents were assessed using a method published by Chang (1983): the Colebrook-White or Manning equation would provide the boundary friction loss: but losses due to the interface shear were omitted. Assembling the various head loss terms and taking account of continuity, an equation was developed that could be used to obtain the stage-discharge function for a given geometry.

8.3.4   This method was tested against the same US WES data used earlier (US WES, 1956) with promising results. These are illustrated in figure 8.6 (taken from Ervine and Ellis, 1987). This shows for two of the sinuosities and two of the flood plain roughnesses tested at Vicksburg how the theoretical prediction compared with observation. Ervine and Ellis commented as follows: "The most obvious conclusion is that the predicted discharge is generally underestimated at higher flood plain depths and overestimated at lower flood plain depths. .... The reason for overestimating discharge at low flood plain depth may be related to the omission of the co-flowing turbulent shear stress term .... In this region, the predicted discharges are of the order of 0 - 20% greater than the experimental data. For larger flood plain depths the predicted discharges are of the order of 10% too low. It should be noted that the assumption for energy loss due to secondary cells in the main channel was derived for in-bank flow and may be greatly repressed at higher flood plain depths. This is combined with the fact that the assumption of three sub-sections of cross-sectional area acting independently of each other, with no interaction between each section, represents a crude attempt to rationalise a complex three-dimensional situation."

8.3.5.   Ervine and Ellis also compared their theory with smaller scale research by Toebes and Sooky (1967), which had the advantage of separate measurements of discharge distribution across the floodway. They concluded

"...predicted discharge is low compared with the experimental data in the area of the main channel and inner flood plain, with the opposite occurring in the outer flood plain. This would imply an overestimation of head loss

34

in the inner regions either in the secondary cells or expansion and contraction losses". The graphical comparison between the Ervine and Ellis theory and Toebes and Sooky data is shown in figure 8.7.

8.3.6   Preliminary analysis of the very detailed data on flow pattern, velocity vectors and secondary currents obtained from the FCF at Wallingford indicates that the above hydromechanics model would require appreciable modification to conform closely to the reality of flow in meandered channels, but the general approach via component head losses remains a valid avenue of development.

8.3.7   A somewhat more fundamental hydromechanics model might be developed through the momentum equations, though their full solution depends on a knowledge of all boundary shears and pressures. It would be easy to assume hydrostatic pressures, but this begs the question: the water surface is not a simple sloping plane, and the flow separations where the flood plain discharges enter the deeper main channel will create non-hydrostatic conditions at the channel margins. However, it is possible that a model could be developed with the simplifying assumptions that could then be calibrated against the available data.

8.3.8   A stage beyond the above would be to use refined grid numerical modelling in two dimensions on plan, solving the 2-D St Venant momentum and continuity equations for the geometries for which data is available. No doubt there would be some need for empirical adjustments to obtain good agreement, but once achieved the model could be used to generate stage discharge functions, or conveyance functions, for any other geometry of sinuous, meandering or irregular compound channel with over-bank flow. However, it may be necessary to add a third dimension, effectively using a layered model, to obtain satisfactory simulation. These are questions for future study but are essential if hydraulic design information on complex channels is to achieve the standard of accuracy and reliability that is now becoming available for straight compound channels. In the meantime, the methods available are somewhat crude and inadequately confirmed by wide ranging data at large scale.

8.3.9   Design methods for irregular compound channels are outside the scope of this report. The treatment of the subject here is intended to illustrate

35

the need for and importance of further analysis before a comparable design method for irregular channels can be prepared, whilst providing the reader with some indication of the order of magnitude of the interference effects in such systems.
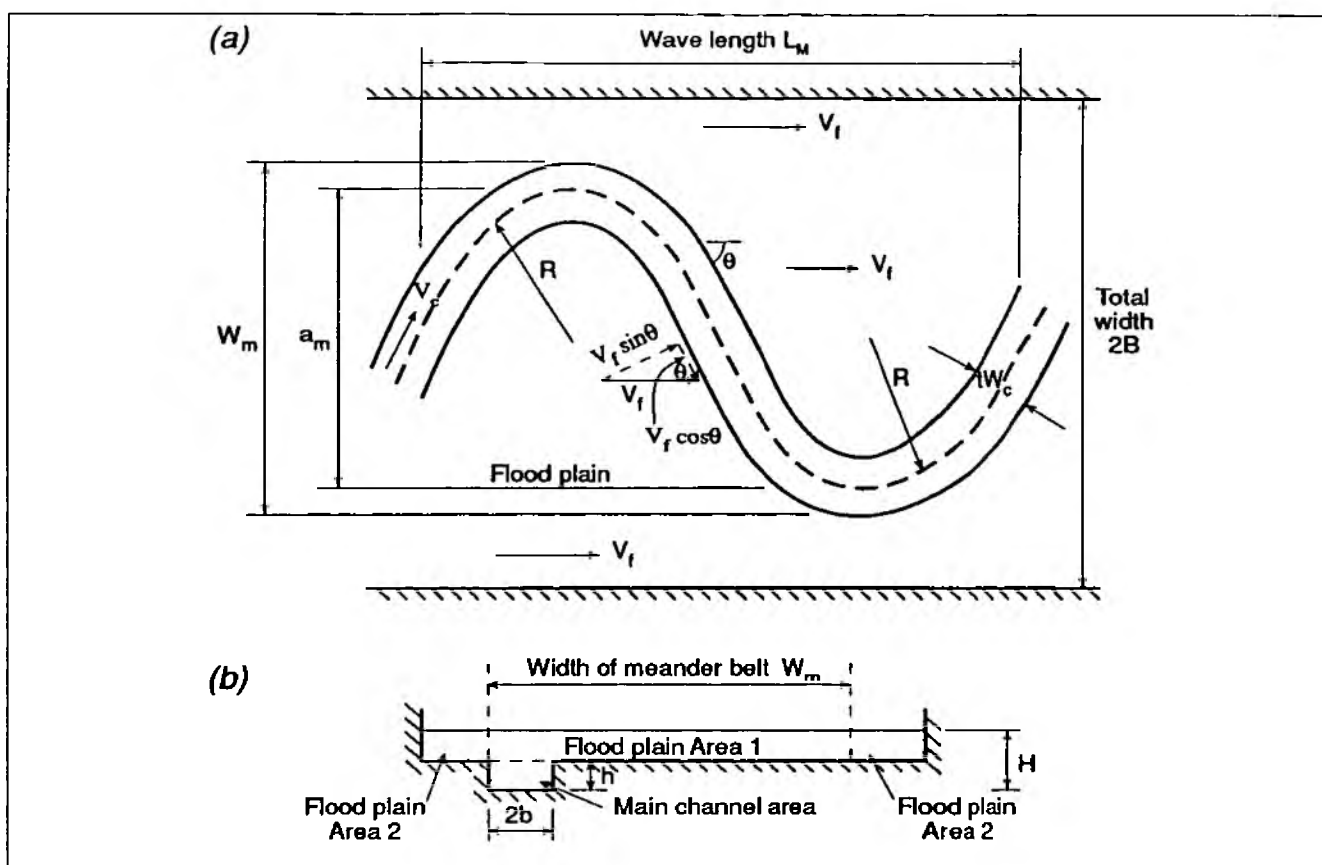
Fig 8.1 **Plan and cross-section of meandered channel, with definition of main symbols used. Cross-section shows subdivisions of area used in Ervine and Ellis (1987) theory**
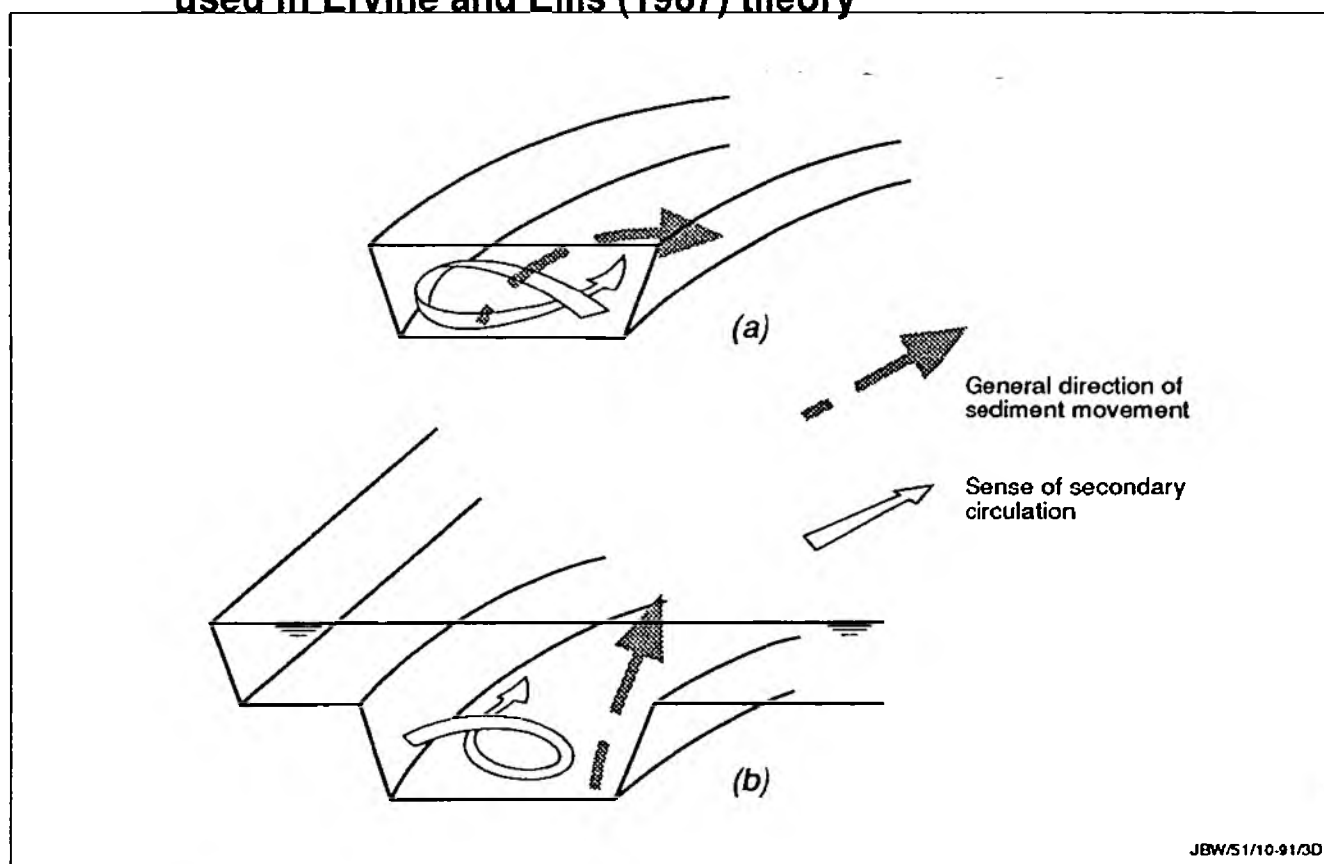
Fig 8.2 **Established secondary currents in bend and main direction of bed movement in meandered channels: (a) within bank flow; (b) over-bank flow**
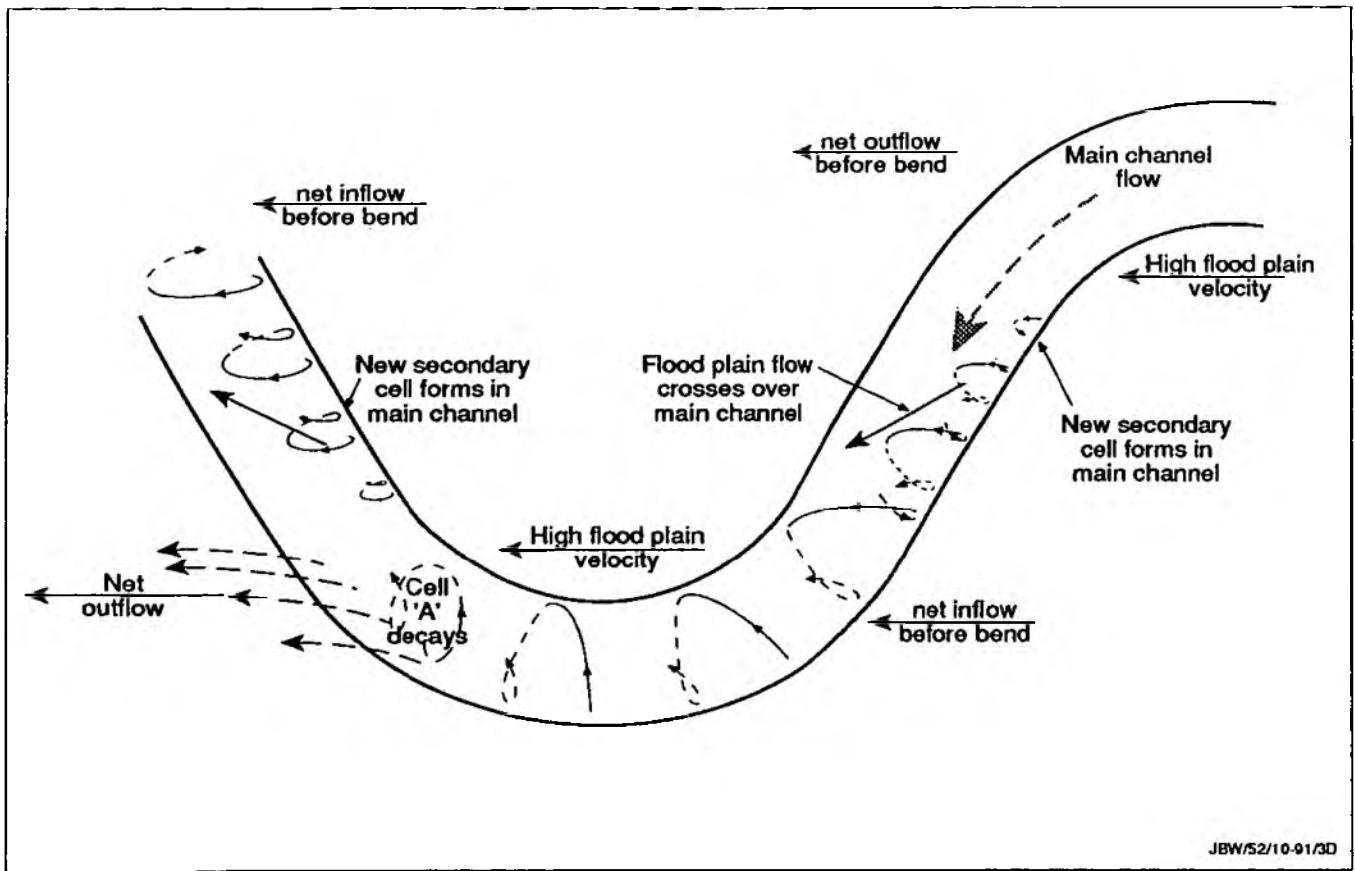
Fig 8.3   **Illustration of flow exchanges and secondary cell development in successive meander bends, Ervine and Jasem (1991).**
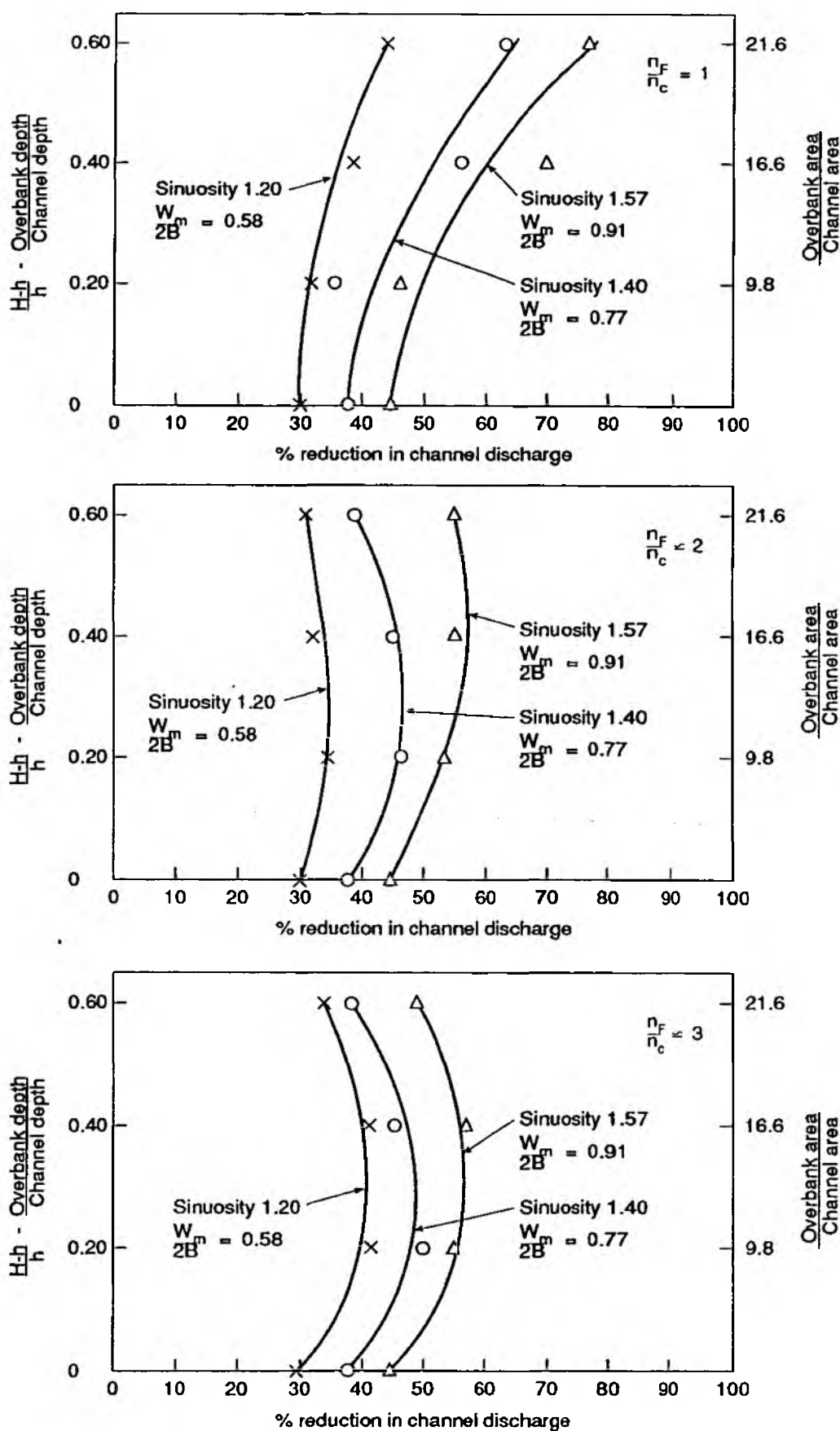
Fig 8.4   Reduction in channel discharge (assuming flood plain flow is unaffected) for three channel sinuosities and three ratios of flood plain roughness to main channel roughness: US WES (1956)
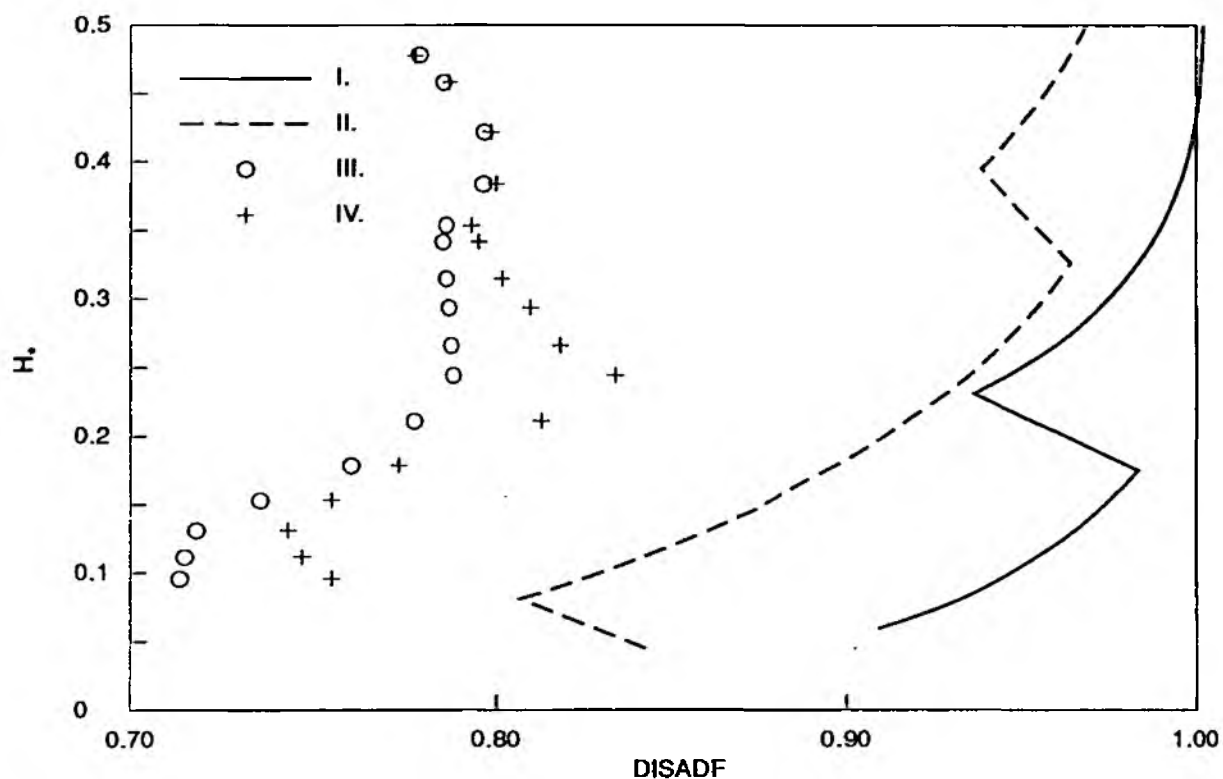
Key

I. Predicted function for equivalent straight system, but with main channel flow computation based on thalweg slope and allowing for planform losses.

II. Predicted function for straight system of same basic cross-section.

III. Observed data in comparison with basic zonal computations, with main channel calculation using thalweg slope and allowing for planform losses.

IV. The ratio of observed discharges to the computations under I, i.e. the interference effect with meandering additional to the allowance for thalweg slope and planform losses in main channel.

JBW/54/10-91/3D

Fig 8.5 Discharge adjustment factors for straight and meandered channels, FCF experimental results for meandered case for B/b = 5.56, 2b/h = 6, 60° cross-over, L_M/W_C = 10, Sy = 1.37, with prediction for equivalent straight system.
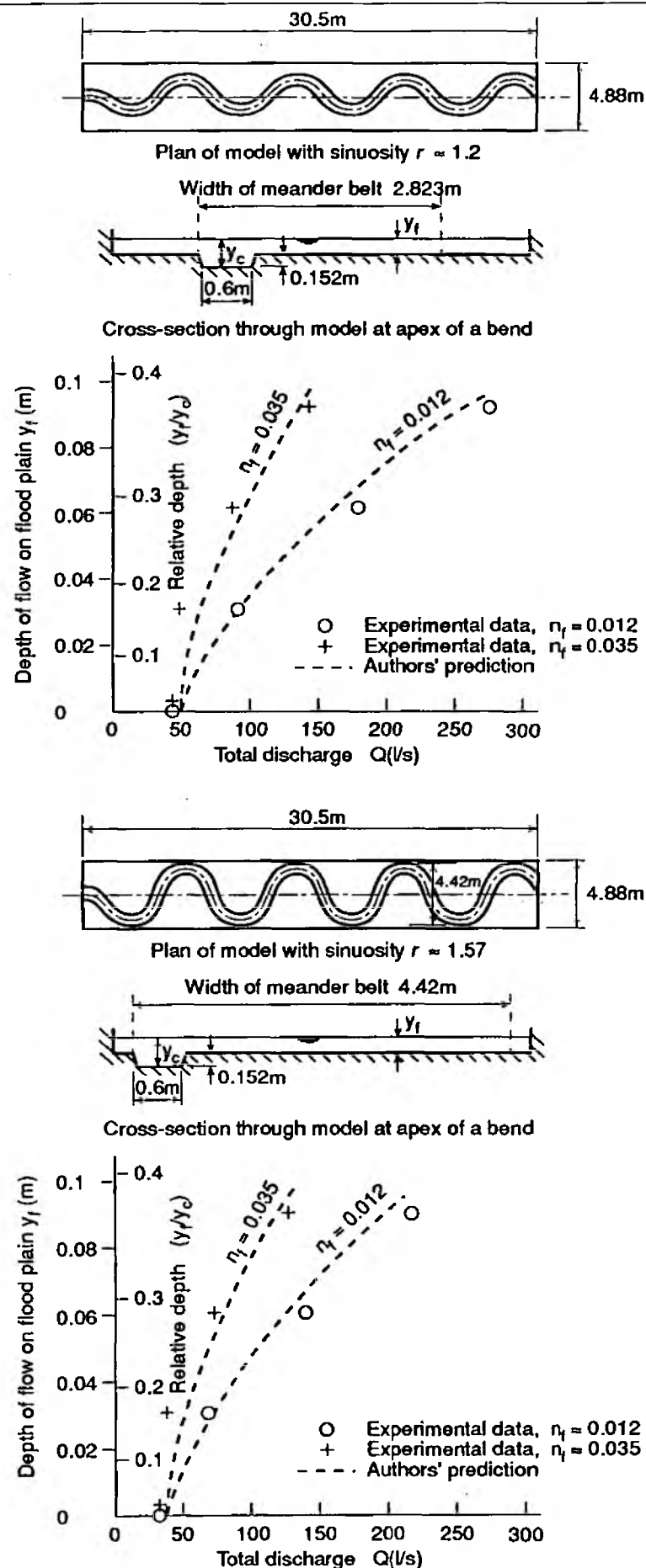
Fig 8.6   Comparison by Ervine and Ellis (1967) of their theory with selected cases from the US WES (1956) report: ratios of flood plain roughness to main channel roughness of 1 and approx. 3 (Manning coefficients); for two sinuosities. Geometries shown above.
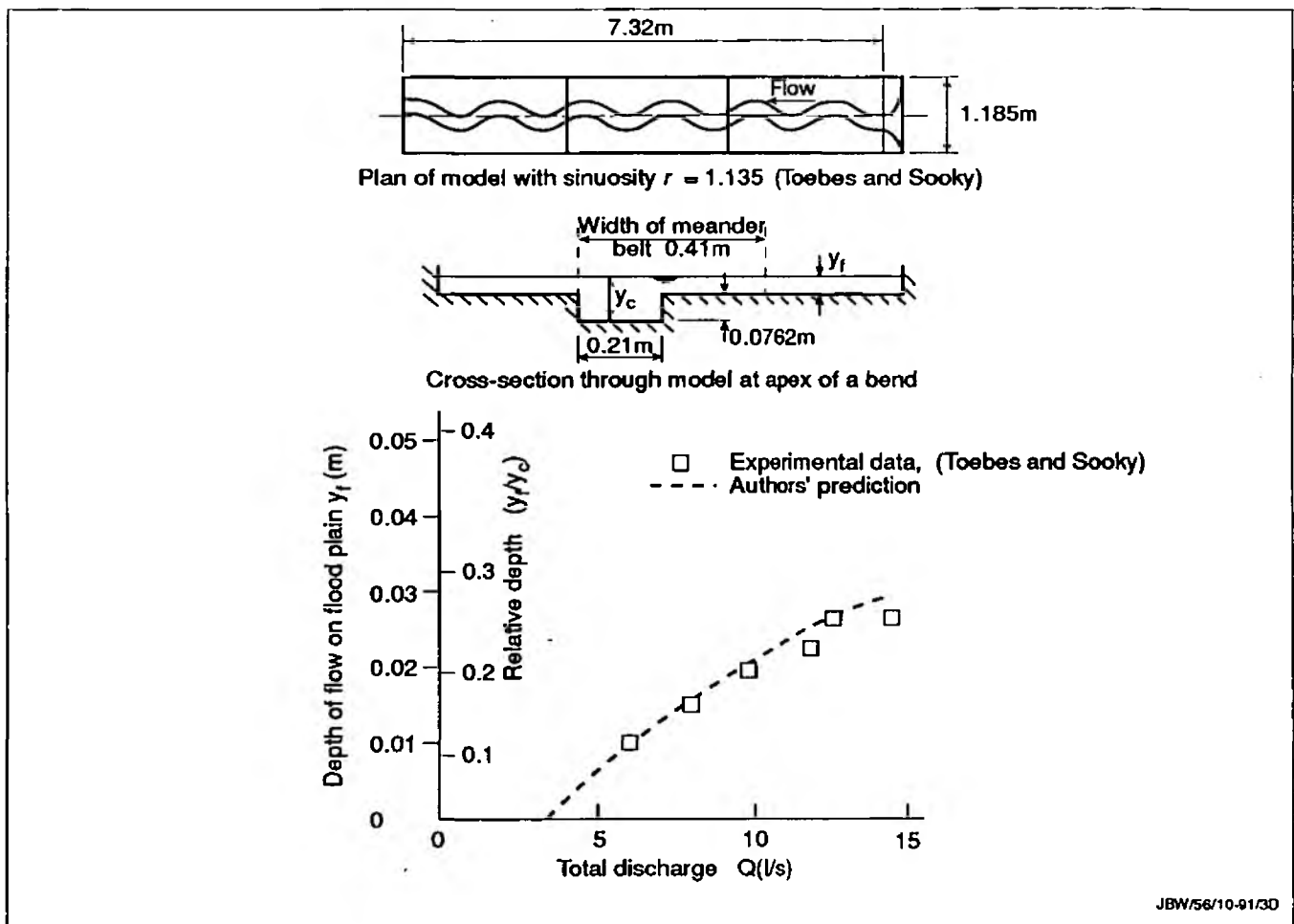
Fig 8.7 Comparison by Ervine and Ellis (1967) of their theory with Toebes and Sooky (1967) report: equal flood plain and main channel roughness; Sy = 1.135. Geometry shown above.

9. SEDIMENT TRANSPORT

9.1 General aspects of sediment transport

9.1.1 The development and utilisation of water resources for irrigation, hydro-power and public supply can be severely affected by sediment in many parts of the world. Where there is a mature and well vegetated landscape, sediment problems may be relatively minor; but where slopes are steep and vegetation sparse, the yield of sediment from the catchment gives high concentrations in the rivers. In utilising these water resources, and also in managing rivers in terms of flood protection, an understanding of the hydraulics of alluvial channels is vital. So far only the water conveyance aspects have been considered, but it is also important to review the impact of the research on flow and resistance in channels with flood berms in the context of its implications for sediment movement. Only through better understanding of fluvial morphology can the rivers be controlled and managed sympathetically in respect of the environmental requirements, and the long term success of engineering projects in rivers carrying sediment be secured.

9.1.2 Sediment may be transported either in suspension (fine material in turbulent flow) or as bed load (by the creep and saltation of particles close to the bed). These modes of transport are governed by somewhat different laws. In practice a range of sediment sizes may exist in a river - or an intermediate size even if of narrow grading - so that design methods for handling sediment problems have also to deal with all conditions between the extremes of fully suspended wash loads and coarse gravel and boulders moving in contact with the bed. Over the years, many formulae have been derived relating the transport of bed material, whatever its size, to the hydraulic properties of flow, but in the last decade or so it has been shown that few are of acceptable accuracy and even the best are far from precise as predictive equations. Nevertheless, recent theories are sufficiently comprehensive to represent not only fine and coarse material but the intermediate sand sizes which dominate many alluvial systems.

9.1.3 Because of the range of sediment sizes of interest and differing transport mechanisms involved, a few definitions are in order:

37

Bed load: The material that moves in close contact with the bed.
Suspended bed material load: That part of the suspended load
consisting of particle sizes found in samples taken from the bed.
Total bed material load: The sum of the above, i.e. the total
transport of those particle sizes present in bed samples.
Wash load: That part of the total sediment discharge consisting of
particle sizes smaller than are present in the bed; frequently taken to be
sizes below 0.06 mm.

9.2. Transport process and theory

9.2.1   The transport of sediment by even a steady uniform flow is a complex
process as yet incompletely understood. Many theories have been put forward
to provide frameworks for the analysis of data on sediment transport, and
very many experiments have been carried out over a period of some 50 years
under controlled conditions in laboratory flumes. Some theories begin from
the analysis of the mechanics of motion of individual particles, others use
similarity principles or dimensional analysis as the starting point. All,
however, include a measure of empiricism in providing coefficient values
based on laboratory experiments or field measurements. Dimensional analysis
provides a set of governing variables as follows:

9.2.2   The minimum set of basic quantities which influence the process of
sediment transport in two-dimensional, free-surface flow are the unit mass
of fluid, ρ, the unit mass of solids, ρ_s, the viscosity of the fluid, υ,
particle diameter, D, water depth, d, shear velocity at the bed $\sqrt{(gdS)}$,
denoted v_*, and acceleration due to gravity, g. Dimensional analysis yields
four groups:

$$Re_* = v_* D/\upsilon \qquad \qquad \ldots 9.1$$

$$Y = v_*^2/(s-1)gD \qquad \qquad \ldots 9.2$$

$$Z = d/D \qquad \qquad \ldots 9.3$$

$$s = \rho_s/\rho \qquad \qquad \ldots 9.4$$

9.2.3   One of the most significant contributions to the science of
sediment motion was made by Shields (1936), who analysed experimental data

38

on the initiation of movement of granular material using the first two of the above four non-dimensional groups. For established motion, an additional parameter is needed to represent the transport rate, for example Einstein's (1950) non-dimensional expression:

$$\Phi = qs/\rho[(s - 1)gD]^{3/2} \qquad \qquad ... 9.5$$

where qs is the sediment transport rate as submerged weight per unit time per unit width. It follows that:

$$\Phi = function [Re_*; Y; Z; s] \qquad \qquad ... 9.6$$

Most transport theories use the above parameters or their equivalent. For example, Ackers and White (1973) replaced the above particle Reynolds number, Re_*, by:

$$D_{gr} = D[g(s - 1)/v^2]^{1/3}. \qquad \qquad ... 9.7$$

9.2.4   One of the more significant studies of the total load of non-cohesive sediments was by Engelund and Hansen (1967). They used a sub-set of the functions indicated by equation 9.6, to provide a simple relationship between transport and channel hydraulics:

$$\Phi f/4 = 0.1 Y^{5/2} \qquad \qquad ... 9.8$$

9.2.5   The Ackers and White (1973) theory considered coarse sediment and fine sediment separately, and then sought a transitional function between them. These transitional sizes include the sands and silts that are of great practical interest in alluvial systems. Their analysis is typical of several in the last fifteen years which have used the power of modern computation to make the fullest use of the mass of data available from laboratory and field. Their results are also typical in that the optimisation procedures used to "calibrate" the theory provided a set of equations from which the total transport of bed material could be calculated within a factor of two on about two occasions out of three. The transport rate was based on the stream power concept introduced by Bagnold (1966), and the different mechanisms applicable to coarse and fine sediments led to two sets of parameters derived from Y,Z and D_{gr} which were

linked by a transition parameter n_{gr} which was expected to be – and confirmed as – a function of Dgr.

$$G_{gr} = C_{gr}[(F_{gr} - A_{gr})/ A_{gr}]^{mgr} \qquad \dots 9.9$$

where:

Transport rate –

$$G_{gr} = \frac{Xd}{SD} \left(\frac{v_*}{V}\right)^{ngr} \qquad \dots 9.10$$

Sediment mobility –

$$F_{gr} = \frac{v_*^{ngr}}{\sqrt{(gD(s-1))}} \left(\frac{V}{\sqrt{32} \log(10d/D)}\right)^{(1-ngr)} \qquad \dots 9.11$$

and

$$A_{gr}, C_{gr}, m_{gr}, n_{gr} = \text{functions} (D_{gr}) \qquad \dots 9.12$$

X is the transport rate expressed as the ratio of sediment flux to fluid flux, by mass or weight, akin to a concentration which will be referred to as the "sediment charge". Data correlations provided simple algebraic formulae for all the functions 9.12, so forming a direct method of prediction. The original data analysis of Ackers and White (1973) has recently been updated, providing improved formulae for the functions 9.12, HR, Wallingford (1990c).

9.2.6   White, Milli and Crabbe (1975) reviewed the then available methods and found that few could approach the level of prediction of the Ackers and White method, the nearest comparable formulation being by Engelund and Hansen (1967). Since then, there have been other contenders, for example van Rijn (1984), (rather complex to detail here) as well as the contemporary multi-dimensional empirical correlation of Yang (1972).

$$\log X' = 5.435 - 0.286 \log (wD/\nu) - 0.457 \log (v_*/w)$$
$$+ [1.799 - 0.409 \log (wD/\nu) - 0.314 \log (v_*/w)]$$
$$\times \log [(V - V_{cr})(S/w)] \qquad \qquad \ldots 9.13$$

In the above, X' is in parts per million, V_{cr} is the mean channel velocity
at initial motion, w is the fall velocity of the particles. The above
formula requires evaluation of V_{cr} and Yang gave a group of expressions
depending on the value v_*D/ν.

9.2.7 These formulae for the total load of bed material are of similar
reliability, but are not precise predictors. In fact it is by now clear
that sediment transport is so sensitive to the hydraulics of the stream and
the grading and condition of the stream bed that it is unlikely that it
will ever be possible to predict transport rates from the overall hydraulic
parameters to much greater accuracy than at present. It is this
sensitivity to hydraulic conditions, especially the mean flow velocity and
the consequent stress on the bed, that makes a consideration of the
interference effects of flood plain flows on main channel flows
particularly significant. In what follows in this Chapter, the 1990
up-date of the Ackers-White transport functions is used to examine the
effect of compound flow on bed material transport, though very similar
conclusions would emerge whichever of the relatively reliable calculation
procedures mentioned above was used.

9.2.8 The suspension of finer material by the stream turbulence is
broadly described by the theory developed by Rouse (1937). In this the
gravitational effect through the fall velocity of particles is countered by
the upward turbulent movement that arises from the vertical distribution of
sediment. The concentration, C, at elevation, z, above the bed is related
to that at some reference elevation, C_o at z_o, through the equation:

$$\frac{C}{C_o} = \frac{(y - z) z_o}{z (y - z_o)}^{\Omega} \qquad \qquad \ldots 9.14$$

where

y = flow depth
Ω = a turbulence parameter given by w/v_*K

v_* = shear velocity, $\sqrt{(gRS)}$

K = von Karman turbulence constant

9.2.9   The period of developing understanding has brought a number of text books on the subject of sediment transport, for example Yalin (1977), Graf (1971), Garde and Ranga Raju (1977), Allen (1985) and Thorne, Bathurst and Hey (eds) (1987). Papers by the originators of the more reliable transport functions should be read for full details of their methods.

9.3. The influence of compound flow on bed material transport

9.3.1   It is clear that there is considerable interference of the flood plain flow with the main channel flow through lateral shear effects and exchange of momentum via secondary circulations, and that this interference increases the apparent hydraulic resistance of the main channel, reducing the mean velocity therein significantly. It is this change in hydraulic conditions in the main river that will give rise to changes in the rate of transport of bed sediment. This sediment charge is a function of velocity (and other factors to a lesser degree), and velocity dependence is to a power above one: hence the sensitivity to the hydraulic conditions. Using sediment transport theory, it is therefore possible to assess the effect of compound flow, taking account of the interference effect by using the calculation procedures developed earlier. This is the basis of what follows: in effect they are computed examples using the best of the available knowledge, though it is hoped in due course that research on transport in compound channels will be carried out to confirm, or up-date as necessary, these forecasts.

9.3.2   The Ackers-White functions are straight forward to apply: no iterations are required and the equations for the various parameters are readily programmable for computation. They have the advantage of covering a very wide range of sediment sizes, and also by working in terms of the total transport of bed material they automatically take account of the balance between suspended load and bed load. The transition parameter n_{gr} allows for the fact that the transport of fine material is a suspension

42

process, depending on the overall turbulence level in the stream, whilst the transport of coarse material is a bed process depending more on the bottom shear stress developed by the average velocity. In applying the equations, some assumptions were necessary:

- the turbulence level relevant to sediment processes in the main channel of a compound section is determined by the stream gradient, through the shear velocity, $v_* = \sqrt{(gRS)}$.

- the bed stress relevant to sediment transport is dependant on the mean channel velocity in the same way in a compound section as in a simple section.

- the effect of the flood plains on the main channel velocity is given by the methods described in Chapters 3 and 5. This is directly calculable in flow Region 1, but in the higher Regions of flow, the assumption is made that the main channel discharge adjustment factor remains the same as at the limit of Region 1. See Chapter 3, para 3.5.10.

- there is no transport of channel bed sediment over the flood plain. This is consistent with non-availability of such material on the flood plains, which would typically be vegetated, and so no material comparable to the main channel bed sediment would be exposed.

9.3.3   For purposes of illustration, a cross-section was chosen typical of small rivers: bed width 15m, channel depth 1.5m, flood plain width, 2 x 20m, channel and flood plain side slopes 1 in 1, thus 2b/h = 10, and B/b = 3.87. Two gradients were examined: 0.3/1000 which might represent a river with an active sand bed, and 3/1000 to represent a gravel bed stream. The Manning equation was used for the basic hydraulic calculations, with n_C = 0.03 and two values of flood plain coefficient, n_F = 0.03 and 0.06. The smoother of the flood plain conditions gave equal roughnesses over the perimeter, so was akin to most of the tests in the FCF, with flow progressing with depth through Regions 1 to 4. With the rougher flood plain condition, the flow stayed in region 1, as expected from the work with roughened flood plains. The range of depths considered covered within-bank flows and relative flow depths, H_*, up to 0.5, i.e. a depth of

flow on the flood plain equal to the actual main channel depth, 1.5m. The channel of lower gradient was assumed to have a bed of 0.25mm sand, while the steeper channel bed was taken as gravel of 30mm dia. These were chosen with some trial and error to provide interesting illustrations: obviously the sediment size chosen should provide transport at bank full flow if it was to provide any simulation of a real alluvial channel.

9.3.4   Figure 9.2 shows the calculated stage-discharge functions for all four cases. These show the by now characteristic change of slope and curvature when flow first goes over-bank. Figure 9.2 shows the calculated sediment charge in the main channel for the four cases considered. Taking the sand bed case first (shown by full lines) sand movement occurs from quite shallow depths in the main channel increasing to over 100×10^{-6} (100 mgm/l) at bank full. With the rougher flood plain, this is effectively the maximum sediment charge at any discharge. Above bank full the charge diminishes because of interference effects from the flood plain, before rising again at depths above about 2m. With the smoother flood plain, interference effects are less, and so after some hesitation in the rate of increase in charge with depth above bank full, at higher depths the charge rises above 200×10^{-6}.

9.3.5   The gravel bed case in figure 9.2 shows initial sediment movement in the main channel at a flow depth of 1.0m, 2/3rds channel depth. The charge increases to about 60×10^{-6} at bank full, with a steep rate of increase up to that depth. Beyond bank full, with the rougher flood plain the diminution of transport above bank full due to interference effects is also sharp, with the charge, X, dropping to perhaps a third of its bank full value at depth 2.0m, i.e. 0.5m depth over the flood plain. There is a sharp drop in X just above bank full flow with the smoother flood plains too, though the drop is short lived giving a return to rapid increase with depth again at depths over 2m.

9.3.6   These estimates of how compounding may affect sediment transport in natural rivers are of considerable interest, and although different examples would show somewhat different results, the broad picture would be expected to remain: a significant change in the sediment transport function when flow goes above bank, with the main channel becoming less effective than it would be in the absence of flood plains or channel berms.

44

9.3.7   Figure 9.3 shows the information in several different ways. Here sediment charge, X, is plotted against water discharge, Q. The upper diagram is for the sand bed river, with the rougher of the two flood plain conditions. Graph I is the same data as shown in figure 9.2, the charge obtained by calculating conditions in the main channel. Graph II also refers to the main channel, but here the interference effect from the flood plains has been ignored to demonstrate what the trend in the transport function would have been like if there was no information on interference and the sediment transport calculation had been based on the main channel in isolation. The latter becomes seriously in error as depth increases, by a factor exceeding 2. Graph III converts the estimated charge shown in graph I to the average over the whole stream, on the basis that there will be no additional transport of this material generated by the flow over the flood plain, but the flow over the flood plain is an additional diluent. Graph IV will be referred to later.

9.3.8   The lower diagram of figure 9.3 is similar information for the gravel bed river. Graph I and III show a very pronounced peak at bank full, indicating that in terms of transport capacity the system becomes much less efficient above bank full, with the interference effect generated by rough flood plains so severe in the example given that transport almost stops again. In fact parallel computations were also made for gravel sizes of 40mm and 50mm: 50mm material is just mobile at bank full but not at lesser or greater depths, 40 mm material is mobile over a range of depth but virtually ceases moving again at about 0.5m depth on the flood plain.

9.3.9   The results for flood plains with equal roughness to the main channel show similar but rather less dramatic effects. They form graphs V (charge based on main channel discharge) and VI (charge based on total discharge).

9.3.10   There is often discussion as to whether a compound channel is more efficient at transporting sediment than a single section without berms. To examine this question, some assumption has to be made about the hydraulic equivalence, and a simple trapezoidal section has been assumed, with side slopes 1/1, giving the same conveyance at depth of 3m as the compound section with flood plains having double the Manning's n value of the main channel. The equivalent simple section has bed width 17.15m compared with

15m in the compound section: their stage discharge curves intersect at 3m. The sediment calculations for this equivalent section form graphs IV on figure 9.3. Below bank full this wider section is less efficient in terms of sediment transport that the compound one: graph IV lies below graph I (graphs I, II and III are identical below bank full, of course). The drop in efficiency within bank is small with sand, but rather more significant in the gravel bed case where initial motion is delayed to a higher discharge. However, for above bank flow the interference effect diminishes the compound channel transport efficiency so much that the single channel has a much better performance: this is shown by comparing graph IV with graph III.

9.3.11   This comparison of graph IV with graph III may also be regarded as representing the situation where a small river confined in a narrow valley without flood plains disgorges into a wider valley or on to an alluvial plain. Under the confined valley condition, major floods will carry sediment according to graph IV, but where the valley opens out to provide flood plains then graph III will apply. The morphological inference is that in high floods the reach with flood plains can not carry forward an excess of sediment delivered from the confined valley. The river channel itself will accrete, partially block, force more flow on to the flood berms and in due course deposit the load of sand or gravel on those berms. These theoretical sediment forecasts for typical systems are consistent with geomorphological information on the development of alluvial plains and with experience of river behaviour in major floods.

9.3.12   The purpose here is to draw attention to the influence of a compound cross section with flood berms on the transport of bed material. The improved knowledge of the conveyance of such sections, allowing for the interference between flood plain and main channel, can feed forward into improved computations for river morphology. Even these preliminary sample calculations are of significance in respect of fluvial morphology, but they are theoretical and involve assumptions, and so should not be regarded as factual until there has been some experimental confirmation. There is ample scope for research on transport in compound channel systems, with much of interest in straight systems as well as in meandered systems. Until the results of such research are available, the method used here

provides evidence of the importance of compounding on sediment transport
capacity and a provisional calculation procedure.

9.4. Suspended solids in compound channels

9.4.1   The turbulent structure in compound channels is undoubtedly
different from that in simple channels without flood berms, and so the
basic turbulent suspension theory summarised in equation 9.14 will not be
applicable without some modification. In terms of broad effects, however,
the most significant feature that arises with compounding is the strong
lateral shear generated around the bank line which will diffuse the
sediment in the upper layers of the main channel across on to the flood
plains, where the flow's capacity for keeping the sediment in suspension
will be less. Hence there will be deposition on the flood plains of
suspended load originating in the main channel.

9.4.2   Allen (1948) has described this process in some detail, as well as
reminding us of the ample evidence from the field through levee building
etc. that this is indeed a well authenticated process. Using the general
concept that the capacity to maintain material of a given size in
suspension is a function of the velocity, and that the velocity will be
less on the berms than in the deep channel, Allen shows that the
concentration sustainable on the flood plains would be less than that in
the main channel by the factor (h/H). The lateral dispersion from main
channel to flood plain thus increases the concentration above the
sustainable value, so a balance can only be achieved through deposition.

9.4.3   Much detailed information on turbulence under the conditions of
compound flow has been obtained from the programme of research on the FCF,
including dispersion tests using dyes. This new information should provide
a basis for better understanding of sediment dispersion, but it is hoped
that a subsequent research programme will examine this topic directly, by
using suspended solids.
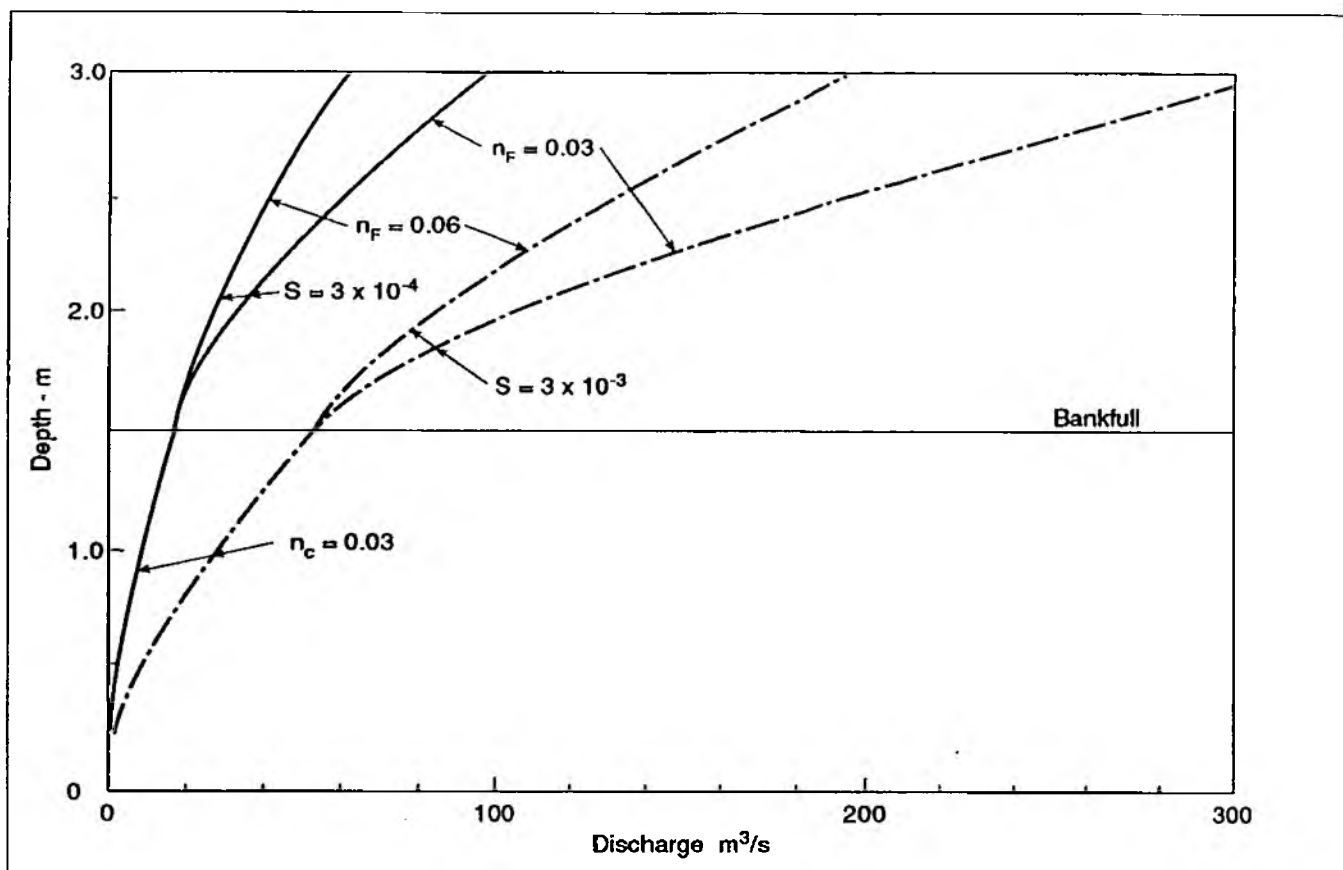
Fig 9.1   Stage discharge curves for example rivers: main channel 15m bed width, 1.5m deep, 1/1 side slopes; flood plains 20m wide, 1/1 side slopes, main channel Manning's n = 0.03
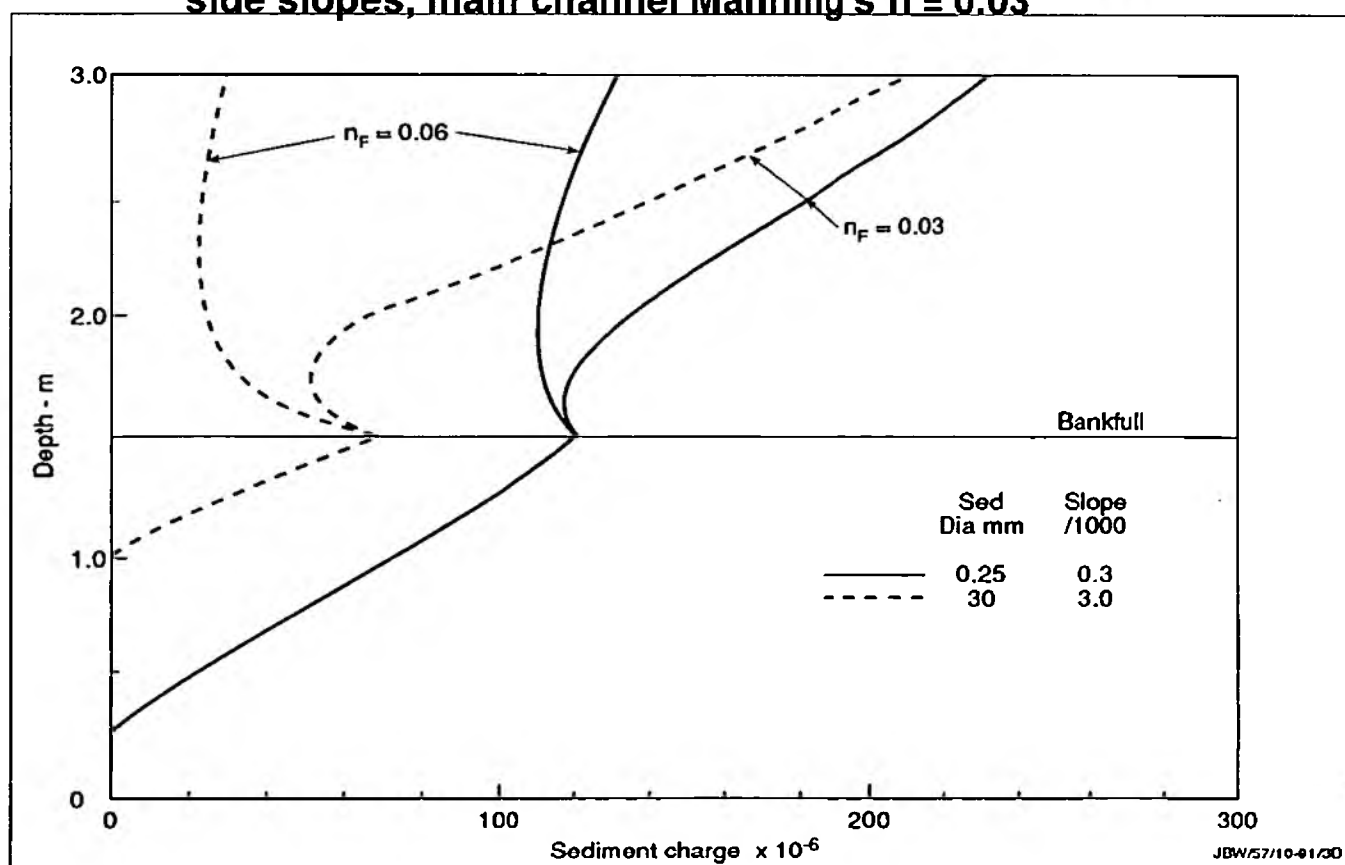
Fig 9.2   Sediment charge - X, versus stage, for sand river at S = 0.3/1000 and for gravel bed river at S = 3/1000
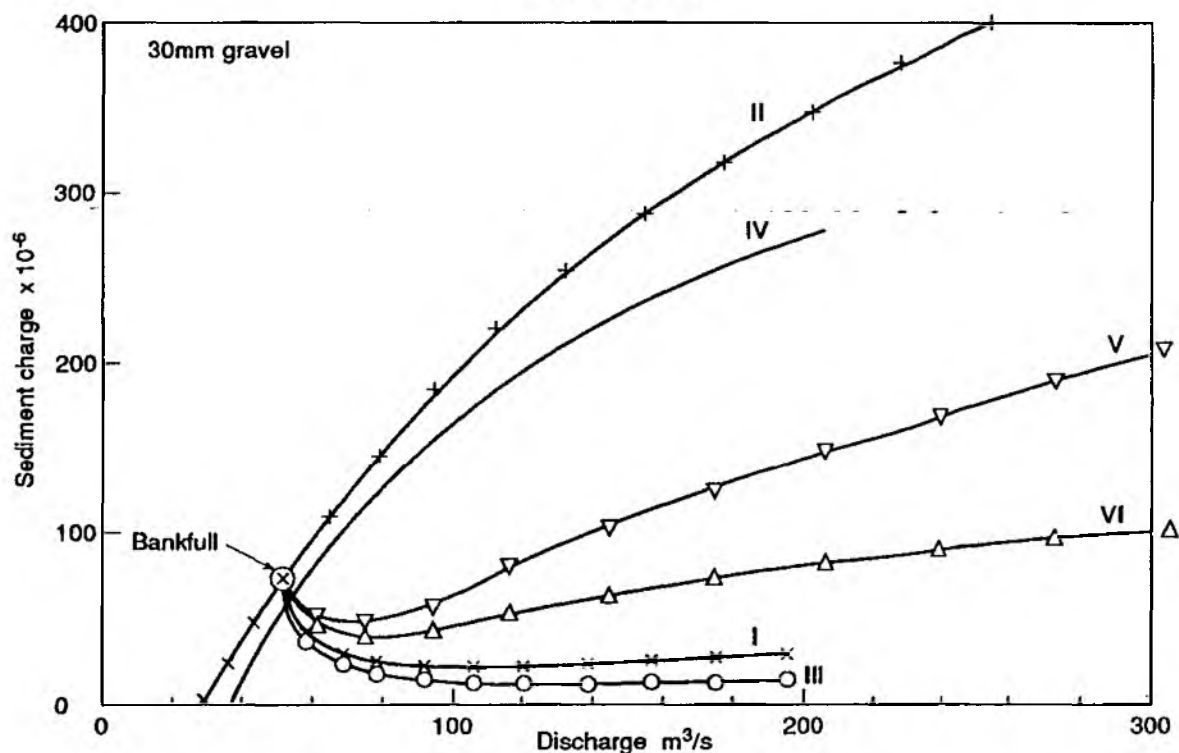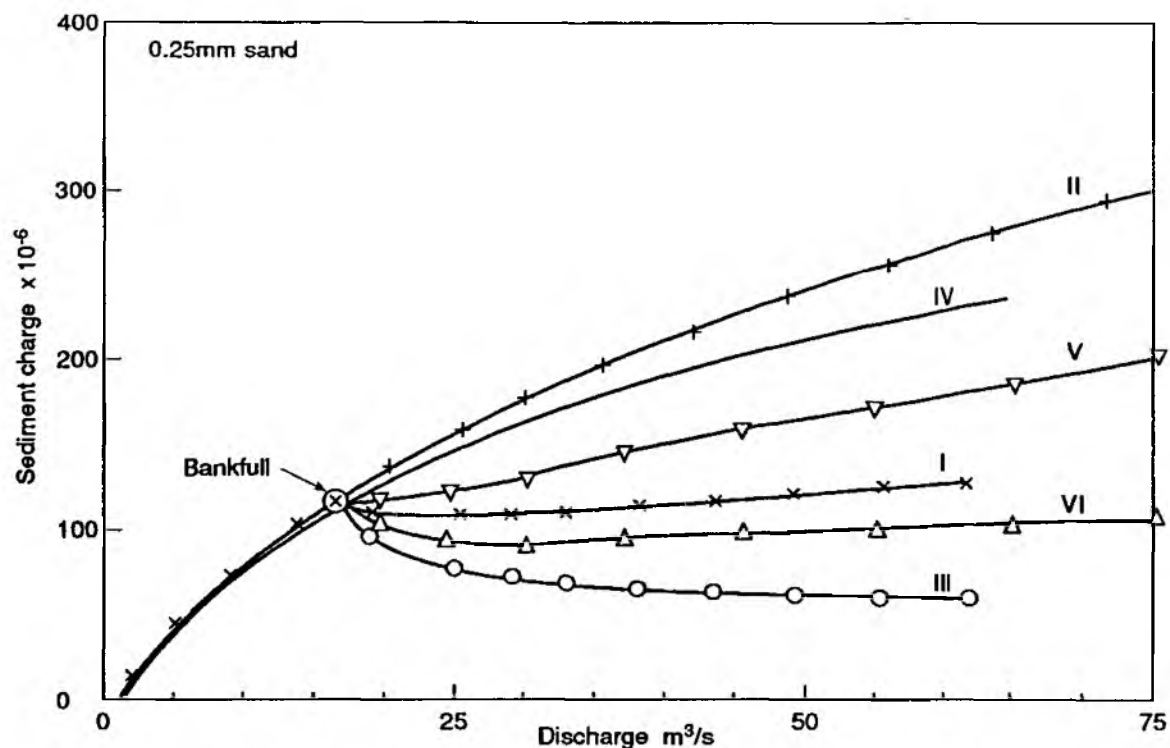
Key:

Graph I, X calculated for main channel allowing for interference from flood plain with n_F double that in main channel
Graph II, values of main channel X if interference is ignored
Graph III, sediment transport as calculated in I but expressed as ratio to total fluid.flux
Graph IV, X calculated for an equivalent trapezoidal section (equal conveyance at depth 3m)
Graph V, as I but with flood plain roughness same as main channel
Graph VI, sediment transport as calculated in V but expressed as ratio to total fluid flux

JBW/58/10-91/3D

Fig 9.3   Sediment charge - X, versus total discharge: upper diagram for 0.25mm sand, lower diagram for 30mm gravel

10. CONCLUDING REMARKS

10.1 <u>Summary of hydraulic design formulae for the conveyance of straight compound channels.</u>

10.1.1 As a result of the analysis of the new information from the large scale flood channel facility at Wallingford, as described in Chapter 3, a set of equations was derived for assessing the stage/discharge relationship for compound channels, or in other words the conveyance of their cross-section. The basic method is a development of the common approach dividing the cross-section into zones by vertical interfaces at the channel bank line. The basic discharges in the main channel and on the flood plains are first calculated separately from an appropriate conventional friction formula and roughness coefficients consistent with the character of the boundaries, excluding the vertical division planes from the wetted perimeters. The sum of these basic discharges have then to be adjusted to allow for the effects of the interaction between the zones, which has a significant effect on the channel conveyance. Several alternative methods of adjustment were considered within the broad framework provided by dimensional analysis, and they were progressively developed to be able to cope with the full range of conditions tested. Because of the complexity of the flow structure involving different regions of behaviour, no single formula could cover all conditions. Moreover, the form of equation and the parameters it depends on were found to differ from one region to the next, and so a logical method was established for determining which flow region applies at any particular flow depth. The equations derived are basically simple in form, with linear variation with the governing parameters, but it is expected that application in practice will utilise a computer program that incorporates the logic for determining which region of flow applies.

10.1.2 Being empirical functions based on data from channels with a main channel bed width/depth ratio of ten, it was necessary to confirm the general application of these equations by reference to data from other sources. Although the predictive equations turned out to be robust in the sense of being transferable in the main to most cross-sections and types and combinations of roughness, as explained in Chapter 5, the equations for Region 1 flow – that covering the lower range of depths – required revision for general application. This possibility had been envisaged in the

dimensional analysis of Appendix 1: the question hinged on whether or not the main channel was wide in relation to the zone of interaction from the flood plains. The wide channel assumption proved not to be valid for width/depth ratios below, say, twenty but a relatively simple modification was found adequate to cover the range of width/depth ratios for which research data was available, and those of practical interest. This involved introducing an aspect ratio factor, ARF, proportional to the main channel width/depth ratio. The resulting set of design equations for straight compound channels is as follows:

10.1.3 **REGION 1:** This is the region of relatively shallow depths where interference effects increase progressively with depth. The formula for this region is based on Q_{*2}, the discharge deficit normalised by the product $(V_C - V_F)Hh$ (see Appendix 1 for nomenclature), with adjustment for aspect ratio. The discharge deficit is the deduction required from the basic calculation, i.e. the sum of the basic flows in the flood plains and main channel, to obtain the 'true' discharge. This is calculated as the sum of the separate deficits for flood plains and main channel. The flood plain deficit proved to be the minor part and is negative, i.e. an addition to flood plain flow. It depends linearly on the depth ratio, H_*, but to cover the case with roughened flood plains is progressively reduced by the factor f_C/f_F as the flood plain friction increased. The major part, the main channel deficit, depends linearly on both the width ratio (width over flood plains divided by top width of main channel) and relative depth, the relative depth multiplier also depending (though not very strongly) on friction factor ratio and channel side slope. Thus for region 1:

$$Q_{*2F} = -1.0 \, H_* \, f_C/f_F \qquad\qquad \dots 10.1$$

$$Q_{*2C} = -1.240 + 0.395 \, B/w_C + G \, H_* \qquad\qquad \dots 10.2$$

(Q_{*2C} is never permitted to be negative, and perhaps should not be less than 0.5, to provide some minimum interaction effect: if this limit applies then also $Q_{*2F} = 0$: see para 5.5.10)

For $s_C \geq 1.0$:

$$G = 10.42 + 0.17 \, f_F/f_C \qquad\qquad \dots 10.3$$

For $s_C < 1.0$:

$$G = 10.42 + 0.17 \, s_C f_F / f_C + 0.34 \, (1-s_C) \qquad \ldots \, 10.4$$

10.1.4   **REGION 2.** This is the zone of greater depth where the
interference effect reduces again. The most appropriate form of design
function for this region relates the requisite discharge adjustment factor
to the channel coherence, which is an expression for the degree of
similarity of hydraulic conditions within the main channel and on the flood
plains. Channel coherence itself is dependent on the section geometry and
roughnesses involved and is defined and explained in paras 3.3.4 to 3.3.6,
and by equations 3.1, 3.2 and 3.3. It was found that the correction factor
to allow for interference effects is rather more than the calculated value
of coherence at that depth: it is nearer to the coherence value at a
somewhat greater depth, in other words requiring a shift in relative depth.
The basic discharge calculation has thus to be factored as follows in region
2:

DISADF (H_*, channel geometry and roughness)

$\qquad$ = COH((H_*+shift), channel geometry and roughness) $\qquad \ldots \, 10.5$

where for $s_C \geq 1.0$,

shift = 0.05 + 0.05 N_F $\qquad\qquad\qquad\qquad\qquad\qquad\qquad$ ... 10.6

for $s_C < 1.0$,

shift = -0.01 + 0.05 N_F + 0.06 s_C $\qquad\qquad\qquad\qquad\qquad$ ... 10.7

In the above N_F is the number of flood plains. The test conditions in the
FCF did not provide any Region 2 results with different roughnesses on flood
plain and in main channel - the FCF rough flood plain results remained in
Region 1 at all depths - but data from other sources has provided reasonable
confirmation of this approach for more modest differences of roughnesses.

10.1.5   **REGION 3.** This is a relatively narrow transitional region of
flow, for which alternative approaches were considered, a simple constant
discharge adustment factor for the zone or an equation giving DISADF as a

50

function of COH_3. Further data analysis showed that the latter was a somewhat more accurate representataion of the FCF data and so for Region 3 the following function is recommended:

$$DISADF = 1.567 - 0.667 \, COH \qquad \ldots 10.8$$

However, the alternative form:

$$DISADF = 0.95 \qquad \ldots 10.9$$

is almost as accurate overall.

10.1.6   **REGION 4.** This is the region where the coherence of the cross-section is such that it may be treated as a single section when calculating overall flow, with perimeter weighting of friction factors. This does not, however, mean that the separate zonal flows calculated provide accurate assessments of the flows in those zones: significant interaction effects remain, and the method for adjusting the main channel flow separately is given later. For total flow computation however, in region 4:

$$DISADF = COH \qquad \ldots 10.10$$

10.1.7   **ASPECT RATIO FACTOR.** The aspect ratio factor, ARF, is generally given by the main channel width/depth ratio/10, i.e. 2b/10h. However, if the aspect ratio exceeds 20, the channel should be assumed to be "wide", when ARF = 2.

10.1.8   **COMPUTATION PROCEDURE.** The actual computation of discharge depends on the choice of basic friction formula and associated coefficient for the conditions under review, as well as on the cross-section geometry and hydraulic gradient. Nothing in the derivation of the set of predictive equations limits that choice of friction formula: the engineer is free to choose Manning, Colebrook-White or whatever is most appropriate for the particular situation. The cross-section geometry provides the values of area, wetted perimeter (excluding the vertical division plane) and hence hydraulic mean depths for the main channel and flood plain zones. The friction formula then provides "basic" values of Q_{FB}, Q_{CB} and hence Q_{TB}.

51

The calculation of the various parameters to permit the use of equations based on a classical compound channel form was explained in section 7.1. The best estimate for flow if in region 1 is then obtained from:

$$Q_{R1} = Q_{TB} - (Q_{*2C} + N_F Q_{*2F})(V_C - V_F) Hh*ARF \qquad \ldots 10.11$$

If flow is in regions 2, 3 or 4, then the best estimate is obtained from:

$$Q_{R2, 3 \text{ or } 4} = DISADF_{R2, 3 \text{ or } 4} Q_{TB} \qquad \ldots 10.12$$

10.1.9   CHOICE OF REGION. The logic behind the selection of the appropriate predictive equation is dependent upon the calculation of discharge for all regions in turn, referred to as Q_{R1}, Q_{R2}, Q_{R3} and Q_{R4} respectively. The choice of the appropriate region and hence appropriate total discharge proceeds as follows:

Region 1 or 2?

If $Q_{R1} \geq Q_{R2}$ then $Q = Q_{R1}$ $\qquad \ldots 10.13$

Region 2 or 3?

If $Q_{R1} < Q_{R2}$ and $Q_{R2} \leq Q_{R3}$ then $Q = Q_{R2}$ $\qquad \ldots 10.14$

Region 3 or 4?

If $Q_{R1} < Q_{R2}$ and $Q_{R3} < Q_{R2}$ then $Q = Q_{R3}$ unless $Q_{R4} > Q_{R3}$ when $Q = Q_{R4}$
$\qquad \ldots 10.15$

10.1.10   The calculation of Q_{R1} etc utilises the equations summarised above, equs 1.1 to 1.12, together with the respective definitions of the dimensionless groups used, namely Q_{*2F}, Q_{*2C} and DISADF. The logic route given in the previous paragraph then selects the appropriate value. There is no transition between them, in accordance with the individual test results: there was little if any evidence of a curved transition between the regional equations.

10.1.11   TOLERANCES. The performance of this set of predictive
equations was checked by reference back to the original Wallingford
experimental data, and the percentage discrepancies between the individual
results and the predicted discharges for the observed depths, geometries etc
were assessed. These discrepancies were subjected to statistical analysis,
to obtain mean errors and the standard error of estimate. The former
statistic indicates the overall goodness of fit, and the latter the
variability. This variability can have two components: any imperfection in
the trend of the predictive equations and also the inevitable experimental
scatter due to random errors of measurement. With main channel and flood
plains of equal roughness, the mean errors for the various groups of tests
were all found to be under a third of a percent; and variability under half
a percent (standard error of estimate: some two-thirds will lie within this
with normal distribution of errors). The former shows the excellence of the
set of predictive equations in fitting the experimental trends; the latter
could hardly be bettered in terms of consistency of laboratory measurement.
The tests with roughened flood plains were not represented quite so well:
although the mean error of 0.07% indicates good agreement on average, the
standard error of 1.5% indicated greater variability in the predictions.
The complete data set was fitted almost exactly on average by these
predictive methods: mean error -0.001%. The variability of 0.8% was very
satisfactory, bearing in mind that perhaps 0.5% arose from the experimental
observations themselves, and that the one set of equations was applied to
smooth and rough conditions, to asymmetric as well as symmetric cases, to a
range of flood plain widths and channel bank slopes, over a range of flow
depths covering four different regions of flow.

10.1.12   The purpose of the analyses of data from other sources covered in
Chapter 5 was to validate - and to adjust and calibrate further as
necessary - the method based on the FCF results by comparing its
predictions with a wider range of experimental data, covering many more
geometries and roughness combinations. The only adjustment found necessary
was the inclusion of the parameter ARF in the formula for Region 1:
otherwise the formulae transferred well and were able to explain several
unsuspected differences in trends of behaviour. However, many of these
other results were obtained at small scale, when measurement problems,
especially the setting of uniform flow and measurement of gradient, give
higher tolerances than were obtainable in the large FCF at Wallingford.

Consequently the degree of agreement between prediction and observation was variable and in nearly all cases not as good as for the main data base. Some of this increased discrepancy was undoubtedly due to wider experimental tolerances, but some may have arisen because of inaccuracy in transferring the set of empirical equations to geometries and roughnesses well outside the range covered by the original derivation. It is therefore difficult to specify tolerances on the formulae themselves. The probable error in predicting discharge at 95% confidence level due to deficiency in the prediction method could be as low as 2%, but for most circumstances is almost certainly below 5%. To this must be added the tolerances in the basic friction formula and the knowledge of the roughness of the channel boundaries.

10.1.13   CALCULATION OF MAIN CHANNEL CONDITIONS. For some purposes it is not sufficient to calculate the stage/discharge curve: separate assessments of discharge in the main channel and flood plain are required, duly corrected for interaction effects. One such example is in the calculation of bed material load in the river itself. The method of obtaining the adjusted value of the main channel and flood plain flows in Region 1 will be evident from the definitions of Q_{*C} and Q_{*F}. Equations 10.1 to 10.4 yield those values, and then:

$$Q_{CR1} = Q_{CB} - Q_{*2C}*(V_C-V_F)Hh*ARF \qquad \ldots 10.16$$

$$Q_{FR1} = Q_{FB} - Q_{*2F}*(V_C-V_F)Hh*ARF \qquad \ldots 10.17$$

Other parameters such as the mean velocities in those zones can then be calculated.

10.1.14   Extending this separate zone adjustment to the higher regions of flow has not been so well established, because of lack of data. However, this may be achieved to engineering accuracy by the method indicated in paragraph 3.5.10. As the calculations proceed from shallow depths through Region 1, the value of $DISADF_C$ may be calculated from Q_{CR1}/Q_{CB}, depth by depth. The logic for choosing the regions (based on total flow) will in due course indicate a change to Region 2, but the value of the main channel discharge adjustment factor for region 1 is then taken to apply at all higher flows. This is simply achieved by retaining the value of $DISADF_C$

calculated at the limit of region 1 at all higher stages, so that in Regions 2, 3 and 4:

$$Q_{CR2,3,4} = Q_{CB} * DISADF_C \text{ at R1 limit} \qquad \text{... 10.18}$$

10.2   The advantages of compound channels.

10.2.1   The environmental and ecological advantages of two-stage channels stem partly from their more natural appearance, but also because berms or flood plains provide useful amenities. Their use has, of course, to be compatable with inundation from time to time. The most general use of flood plains is for agriculture, especially where they are a natural feature of the landscape, but they may also form parks or playing fields, and even relatively narrow berms alongside urban drainage channels can be developed as linear parks. There are, however, precautions to be followed, such as making good forecasts of frequency and duration of inundation, and the elevation of the normal water table which will have an important bearing on the vegetation growth, and hence the cost of maintenance and the consequent hydraulic resistance.

10.2.2   A case is described by Sellin, Giles and van Beeston (1990) of a small river improvement project which was designed with the ecology very much in mind. This proved less efficient than expected hydraulically and also in terms of the need for and access arrangements for maintenance. This is the River Roding in Essex, draining a catchment of 250 km to the project location. The scheme in reality forms a three stage system. There is a curvilinear main channel with some straighter but skewed reaches, with berms out to a fairly regular retired bank line, all set below the general level of an extensive flood plain. Because the berms are not much higher than normal water level, they provide a wet habitat, which may be the delight of ecologists but because of the luxuriant growth of water-loving reeds and other plants, offers a very high resistance except just after cutting. The object of the scheme had been to provide a 70 year standard of protection to a neighbouring town through the provision of flood berms, but in practice this is not normally achievable, even with considerable maintenance effort. Cutting the growth on the berm increases the flood capacity at 1.35m depth on the berm by 50%. The actual capacity can be as low as 15 m³/s with uncut vegetation, trees, tussock development and debris,

but is typically 25 m³/s after a full season's growth, rising to to 40 m³/s after cutting, compared with a design standard of 50 m³/s. This example shows that the use of two-stage channels is not without its problems. What is ecologically highly beneficial in a river corridor has to be reconciled with the social requirement of limited flood frequency. This depends on hydraulic performance, which in turn depends on the normal use of the berms or flood plains and on the vegetation thereon.

10.2.3 The environmental implications of river engineering are covered in a report by Hey (1990). He also draws particular attention to the problems of a high water table relative to the berm elevation and to the impact of vegetation on flow capacity, whilst pointing the way through river corridor surveys and post-construction audit surveys to achieving the desired balance between what is environmentally desirable and what may be essential in meeting hydraulic objectives. This involves not only vegetation, of course, but also within channel features such as shoals and embayments which may attract fish and provide attractive habitats for much wild life and plant species. Brookes (1988) treats the environmental management of channelized rivers in detail, with many examples of good and bad practice. This contains a wealth of experience and expertise on all aspects of environmental assessment: habitat evaluation procedures, biotic indices, aesthetic evaluation, stream morphology, fish and fisheries, aquatic plants. Figure 10.1 illustrates improvements to river cross-sections to increase their conveyance whilst retaining desirable ecological features within a two-stage channel, though of course the river engineer has still to assess the likely roughness coefficients and meet the hydraulic objectives of the project.

10.2.4 The hydraulic advantage of a compound channel when drainage improvements are required is the increased flood capacity for a given increase in stage, arising from the flow over the berms or flood plains. This advantage may not always be as great as might have appeared from the traditional methods of calculation, because the interaction between the zones of different flow depth increases energy dissipation, as clearly demonstrated by research and now calculable with the methods recommended herein. Nevertheless, the advantage is very real in practice where the available flow depth is limited. Irrespective of any hydraulic advantage, a knowledge of two-stage channel behaviour is necessary because they occur

naturally: the cross-section of typical river channels is determined by the discharge which occurs for a combined period of the order of 2 days per year, so it is obvious that major floods will inundate their associated flood plains, so that the design condition is when they are indeed two-stage systems.

10.2.5 The provision of berms alongside artificial channels has also advantages in terms of access for maintenance. There is no need for such access to be above water level even during floods, as maintenance work is almost invariably carried out when the system is not near capacity. It therefore makes good sense to provide two-stage channels, even in circumstances where they may have little or no amenity value: they combine good access with increased hydraulic conveyance.

10.3 State of knowledge and need for further reseach

10.3.1 The detailed and extensive research programme carried out on the SERC-FCF at Wallingford has reaped the benefit of being the first major programme to combine large scale, a high standard of accuracy of measurement, attention to detail and collaboration between different groups with complementary interests. The large scale has permitted the use of a width/depth ratio more in line with the practical range of main channel aspect ratios, and in several respects has provided results quite different from those reported from small scale narrow faciliies that typified much of the earlier research. This research investment has been rewarded with a detailed knowledge of the flow in two-stage channels that was not previously available from any source, and this new data base confirms that a radically different approach is required to the hydraulic design and assessment of such systems. Previous methods were seriously in error.

10.3.2 The analysis of the research results and the application of those findings to related topics such as the extrapolation of stage/discharge functions and the transport of bed material shows that the consequences of the new knowledge are not confined to improved estimates of channel conveyance. They cut across established practice by providing new insights into channel morphology, the computational modelling of river systems, the hydraulic consequences of following environmentally desirable river management practices, etc. This report deals only with the results

relevant to straight channels aligned with, or only mildly skew to, their berms or flood plains, but subsequent aspects of the research programme have concerned meandering channels and will undoubtedly give rise to equally significant changes in the approach to the hydraulics of irregular channels when the analysis and interpretaion is completed.

10.3.3   Even with straight aligned channels, the research programme in the FCF has left some question marks; some gaps in the coverage and confirmation of ideas and concepts. The following items deserve further study at large scale when opportunity and funding levels permit:

-    Stage discharge data is required of comparable detail and accuracy for channels with differing aspoect ratios. The limitation of the FCF to a main channel width/depth ratio of 10 has made confirmation of the influence of this feature somewhat elusive.

-    Stage discharge data is also required with boundary roughness of various degrees on the flood plains. Any artificial roughness would require accurate and detailed calibration, of course, but without such research there remains a possibility that the influence of flood plain roughening in the form of surface piercing rods may not be the same as that of boundary-type roughening: the design equations using the ratio of the flood plain to main channel friction factors may leave scope for refinement for application to the more usual roughness condition.

-    The different regions of flow apparently include Region 3 as a transition between Regions 2 and 4, and this may be associated with an unstable re-organisation of secondary circulations. There is scope for using the existing detailed information on flow structure to seek a cause for this transition in the stage discharge function.

-    Turbulence methods will undoubtedly oust the empirical procedure recommended here in course of time, but their adoption requires better understanding of the role of different interactions between the main channel and flood plain, and any dependence of their relative importance on flow depth and cross-section geometry. A careful study of the formulation of the turbulence coefficent in the lateral distribution method is required, making full use of the data set now

58

available, with particular attention paid to accuracy of simulation of total flow and also the division of flow, and any variation with flow depth.

- The implications for sediment transport of the reduction in main channel discharge and velocity consequent upon interaction from the flood plains requires experimental study. Without experimental verification, the methods used to indicate the order of magnitude of the likely effect used in Chapter 9 are open to question, and in any event are unlikely to have taken adequately into account all the complexities of the flow structure.

10.3.4 Regarding the later phases of research on meandering channels, it is important that the results are reviewed within the context of simulating the fluid and momentum exchanges in computational models with two-dimensions on plan. Only thus can the work on meandering channels be extrapolated to irregular plan geometries in general: they clearly can not be handled as a simple extension of the methods developed here for straight channels. The new insights already gained on the flow structures in such systems with overbank flow, as illustrated in Chapter 8, provide a vital starting point for incorporating appropriate mechanisms into any model.
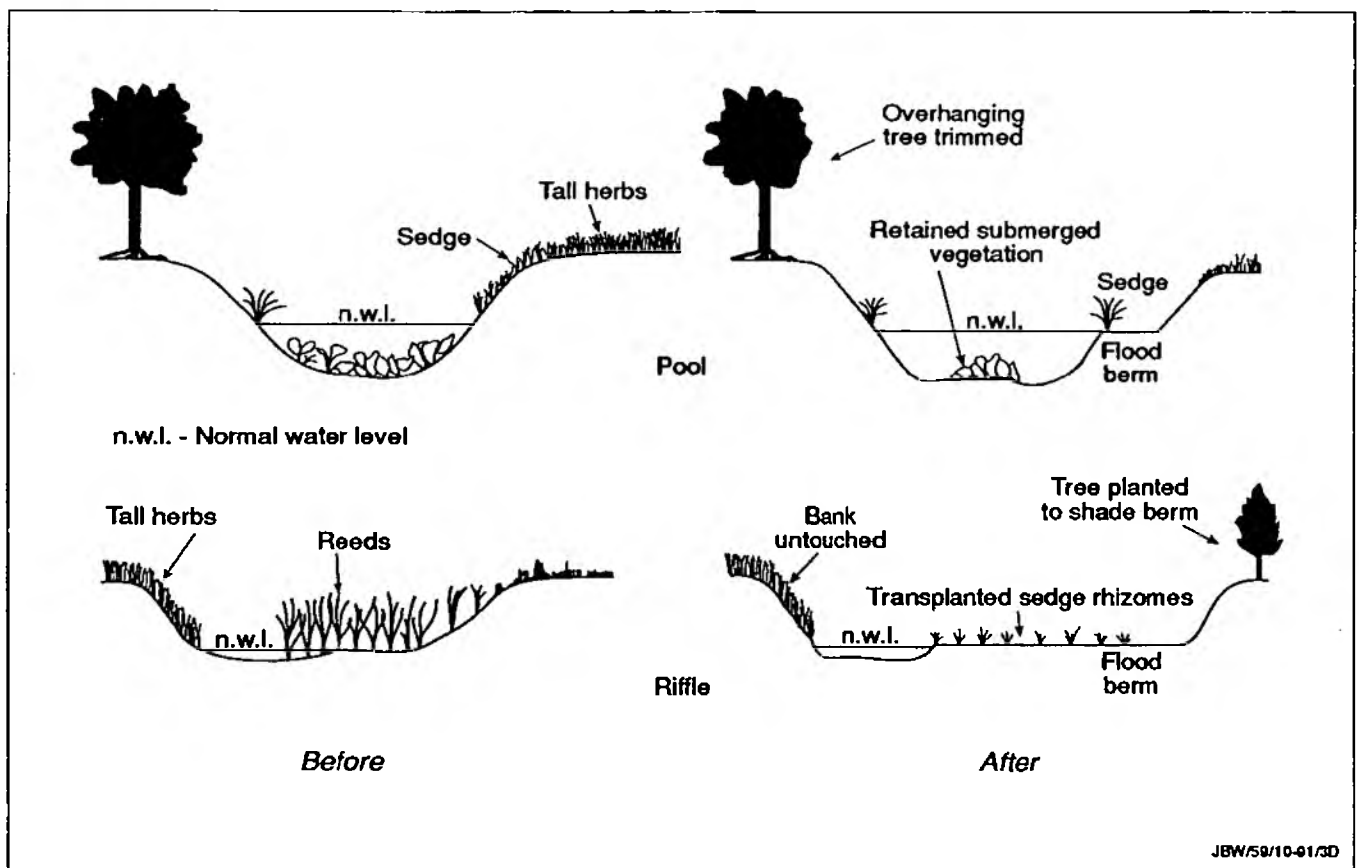
Fig 10.1 Ecologically attractive two-stage channel design proposed for River Ray in Oxfordshire (Brookes, 1988, after Hinge and Hollis)

11. ACKNOWLEDGEMENTS

12. REFERENCES

Ackers P, (1958), Resistance of fluids flowing in channels and pipes, Hydraulics Research Paper no 1, HMSO, London, 1958.

Ackers P, (1980) Use of sediment transport concepts in stable channel design, Int. Workshop on Alluvial River Problems, Roorkee, India, 1980.

Ackers P and White W R, (1973), Sediment transport: new approach and analysis, Proc American SCE, Nov 1973, vol 99, HY11, pp 2041 - 2060.

Allen J R L, (1985), Principles of physical sedimentatology, George Allen and Unwin, London, (1985), ISB 0-04-551096-2.

Asano, T, Hashimoto, H and Fujita, K, (1985), Characteristics of variation of Manning's roughness coefficient in a compound cross section. International Association for Hydraulic Research, Proc 21st Congress, Melbourne, Vol 6, August 1985, pp 30-34.

Baird J I and Ervine D A, (1984), Resistance to flow in channels with overbank flood plain flow, Proc 1st Int Conf on Channels and Channel Control Structures, Southampton, UK, p 4-137-150.

Bagnold R A, (1966), An approach to the sediment transport problem from general physics, US Geological Survey, Prof. paper 422-1, US Gov. Printing Office, Washington, 1966.

Blasius H, (1913), Das ahnlichkeitsgesetz bei reibungsvorgangen in flussigkeiten, V D I Forschungshaft, no 131.

Bray D I, (1982), Flow resistance in gravel bed rivers, In: R D Hey et al. (1982)

Bridge J S and Jarvis J, (1982), The dynamics of a river bend: a study in flow and sedimentary processes, Sedimentology, vol 29, 1982, 499-541.

Brookes A, (1988), Channelized rivers: perspectives for environmental management, John Wiley and Sons, Chichester, UK.

Chadwick A and Morfett J, (1986), Hydraulics in civil engineering, Allen and Unwin, London.

Chang H H, (1983), Energy expenditure in curved open channels, Proc ASCE, vol 109, J Hydraulic Engineering, no 7, July 1983, 1012-1022.

Chang H H, (1988), Fluvial processes in river engineering, John Wiley and Sons, 1988.

Clauser F H, (1954), Turbulent boundary layers in adverse pressure gradients, J Aeronuatical Sciences, Feb 1954.

Colebrook C F, (1939), Turbulent flow in pipes, with particular reference to the transition region between the smooth and rough pipe laws, Journal Instn. Civil Engineers, London, vol 11, p 133.

Cowan W L, (1956), Estimating hydraulic roughness coefficients, Agricultural Engineering, vol 37, no 7, July 1956, 473-475.

Cunge J A, (1969), On the subject of a flood propagation computation method (Muskingum method), J. Hydraulics Res., vol 7, no 2, 1969, 205-230

Einstein H A, (1950), The bed load for sediment transportation in open channel flow, Ser. Tech. Bull. US Dept Agriculture and Soil Conservation, 1026, 1950

Elsawy E M, McKee P M and McKeogh E J, (1983), Application of LDA techniques to velocity and turbulence measurements in open channels of compound section, Proc 20th Int Congress IAHR, vol 3, Moscow, p255-263.

Elliott S C A and Sellin R H J, (1990), SERC flood channel facility: skewed flow experiments, Journal of Hydraulics Research, Vol 28, 1990, no 2, p197-214

Engelund F and Hansen E, (1967), A monograph on sediment transport in alluvial streams, Teknisk Vorlag, Copenhagen, Sweden, 1967.

Ervine D A and Ellis J, (1987), Experimental and computational aspects of overbank flood plain flow, Trans. Royal Society of Edinburgh: Earth Sciences, vol 78, 1987, 315-325.

Ervine A and Jasem H K, (1991), unpublished PhD thesis and private communication.

Fread D L (1984), DAMBRK: the NWS dam-break flood forecasting model, Office of Hydrology, National Wether Service, National Oceanic and Atmospheric Admin., U S Dept. Commerce, Silver Spring, Md, USA.

Garbrecht J and Brunner G, (1991), Hydrologic channel-flow routing for compound sections, J Hydraulic Eng., American Soc. Civil Engrs, vol 117, 5, May 1991, 629-642.

Garde R J and Ranga Raju K G, (1977), Mechanics of sediment transportation and alluvial stream problems, Wiley Eastern Ltd, 1977.

Graf W H, (1971), Hydraulics of sediment transport, McGraw-Hill, 1971.

Herschy R W, ed. (1978), Hydrometry, John Wiley and Sons, Chichester, UK, 1978.

Henderson F M, (1966), Open channel flow, Macmillan Company, New York, 1966.

Hey R D, (1979), Flow resistance in gravel-bed rivers, ASCE, J Hyd. Div, vol 105, HY4, April 1979, 365-379.

Hey R D, (1990), Environmental river engineering, J. Inst. Water an Environmental Management, vol 4, no 4, Aug 1990, 335-340.

Hey R D, Bathurst J C and Thorne C R, (editors) (1982), Gravel bed rivers, fluvial processes, engineering and management, Wiley, New York, 1982.

Higginson N N J, Johnston H T and Myers W R C, (1990), Effect of scale distortion in a compound river channel model study, Proc. Int. Conf. on River Flood Hydraulics, Wallingford, Sept 1990, ed. W R White, John Wiley and Sons, 391-403.

Hogg I G G, Guganesharajah K, Gunn P D S and Ackers p (1988), The influence of river regime on the flood management of the Sukkur Barrage, Pakistan, Int Conf. on River Regime, ed White W R, Hydraulics Research, Wallingford, UK, May 1988.

Hollinrake P G, (1987, 1988, 1989), The structure of flow in open channels – a literature search, vols 1, 2 and 3, Reports SR 96, SR153 and SR209, Hydraulics Research, Wallingford, UK.

Hydraulics Research, (1988), Hydraulic performance of environmentally acceptable river engineering schemes, Report EX 1799, Hydraulics Research, Wallingford, UK.

Hydraulics Research, (1990a), Charts for the hydraulic design of pipes and channels, 6th edition, Hydraulics Research, Wallingford, UK, pub. Thomas Telford, London.

Hydraulics Research, (1990b), Tables for the hydraulic design of pipes, 5th edition, Hydraulics Research, Wallingford, UK, pub. Thomas Telford, London.

Hydraulics Research, Wallingford (1990c), Sediment transport: The Ackers and White theory revised, Report SR 237, HR Wallingford, Oxon, UK

Jaeger C (1956), Engineering fluid mechanics, Blackie and sons, London, 1956.

Jansen P Ph, van Bendegom L, van den Berg J, de Vries M and Zanen A, (1979), Principles of river engineering, Pitman, London, 1979.

Kiely G, (1991), unpublished thesis plus personal communication.

Keller R J and Rodi W, (1984), Prediction of two-dimensional flow characteristics in complex channel cross-section, Proc Hydrosoft 84 conf., Portorez, Yugoslavia, Elsevier, p 3-3-14.

Keller R J and Rodi W, (1988), Prediction of main channel/flood plain flows, J Hydraulic Research, vol 26, no 4, p 425-441.

Keulegan G H, (1938), Laws of turbulent flow in open channels, Journal of Research, Nat. Bureau of Standards, Washington D C, Res. Paper 1151, vol 21, no 6, pp 707-741.

Klaassen G J and Van der Zwaard J J, (1974), Roughness coefficients of vegetated flood plains, J Hydraulics Research, vol 12, 1974.

Knight D W and Demetriou J D, (1983), Flood plain and main channel interaction, Proc ASCE, J Hydraulic Eng, vol 109, no 8, Aug 1983, 1073-1092.

Knight D W, Demetriou J D and Hamed M E, (1983), Hydraulic analysis of channels with flood plains, Proc Int Conf on Hydrol Aspects of Floods, BHRA, Bedford, UK, p 129-144.

Knight D W, Demetriou J D and Hamed M E, (1984), Stage discharge relations for compound channels, Proc 1st Int Conf, Channels and Channel Control Structures, April 1984, ed Smith K V H, Springer Verlag, 1984, 4.21-4.36.

Knight D W and Hamed M E (1984), Boundary shear in symmetrical compound channels, Proc ASCE, J Hydreaulic Eng., vol 110, HY10, Oct. 1984, 1412-1430.

Knight D W and Sellin R H J, (1987), The SERC Flood Channel Facility, J Inst Water and Env. Management, London, vol 1, no 2, 1987, 198-204.

Knight D W and Shiono K, (1990), Turbulence measurements in a shear layer region of a compound channel, J Hydraulic Research, vol 28, no 2, 1990, IAHR, Delft, 175-196

Knight D W, Shiono K and Pirt J, (1989), Prediction of depth mean velocity and discharge in natural rivers with overbank flow, Conf. on Hydraulic and Environmental Modelling of Coastal, Estuarine and River Waters, ed. Falconer, Goodwin and Matthew, Gower Tecnical Press, 1989, 419-428.

Knight D W, Samuels P G and Shiono K, (1990), River flow simulation: research and developments, J. Inst. Water and Environmental Management, vol 4, no 2, April, 1990, 163-175

Knight D W and Yuen K W H (1990), Critical flow in a two stage channel, Int. Conf. on River Flood Hydraulics, Sept 1990. Hydraulics Research, Wallingford, Wiley and Sons, 1990.

Kouwen N, Li R N and Simons D B, (1981), Flow resitance in vegetated waterways, Trans Amer. Soc Agric. Engrs, vol 24,(3), 684-690, 698.

Larsen T, Frier J-O and Vestergaard K (1990), Discharge/stage relations in vegetated Danish streams, Int. Conf. on River Flood Hydraulics, Wallingford, Sept 1990, John Wiley and Sons, 187-196.

Leopold L B and Wolman M G, (1957), River channel patterns: braided meandering and straight, USGS Prof. Paper 282-B, 1957.

Limerinos J T, (1970), Determination of the Manning coefficient from measured bed roughness in natural channels, U S Geological Survey Water Supply Paper 1898-B, 1970.

Manning R, (1891), On the flow of water in open channels and pipes, Proc Inst Civil Engrs, Ireland, 1891 vol 20, p161, 1895 vol 24, p 179.

Morris H M, (1959), Design methods for flow in rough conduits, Proc American Soc. Civil Engineers, vol 85, HY7, July 1959, p 43.

Myers W R C, (1978), Physical modelling of a compound river channel, Proc. Int. Conf. on River Flood Hydraulics, Wallingford, Sept 1990, ed. W R White, John Wiley and Sons, 381-390.

Myers W R C, (1978), Momentum transfer in a compound channel, J Hydraulic Research, vol 16, IAHR Delft

Myers W R C, (1984), Frictional Resistance in channels with flood plains; Channels and channel control structures, 1st Int Conf, Southampton, England, 1984, ed K V H Smith, pub Springer-Verlag, 1984, p 4.73-4.87.

Myers W R C, (1985), Flow resistance in smooth compound channels, experimental data, University of Ulster, March 1985.

Myers W R C and Brennan E K, (1990), Flow resistance in compound channels, J Hydraulic Research, vol 28, no 2, 1990, IAHR, Delft, 141-156.

Nalluri C and Judy N D, (1985), Interaction between main channel and flood plain flows, Proc 21st Congress IAHR, Melbourne, Australia, p 377-382.

Nikuradse J, (1933), Stronungsgesetze in rauhen rohren, VDI Forschungsheft, 1933, p 361.

Nikuradse J, (1932), Gesetzmabigkeit der turbulenten stromung in glatten rohhren, VDI Forschungsheft, 1932, p 356.

Patel V C, (1965), Calibration of the Preston tube and limitations on its use in pressure gradients, J Fluid Mechanics, vol 23, Part 1, 1965, 185-195

Petryk S and Grant E U, (1978), Critical flow in compound channels, ASCE, J Hyd Div, vol 104, HY5, 1978, 583-594

Powell K E C, (1978), Weed growth – a factor in channel roughness, Hydrometry, ed Herschy R W, John Wiley and Sons, 1978, 327-352.

Prandtl 1, (1933), Neuere Ergebnisse der Turbulenzforschung, ZVDI vol 77, p 105.

Prinos P and Townsend R D, (1983), Estimating discharge in compound open chanels, Canadian Soc for Civil Engineering, 6th Canadian Hydrotechnical Conference, Ottawa, Ontario, June 1983, p129-146.

Prinos P and Townsend R D, (1984), Comparison of methods for predicting discharge in compound open channels, Advances in Water Resources, 1984, vol 7, Dec, CML Publications, 180-187.

Radojkovic M, (1976), Mathematical modelling of rivers with flood plains, 3rd annual symp. Waterways, Harbours and Coastal div, ASCE, vol 1, rivers.

Radojkovic M and Djordjevic S, (1985), Proc 21st Congress IAHR, Melbourne, Australia, vol 3, p 368-371.

Rajaratnam N and Ahmadi R M, (1981), Hydraulics of channels with flood plains, J Hyd Research, vol 19, 1, 1981.

Ramsbottom D M, (1989), Flood discharge assessment – interim report, Hydraulics Research, Wallingford, SR 195, March 1989.

van Rijn L C, (1984) Sediment transport: part I: bed load transport; part II: suspended load transport; part III: bed forms and alluvial roughness, Proc ASCE, vol 110, HY 10, Oct 84, p 1431; HY11, Nov 84, 1613-1641; HY12, Dec 84, 1733-1754.

Rouse H, (1937), Modern conceptions of mechanics of fluid turbulence, Trans Amer. Soc. Civ. Engrs, vol 102, 1937.

Rouse H, ed (1950), Engineering Hydraulics, John Wiley and Sons, New York, 1950, reprinted 1961 etc.

Samuels P, (1989), The hydraulics of two-stage channels - review of current knowledge, Inst Water and Environmental Management, River Eng's Conf., University of Loughborough, July, 1989.

Samuels P, (1988), Lateral shear layers in compound channels, Fluvial Hydraulics 88 conf, VITUKI, Budapest, Hungary.

Sargent R J, Variation of Manning's n roughness coefficient with flow in open river channels, J. Inst Water Engineers, vol 33, no 3, 1979, 290-294

Sellin R H J, Giles A and van Beeston D P, (1990), Post-implementation appraisal of a two-stage channel in the River Roding, Essex, J. Inst Water and Environmental Mnagement, vol 4, no 2, April 1990, 119-130

Shields A,(1936), Anwendung der Ahnlichkeitsmechanik und Turbulenz-forschung auf die Geschiebebewegung, Mittiel., PVWES, Berlin, no 26, 1936.

Shiono K and Knight D W, (1988), Two dimensional analytical solution for a compound channel, Proc 3rd Int. Symp. on Refined Flow Modelling and Turbulence Measurement, Tokyo, Japan, July 1988, 503-510.

Shiono K and Knight D W, (1990a), Mathematical models of flow in two or multi-stage straight channels, Int. Conf. on River Flood Hydraulics, Sept. 1990, Wallingford, ed White W R, John Wiley and Sons, Chichester, 1990, 229-238.

Shiono K and Knight D W, (1991), Turbulent open channel flows with variable depth across the channel - a general model and new data, J Fluid Mechanics, vol 222, September 1991, 617-646.

Strickler A, (1924), Beitrage zur frage der geschwindig-keitsformal und der rauhigkeitsahlen fur strome, kanale und geschlossene leitungen, Eidg. Wasserwirtshaftsamt Bern, Milleilung, 1923; Schweitz. Bauztg, 1924, vol 83, 23.

Thorne C R, Bathurst J C and Hey R D, (eds), (1987), Sediment transport in gravel bed rivers, John Wiley and Sons, 1987.

Toebes G H and Sooky A A, (1967), Hydraulics of meandering rivers with flood plains, Proc ASCE, vol 93, J Waterways and Harbours, no 2, May 1967, 213-236.

US WES, (1956), Hydraulic capacity of meandering channels in straight floodways, Tech. Memo. 2.249, Waterways Experiment Station, Vicksburg, Mississippi, March 1956.

Ven te Chow, (1959), Open channel hydraulics, McGraw-Hill, New York.

Wark J B, Samuels P G and Ervine D A, (1990), A practical method of estimating velocity and discharge in compound channels, Int Conf on River Flood Hydraulics, September 1990, HR, Wallingford, Pub J Wiley and Sons, 163-172.

Willetts B B, (1991), The hydraulics of meandering channels, Seminar on River and Flood Plain Management, 22 March, 1991, Scottish Hydraulics Study Group, Glasgow.

White W R, Paris E and Bettess R (1980), The frictional characteristics of alluvial streams: a new approach, Proc. Inst. Civil Engrs, vol 69, (2), 737-750.

White W R, Bettess R and Wang Shiqiang, (1987), Frictional characteristics of alluvial streams in the lower and upper regimes, Proc. Inst. Civil Engrs, vol 83, (2), 685-700.

White W R, Milli H and Crabbe A D, (1975), Sediment transport theories: a review, Proc Inst Civ Engrs, Part 2, June 1975, vol 59, 265-292.

Wormleaton P R, (1988), Determination of discharge in in compound channels using the dynamic equation for for lateral velocity distribution, Proc IAHR Conf. on Fluvial Hydraulics, Vituki, Budapest.

Wormleaton P R, Allen J and Hadjipanos P, (1982), Discharge assessment in compound channel flow, Proc ASCE, vol 108, J Hy Div, p 975-994

Wormleaton P R and Merrett, (1990), An improved method of calculation for steady uniform flow in prismatic main channel/flood plain sections, J Hydraulic Research, vol 28, no 2, 1990, IAHR, Delft, 157-174.

Yalin M S, (1977), Mechanics of sediment transport, 2nd ed., Pergamon Press, 1977.

Yang C T, (1972) Unit stream power and sediment transport, Proc ASCE, vol 98, HY10, Oct 1972, 1805-1826.

Yen B C and Yen C L, (1983), Flood flow over meandering channels, Rivers Meandering Conf, 1983, 554-561.

Zheleznyakov G V, (1985), Problem of the interaction of the main channel and flood plain flows, Proc 21st Congress IAHR, Melbourne, Australia, vol 3, p373 - 376.

The following form a limited circulation unpublished series "SERC flood channel research, Water Authority funded project for the development of a design manual, Technical Report Series, Consultant P Ackers".

1,   Resistance functions for the Wallingford facility, August 1989.

2,   Resistance functions for the Wallingford facility, rod roughness, Nov 1989.

3,   The hydraulic resistance of compound channels, review and proposed method of approach, Nov 1989.

4,   Review and analysis of research at Wallingford, in the context of empirical design methods, October 1990.

5,   Review and analysis of other sources of data in the context of empirical design equations based on WFCF data, March 1991.

6,   Skew channels, February 1991.

7,   Turbulence methods, April 1991.

8,   Irregular plan form, April 1991.

9,   Sediment transport in compound channels, April 1991.

13. NOMENCLATURE

NOTE: The nomenclature is not unique. To follow established convention and to avoid an excess of subscripts and Greek symbols, some characters are used in more than one sense. The context in which they appear will make clear which is intended.

A	Cross sectional area
A, B	Parameters in the logarithmic smooth-turbulent velocity distribution
A, B	Empirical coefficients
A_{gr}, C_{gr}, F_{gr}, G_{gr}, m_{gr}, n_{gr}	Parameters in sediment transport function
ARF	An adjustment factor in the Region 1 functions to allow for the effect of main channel width/deth ratio (aspect ratio)
B	Half total width of channel plus berm or berms (flood plains), at the elevation of the berms (flood plains). If the berms slope and are partially inudated, B is taken as half the water surface width
b'	Mean width, defined as area/flow depth (normally with subscript for main channel or flood plain)
bw	Bed width (normally with subscript for channel, flood plain)
b_C	Half bed width of main channel
b_F	Bed width of one of a pair of berms or flood plains
B, b	Parameters in a generalised form of the exponential smooth-turbulent Blasius equation
C, D	Parameters in a generalised form of the logarithmic smooth-turbulent law
C, C_o	Concentration of suspended solids, reference value at prescribed elevation, z_o
C_D	Drag coefficient of rods
COH	Channel coherence; subscript indicates method of calculation
D	Pipe diameter; sediment diameter
D_{gr}	A dimensionless indicator of grain size
d	Flow depth; diameter of rods forming roughness
DISADF	Factor by which zonal calculation has to be multipied to allow for interference
DISDEF	Difference between zonal calculation of discharge and actual flow
DISDEFBF	Ratio of DISDEF to bank full discharge
e	Base of Naperian logarithms, denoted by ln
F_T ,C,F	Adjustment factors

72

F_{ROD}	form drag of rods per unit channel length
f	Friction factor, $8gRS/V^2$
f_S	Friction factor arising from smooth channel boundaries
f_{TOT}	Total of rod roughness and smooth perimeter resistance, expressed as friction factor
G	A parameter in predictive equation for region 1
g	Gravitational acceleration
H	Total flow depth; depth of flow in main channel
H_F	Flow depth on flood plain, $H - h$
h	Depth of main channel below berm level
H_*	Ratio of flow depths on flood plain and in main channel
K	Von Karman turbulence constant
K_V	Conveyance as conventionally defined, e.g. in Ven Te Chow
K_D	Conveyance, $Q/\sqrt{(8gS)} = A/\sqrt{(A/fP)}$
k_S	Linear measure of roughness, after Nikuradse and Colebrook White
$\ln$	Logarithm to base e
$\log$	Logarithm to base 10
N	Number of roughening rods per unit channel length
n	Manning's roughness coefficient, from $1/n = V/(R^{2/3}\sqrt{S})$
n	Number of rods in a transverse row
N_F	Number of flood plains
Q	Discharge
Q_{*1}	Discharge deficit (DISDEF) normalised by $(V_C - V_F)(H-h)h$
Q_{*2}	Discharge deficit (DISDEF) normalised by $(V_C - V_F)Hh$
q	Discharge intensity, i.e. discharge per unit width
q_S	Sediment transport rate as submerged weight per unit time per unit width
R	Hydraulic radius (or h.m.d.), cross section area/wetted perimeter
Re	Reynolds number, $4VR/\nu$
Re_*	Grain Reynolds number in sediment transport, v_*D/ν
Re_*	Roughness Reynolds number, $u_* kS/\nu$
s	Channel/flood plain side slope, horizontal/vertical
s	Relative specific weight/mass of sediment to fluid
s_{BF}	Slope of flood plain towards main channel
S	Hydraulic gradient of channel
SF_I	Shear force at interface
tw_c	Top width of channel

U	Mean velocity over the flow depth
u	Local mean stream velocity
u_*, v_*	Friction velocity, $\sqrt{(gRS)}$
V	Average flow velocity through cross-section, or with suscript through one zone of cross-section
W	Water surface width
w	Fall velocity of particles of sediment
w_C	Half width of main channel at elevation of bank top
Y	A non-dimensional form for bed shear stress in sediment transport
y	Local flow depth at point in cross-section
Z	Ratio of flow depth to sediment diameter
Z_*	Ratio of local flow depth to rod diameter, z/d
z	Distance from solid boundary; local flow depth
α	Velocity distribution coefficient
β	Blockage coefficient arising from rod roughness
δ	A correction term
Φ	Radojkovic interaction index; a function of ....
ρ	Density of fluid
τ	Shear stress
μ	Fluid viscosity
ν	Kinematic viscosity of fluid, μ/ρ
Ω	turbulence parameter for solids suspension

Subscripts:

AV	Average
BF	Bank full
B,basic	Basic values before allowing for interaction
C	Main channel
CALC	Calculated value
F	Flood plain
i	Interval: one of a series of values
I	Interface
MEAS	Measured value
R1, R2, R3, R4	Regions of flow behaviour
T	Total i.e. main channel plus flood plains
*	Ratio between flood plain and main channel values (except where otherwise defined)

Appendices

APPENDIX 1

DIMENSIONAL ANALYSIS APPLIED TO COMPOUND CHANNELS

1.   The *independent variables* that determine steady uniform
friction-controlled flow in a prismatic compound trapezoidal channel are the
fluid properties, the roughness of the surfaces, gravity, channel slope and
cross-section geometry:

ρ - mass density of fluid

μ - fluid viscosity

k_{SC} - roughness of main channel perimeter

k_{SF} - roughness of flood plain

g - acceleration due to gravity

S - slope of channel

b_C - half bed width of deep channel

b_F - bed width of each flood plain

s_C - side slopes of deep channel, 1 vertical to sc horizontal

s_F - side slopes of flood plain edges

h - depth of main channel

H - total flow depth, measured over deep channel

The dependent variables include:

Q_T - total discharge in the compound section

Q_C - component discharge in deep channel

Q_F - component discharge in the flood plains

V - average velocity over whole cross section

$V_C;V_F$ - component average velocities etc.

Any *dependent variable* is a function of the independent variables
listed:

$$\text{DVAR} = \Phi \ [\ \rho, \ \mu, \ k_{SC}, \ k_{SC}, \ g, \ S, \ b_C, \ b_F, \ s_C, \ s_F, \ h, \ H \ ] \qquad \ldots A1.1$$

2.   These 12 independent variables will yield 9 dimensionless groups,
which could be derived in many different ways. To proceed, it is desirable
to introduce similarity concepts, such as those familiar when dealing with
friction controlled flow in simple cross-sections. Taking total discharge

as the dependent of immediate practical concern, and also linking S with g because it is the weight component down the slope that has physical significance, and considering the system as one channel:

3. *Single channel method*

$$\frac{Q^2 P}{8gS^3} = \Phi \left\{ \frac{Q/P}{\mu/\rho}; \frac{H}{H-h}; \frac{Q}{\sqrt{(gA/W)}}; \frac{k_{SC}}{H}; \frac{k_{SF}}{H-h}; \frac{b_C}{H}; \frac{b_F}{H-h}; s_C; s_F \right\} \qquad \ldots A1.2$$

where

A = total cross-section area = $\Phi_A [b_C; b_F; s_C; s_F; h; H]$
P = total wetted perimeter = $\Phi_P [$ ditto $]$
W = total water surface width = $\Phi_W [$ ditto $]$
ν = kinematic viscosity, μ/ρ

These dimensionless groups are recognisable as:

$\dfrac{Q^2 P}{8gSA^3}$ = 1/f where f is the friction factor treating the whole section as one

$\dfrac{Q/P}{\nu}$ = Reynolds number of whole section

$\dfrac{Q}{\sqrt{(gA/W)}}$ = Froude number for whole section

$H/(H-h)$ = ratio of channel flow depth to that on flood plain

k_{SC}/H = relative roughness of channel

$k_{SF}/(H-h)$ = relative roughness of flood plain

b_C/H = width/depth (aspect) ratio of main channel

$b_F/(H-h)$ = width/depth (aspect) ratio of flood plain

s_C = side slope of main channel

s_F = side slope of flood plain

4.   If we are to proceed on these lines, treating the whole section, then some simplification is possible if we confine attention to:

(i)   Rough-turbulent conditions on flood plain as well as in the deep channel (when viscous effects are no longer significant)

(ii) Velocities low enough to avoid energy lossses due to surface waves (when the Froude number becomes irrelevant).

Also the side slopes of the main channel may become less significant if the aspect ratios are based on mean channel widths, b_C' and b_F', so that we may then reduce the problem to one with 7 independent variables, with two (bracketted) of lower significance perhaps:

$$\frac{Q}{(8gSA^3/P)} = \frac{1}{\sqrt{f}} = \Phi \left\{ \frac{H}{H-h}; \frac{k_{SC}}{H}; \frac{k_{SF}}{H-h}; \frac{b_C}{H}; \frac{b_F}{H-h}; \frac{b_F}{H-h}; (s_C); (s_F); \right\} \qquad \ldots A1.3$$

If there is equal roughness on flood plain and in channel, this further simplifies to:

$$f = \Phi \left[H/(H-h); k_S/H; b_C'/H; b_F'/(H-h) \right] \qquad \ldots A1.4$$

5.   In general, single channel approaches use a restricted sub-set of the above:

$$f = \phi_1 \left[k_S/R \right] \times \phi \left[H/(H-h); b_F'/b_C' \right] \qquad \ldots A1.5$$
$$\ldots A1.5$$

where R is the hydraulic mean depth of the whole section (replacing H in the preceding form) and the aspect ratios of the separate zones are replaced by the ratio between their widths.

6.   Splitting dimensionless statements in this way is strictly not permissible, however. Consider the general relationship:

$$c = \phi \left[a; b \right] \qquad \ldots A1.6$$

Replacing this by:

$$c = \Phi_1 [\, a \,] \times \Phi_2 [\, b \,] \qquad \qquad \ldots A1.7$$

limits the relationship to one that would plot as a set of parallel curves on a log-log plot, clearly much less general than the function it seeks to replace.

Replacing it by:

$$c = \Phi_1 [\, a \,] + \Phi_2 [\, b \,] \qquad \qquad \ldots A1.8$$

means restricting it to a set of parallel curves when plotted to linear axes. So although split dimensionless statements are convenient, especially in terms of data analysis, whether or not they are acceptable is a matter requiring justification. It is common in design practice to split complex relations by assuming that the various factors influencing a process can be allowed for separately, i.e. assuming the various factors do not interact, but the legitimacy of this procedure requires testing in the particular case under review.

7. Divided channel method

Continuing the assumption that viscous and surface wave influences are negligible, the divided channel approach in its basic form separates the cross-section into deep channel and flood plain zones. Various assumptions about the planes of division between the zones have been considered in the past, but here they are vertical plains at the bank line, and the interface so created is not included in the wetted perimeter of either zone. With the further assumption that the effect of the aspect ratio is solely on friction loss so that it may be accounted for by using the hydraulic mean depth, the method is basically as follows:

$$Q = Q_C + Q_F \qquad \qquad \ldots A1.9$$

where

$$Q_C = \sqrt{(8gSA_C^3/P_C f_C)} \qquad \qquad \ldots A1.10$$

and

$$Q_F = \sqrt{(8gSA_F^3/P_F f_F)} \qquad \qquad \ldots A1.11$$

$$f_C = \Phi_C [k_{SC} P_C/A_C] \qquad \qquad \ldots A1.12$$

$$f_F = \Phi_F [k_{SC} P_F/A_F] \qquad \qquad \ldots A1.13$$

8.   The above is defective as it ignores any interaction effect between the separate zones. Hence we must introduce correction factors, F_C and F_F to adjust the calculated channel and flood plain flows for the effect of their interaction, or an overall correction factor for the total flow, F_T;

$$Q_T = F_T \times (Q_C + Q_F) \qquad \qquad \ldots A1.14$$

9.   In the above, Q_C and Q_F are the basic values calculated from the friction formulae appropriate to their particular features, e.g. smooth, rough or transitional. The correction factors will be functions of other flow or geometric parameters. The minimum requirement from purely dimensional considerations is:

$$F_C = \Phi_1 [H/(H-h); k_{SC}/H; k_{SF}/(H-h); b_C'/H; b_F'/(H-h); s_C; s_F] \qquad \ldots A1.15$$

$$F_F = \Phi_2 [\text{ditto}] \qquad \qquad \ldots A1.16$$

and

$$F_T = \Phi_3 [\text{ditto}] \qquad \qquad \ldots A1.17$$

10.   Different authors have used different restricted forms of the above, perhaps related to the scope of experiments they have made, for example:

$$F_{C,F,T} = \Phi_{(1,2,3)} [H/(H-h); f_F/f_C; b_F/b_C] \qquad \qquad \ldots A1.18$$

For equal roughness on flood plain and in main channel, this would reduce to sets of curves giving correction factors plotted against relative depth, $H/(H-h)$, with the width ratio as the third variable for each set. Different sets would be required for different values of the friction factor ratio – but a further four possibly relevant parameters have also to be accounted for, or shown to be insignificant. (Four because the seven parameters of equs A1.15 to 17 have been reduced to three)

11. Let us consider the features to be expected where both the flood plains and main channel are very wide relative to their flow depths: in the limit this is the junction at a bank line of two semi-infinite sheet flows. The expectation in that case is for the flow to be affected for a limited zone either side of the bank line, and is is worth considering therefore using an *additive/subtractive* correction to the flows either side of the bank rather than using *multiplying* correction factors. In the wide channel case, then:

$$Q = Q_C + Q_F \qquad \qquad \text{...A1.19}$$

where

$$Q_C = Q_{Cb} + \delta Q_C \qquad \qquad \text{...A1.20}$$

$$Q_F = Q_{Fb} + \delta Q_F \qquad \qquad \text{...A1.21}$$

Q_{Cb} and Q_{Fb} are the channel and flood plain flows calculated by the appropriate resistance equation for the main channel and flood plains respectively, ignoring any interaction effects: the additive/subtractive corrections take account of the actual interaction. The question then arises as to how best to "normalise", i.e. convert to non-dimensional form, these discharge corrections. An argument can be developed that they should be normalised by the local flow parameters characterising the junction between the assumed semi-infinite sheet flows, e.g. $(H-h)^2(V_C-V_F)$.

12. The implication behind this is that the cross-section of the zone of influence has dimensions related solely to the depth on the flood plain,

and any velocity defect/increment is basically proportional to the difference between main channel and flood plain velocities. However, Rajaratman and Ahmadi (1981) considered this very point on the basis of experiments in a vertical sided compound channel and demonstrated that the width of the zone of influence was proportional to bank full depth, h, so that normalisatiom by $h^2(V_C-V_F)$ or $hH(V_C-V_F)$ might prove preferable.

13. Zheleznyakov (1985) had earlier suggested the concept of additive or subtractive corrections to the flood plain and main channel flows and demonstrated that it was the loss of main channel flow rather than any increase in flood plain flow that dominated the situation. He went on to suggest that changes could be expressed in terms of bank full flow. This would not be appropriate for very wide systems approaching the semi-infinite situation hypothecated above, however.

14. Thus there are several alternative concepts for normalising the suggested discharge correction. From the pragmatic point of view, bank full discharge is a straight forward quantity to use, but so also are the alternatives. Only by comparing the possible normalising procedures when analysing experiments can we decide on the most relevent non-dimensional groupings. For very wide systems, the semi-infinite concept would lead to:

$$\delta Q_T/(H-h)^2(V_C-V_F) = \Phi_{\delta T} [H/(H-h); f_F/f_C; s_C] \qquad \ldots A1.22$$

though from the dimensional analysis viewpoint the term (H-h) in the left parameter could equally well be any combination of H and h with the dimensions of an area, e.g. (H-h)h or Hh.

15. To cover compound channels in general, the function would have to allow for the restriction of the flow interaction by the channel width and edge of the flood plain. The relevant aspect ratios have therefore to be re-introduced. Also, because of viscous influences, especially in smooth laboratory channels, it is conceivable that the Reynolds number may be significant, although it is hoped that the friction factors would be a sufficient flow description for both smooth and rough situations. The generalised statement thus becomes:

$$\delta Q / (\text{Area}) (V_C - V_F) = \Phi_{\delta T}[\ H/(H-h);\ f_F/f_C;\ s_C;\ b'_C/H;\ b'_F/(H-h);(s_F)]\ \ldots A1.23$$

where (Area) is intended to cover any product of two independent variables
of length dimensions to give a plausible area of influence. Combinations
of interest might be Hh, (H-h)h, 2bH etc. As the FCF at Wallingford has a
fixed value of main channel aspect ratio, $2b/h = 10$, in terms of data
analysis the use of Hh or 2bH would not be distinguishable: the latter is
always 10 times the former, and the issue could only be resolved by
resorting to other data sources with different main channel aspect ratio.

16. This concept, equivalent to additive/subtractive correction to the
overall flow (or more basically in the separate zones of flow) can be tested
alongside other methods, for example the use of discharge adjustment factors
either for the separate zonal calculations or for the sum of those basic
discharges. There is no reason from the dimensional analysis viewpoint to
prefer any particular method of expressing the required correction to the
basic calculated flows. The criteria for choice might include:

- goodness of fit
- insensitivity to some variables
- simplicity of function e.g. linearity
- convenience of application in hydraulic design

APPENDIX 2

RESISTANCE FUNCTIONS FOR THE SERC-FCC AT WALLINGFORD

1.*Background*

1.1 The Flood Channel Facility at Hydraulics Research, Wallingford, consists of a compound channel moulded in cement mortar. It is of fixed gradient, although a number of alternative cross-section geometries has been tested. Tests were conducted by several independent research groups concentrating on different aspects, but in all cases important flow parameters were the discharges at which the experiments have been conducted and the corresponding mean depths of flow relative to the bed of the main channel. From discharge and depth, with the known fixed gradient of about 1 in 1000, all other conventional measures of channel performance can be calculated, e.g. mean velocity, Froude number, friction factor, Reynolds number etc.

1.2 In the context of analysing the experimental results for the preparation of a design manual, the resistance of the channel is of prime importance, and this required the establishment of the most appropriate resistance formula for the Wallingford channel, based on the analysis of experiments conducted on channels without flood plains. If the function were not a good fit for simple channels, there would be much less prospect of identifying and formulating the additional resistance arising under compound flow conditions: and indeed misleading conclusions could emerge. Hence a priority task was a review of the basic resistance function. It must be stressed that the conclusions in this Appendix relate specifically to the Wallingford channel: they do not apply to the rougher channels in engineering practice.

1.3 It might be thought that the choice of the Colebrook-White transition function would have been automatic and uncontentious bearing in mind that it has been in general use, at least for the smoother range of manufactured and constructed surfaces, for both pipes and channels. If that had been the case, all that would have been necessary was to assess a suitable value of k_s. Analyses of the data by the various research teams, however, left the matter in some doubt, because the different groups had used different

basic functions, including forms of smooth turbulent equation, the turbulent transition function of Colebrook-White and Manning's equation, as well as friction factor/Reynolds Number plots.

1.4 A perhaps surprising feature of the previous analyses was that several alternative resistance laws were, at face value, equally valid, even equations such as Manning's, which is normally regarded as restricted to rough channels, providing a good fit with constant n for the simple channels. To avoid continuing confusion, as well as to provide a sound basis for further analysis of stage/discharge data, reconsideration of the basic resistance function was therefore considered essential.

2. *Brief review of resistance functions*

2.1 Most text books on hydraulics contain a review of hydraulic resistance, and include a friction factor/Reynolds number diagram (often ascribed to Moody, see for example Chadwick and Morfett, 1986) based on the Colebrook-White transition function. Almost without exception, this diagram will relate to pipe flow but a method of conversion to open channels or non-circular cross-sections may be given, using the equivalence for circular sections, namely :

$$R = D/4 \qquad \qquad \qquad ...2.1$$

2.2 This is an oversimplification, because the Colebrook-White formula derives from the smooth turbulent and rough turbulent functions obtained by integrating the logarithmic velocity distribution law over the flow cross-section. There are constants of integration that depend on the shape of section, and so an additional adjustment is required over and above the $R = D/4$ conversion. In normal engineering the distinction is not very important (because of uncertainties elsewhere in the design process), but in the accurate analysis of research results it could be significant. The two versions of the rough turbulent equation in the literature, for circular and wide open-channels respectively, are:

Circular sections:

$$1/\sqrt{f} = 2 \log (k_S/3.7D) = 2 \log (k_S/14.8R) \qquad \qquad ...2.2$$

Wide open-channels:

$$1/\sqrt{f} = 2 \log (k_S/12.3R) \qquad \qquad \qquad ...2.3$$

This last form was obtained by Keulegan (1938) who also showed that a
similar correction for channel shape is required for smooth turbulent flow.
The corollary to this is that if the Colebrook-White transition function is
to be adjusted for shape, both elements require the same adjustment
factor (Ackers, 1958) so that the two versions of the function are:

Circular sections:

$$1/\sqrt{f} = -2 \log [(k_S/14.8R) + (1.255\nu/R\sqrt{(32gRS)})] \qquad ...2.4$$

Wide open-channels:

$$1/\sqrt{f} = -2 \log [(k_S/12.3R) + (1.510\nu/R\sqrt{(32gRS)})] \qquad ...2.5$$

Unfortunately the need for adjustment to the smooth term is not so
generally recognised so that sometimes the wide channel adjustment is made
only to the roughness term in the transition function. In what follows,
the wide-channel transition function will be taken as equ. 2.5.

2.3 A major distinction between smooth and rough turbulent flows is the
influence of fluid viscosity on the resistance function: in the former
case, the friction factor, f, depends on Reynolds number, decreasing with
increasing size and velocity; in the latter case, the friction factor is
independent of Reynolds number. This distinction also results in only
rough turbulent flow following a square law of resistance, i.e. velocity
being proportional to the square root of hydraulic gradient (other
parameters of flow being unchanged). The very popular "square law" Manning
equation may be thought of as an approximation to equation 2.2 or 2.3, with
Manning's n given by $k_S^{1/6}/26$ (k_S in mm) It can be shown that the
approximation is close for relative roughnesses R/k_S between about 10 and
100, which confirms application to many of the rougher engineering
constructions and to natural channels. It follows from the form of the
Manning equation that it should only be applied to rough turbulent flow,

when the flow is not being influenced by viscosity and so is independent of Reynolds number.

2.4 The transition between rough and smooth turbulent flows embodied in the Colebrook-White function allows for the progressive change from viscosity dominated flow to roughness dominated flow as the Reynolds number increases. The form this transition takes in a friction factor/ Reynolds number plot is not fixed, but depends on the character of the roughness: for example, the Nikuradse diagram for a uniform coverage of glued-on sand grains has different transitions from the Moody/Colebrook White chart which is for isolated protuberances. The latter has a much more gradual and extended curve into the smooth law and this is thought to arise because the isolated roughness elements continue to exercise a local disruption on the laminar sub-layer: they are not so readily submerged as is the uniform coverage of grains with equal k_S value.

2.5 An important distinction between experiments conducted on pipes and those on open channels is that the former will be at a constant relative roughness, because in any test series both surface texture and flow cross section remain constant: it is the hydraulic gradient (slope) which varies as the discharge is varied. Open channels, on the other hand, have the flexibility of cross-section change: whether they are at constant slope or variable slope will depend on the experimental arrangement, but the Wallingford flood channel facility imposes constant slope, so that relative roughness is not constant. Thus any sequence of test results for a fixed gradient open channel runs across the constant relative roughness lines on a Moody- type diagram rather than following one of them.

2.6 Myers and Brennan (1989) when analysing the Wallingford data generalised the smooth turbulent function to the following:

$$1/\sqrt{f} = C \log (Re\sqrt{f}) - D \qquad \qquad \ldots 2.6$$

The smooth component of the Colebrook-White formula for pipes sets $C = 2.00$ and $D = 0.80$, values deduced from Nikuradse's tests on pipes many years ago. They were empirical adjustments to values deduced theoretically from the velocity distribution: 2.03 was considered a more fundamental value of C, corresponding to the generally accepted value for the turbulence

constant, K, of 0.40. For wide open channels, Keulegan had suggested D = 1.08. Using a slight variant of equ. 2.4 (Henderson, 1966), a k_S value of 0.06mm was deduced for the Wallingford channel. Myers and Brennan reasoned that as $Re_* = u_* k_S / \nu$ had a maximum value about the same as the value of 4 suggested by Henderson as an upper limit for smooth turbulent flow, the flow should indeed be considered as smooth turbulent throughout. However, the limit of 4 is more appropriate to a uniform sand textured surface, being based on Nikuradse's rough pipe experiments: the Colebrook-White transition extends from $Re_* = 0.3$ to 50, so the question about whether the flow should be considered as smooth rather than transitional was unresolved.

2.7 The form of equation 2.6 indicates that the main influence of any variation in the term D is to provide a vertical shift to a plot of $1\sqrt{}/f$ against Re. The effect of channel shape obtained by integrating the velocity distribution accounts for a change in D of 0.17:
(0.5 - In 2) $/K\sqrt{}/8 = 2(\log 14.8 - \log 12.3)$. However, since the time when Keulegan studied the question, a great deal of additional experimental evidence on turbulent flows has become available which has providing updated equations for the turbulent velocity distribution in smooth channels, which in turn lead to up-dated open channel friction functions.

2.8 The logarithmic velocity distribution law for smooth boundaries takes the form:

$$v/v_* = A \ln(v_* z/v) + B \qquad\qquad ...2.7$$

where v is the local velocity at distance z from the wall, and v_* is the shear velocity at the wall $(=\sqrt{(\tau/\rho)})$. There is still some contention over the best values of A and B, which are essentially empirical as they depend on experimental measurement of velocity distribution. The generally accepted values in a historic context have been those due to work by Nikuradse (1932), Clauser (1954), Patel (1965) and the consensus from the Stanford conference of 1968.

2.9 Integrating the velocity distribution over the depth for a wide open channel gives equation 2.6, where:

$$C = 2.3026 \ A/\sqrt{8} \qquad\qquad \ldots 2.8$$

$$D = - \ (1 + \ln 4\sqrt{8})A + B \qquad\qquad \ldots 2.9$$

and on this basis it is possible the smooth channel resistance functions
that may derived from the 'historic' velocity distributions may be
compared:

Source	Date	A	B	C	D
Nikuradse	1932	2.50	5.50	2.035	1.083
Clauser	1954	2.49	4.90	2.027	1.283
Patel	1965	2.39	5.45	1.946	0.968
Stanford	1968	2.44	5.00	1.986	1.188

2.10 From the appearance and feel of the moulded surface at Wallingford, it
is apparent that the surface is not far from smooth: it certainly can not be
characterised as rough. In those circumstances the Manning equation would
not be expected to provide a good fit to resistance data without using the
coefficient, n, in an artificial way to illustrate the departure from rough
turbulent "square law" resistance: yet as previously mentioned it provides a
surprisingly good fit without varying n. The reason for this will be
discussed in detail later, but one factor is that open channel tests at
constant gradient are not well conditioned to distinguish between smooth
turbulent, rough turbulent and transitional conditions, given that all
contain at least one parameter which is based on the particular set of
experiments. A shift from the classical smooth turbulent line on an f, Re
plot, whilst remaining approximately parallel to it, can be obtained by
altering D in the logarithmic smooth-turbulent formula, by a non-zero value
of k_S in the transition formula for a wide channel (or indeed in the
corresponding pipe equation) or by varying depth and hence relative
roughness in a rough turbulent formula.

2.11 These three equations are shown in fig A2.1: the Myers and Brennan
(1990) modified smooth turbulent equation, the wide channel transition
function with kS = 0.07 mm and the Manning equation with n = 0.010. The
upper diagram shows the conditions for the Wallingford main channel

cross-section at a gradient of 1:1000: only at the shallowest flows is there much difference between the three functions.

2.12 On the basis of this review, from purely theoretical considerations the Manning equation should be ruled out on the grounds that applying a rough turbulent equation to a rather smooth channel at slack gradient would be misleading. Any agreement with the Manning equation is the fortuitous result of having a fixed gradient. Had the gradient varied, a fixed Manning's n could not have provided an acceptable fit to the data. In fact, the flow is not rough turbulent and some viscous influence is expected. The appropriate resistance function from theoretical considerations alone is expected to be the transition law or a modification of the smooth turbulent law.

3. *Analysis of resistance calibration data*

3.1 Depth discharge data were obtained in the various phases of the investigation for 'simple', i.e. non-compound flow conditions, with bank side-slopes of 2:1 (hor:vert), 1:1 and vertical. In all cases the bed width was 1.5 m and the channel hydraulic gradient very close to the mean channel gradient of 1.027/1000. The average stage was obtained by taking the mean of the measured depths over the experimental length of well established uniform flow, the discharge was measured by orifice meters in the supply lines, the hydraulic gradient was assessed from the slope of the total energy line. Velocity was derived from continuity, knowing the mean cross sectional area. Viscosity was obtained from the water temperature. On the whole, the water temperature remained close to 15°C. Unfortunately at the time this analysis was carried out not all the measured temperatures had been added to the data set, and where they were missing a figure of 15°C was assumed, but in view of the small variation from this standard value any error introduced would be insignificant. (This assumption did not apply to the analysis of compound channels: measured temperatures were then available.)

3.2 There were four sets of information referred to as channels 1 to 4:

Channel number	Side slope, s	Date of experiments	Number of tests	Depth range mm
1	2	Jan-Feb 89	14	45 - 150
2	1	Nov 86-Sept 87	28	25 - 149
3	1	Sept 87	13	150 - 296
4	0	Oct-Nov 88	11	40 - 148

(These dates refer to the bulk of tests at the stated side-slope: a few tests at other dates are included)

Channel 3 relates to tests carried out as an extension to those on channel 2, having extended the banks upwards with temporary side slopes to cover the range of depths of interest with over-bank flow. One of the tests on channel 2 seemed to be away from the general trend, so some analyses were made omitting it, though with very little effect on the overall picture. As channels 2 and 3 were in essence one channel tested over different depth ranges, some analyses were made combining these data: and also combining all four data sets.

3.3 There has been an observable change in the surface texture of some sections of the main channel with time. There are some hard, possibly calcareous deposits over sections where the bed level was marginally below the perfect line. These have perhaps occurred because of slower draining and subsequent drying out in these zones in the periods between tests, so giving a deposit from the hard laboratory water. The texture of these zones seemed even smoother to the touch than the original surface (they were somewhat slippy) but they may have introduced minor irregularities that could have increased roughness rather than reducing it. A secondary objective of the data analysis was to show whether any change was significant.

3.4 The equations considered were:

- Colebrook-White transition in original form, equ 2.4
- The same but modified for wide channels, equ 2.5

- Manning equation
- Generalised smooth turbulent, equ 2.6

The aim of the analysis was to find the best fit coefficient values for the data set, and then to assess the variation about that function by calculating the root mean square error, both as a percentage and as an absolute error in predicted velocity. The first two equations have k_S as the empirical coefficient; Manning's n applies to the third. The generalised smooth turbulent function has two parameters, C and D, which give greater flexibilty in the fitting procedure - effectively a shift from the smooth turbulent law and a tilt if need be. The results are given in Table A2.1.

3.5 The broad conclusion from the results in Table A2.1 is that there is not much to choose between the four equations tested. The Colebrook-White transitional equation is in most cases marginally the worst whether in terms of percentage discrepancy or absolute discrepancy, but it is also apparent that most of the discrepancy from any of the equations is due to inevitable experimental tolerances rather than basic inadequacy of the theoretical functions. Apart from channel 1 (2:1 side slopes), the wide-channel modification of the C-W equation is a slightly better fit. Perhaps surprisingly, the Manning equation is better than either form of transition, whether taking data sets separately or in combination. Despite its extra degree of freedom, only in one case (channel 4, vertical sides) does the generalised smooth turbulent function turn out to be significantly better than the others. In this particular case, values of A and D have emerged from the best-fit routine that differ considerably from those for the other data sets: they have provided a tilt that better accommodates these particular results.

3.6 The k_S values for the C-W and wide-channel equations provide a sensitive measure of any roughness changes with time. For the wide-channel formula, the mean value of k_S for the first set of experiments carried out from November 1986, to January 1987 on the channel with 1:1 side slopes (channel 2) was 0.071 mm: a low value indicating how nearly smooth the steel floated finish to the channel was. This increased in tests made in September, 1987 on channel 2 to about 0.090 mm, showing marginal roughening but within the range of experimental error. Further tests in with the same

side-slope of 1:1 but at depths above 0.15 m, also in September 1987, gave k_S = 0.046 mm, seemingly smoother. Later tests in October and November 1988 with vertical sides (channel 4) gave a value of 0.111 mm, but then tests made in January and February 1989 with side slopes of 1:2 (channel 1) yielded a mean roughness of 0.010 mm, implying virtual smoothness, and suggesting that the deposition has smoothed rather than roughened the channel. However, the deposits were already present in the 1988 tests.

3.8 The Manning roughness values provide a somewhat less sensitive measure of any change in resistance of the basic channel. The first tests results may be regarded as setting a standard and then the average values from subsequent groups of tests can be used to indicate a percentage increase or reduction in calculated velocity or discharge, as in the following table:

Channel number	Side slope H:V	Test date	Mean n	Percentage change in V	
				Increase Smoother	Reduction Rougher
2	1:1	Nov 86 – Jan 87	0.01000	-	-
2	1:1	Sept 87	0.01014		1.4
3	1:1	Sept 87	0.01002		0.2
4	Vert	Oct – Nov 88	0.01001		0.1
1	2:1	Jan – Feb 89	0.00965	3.5	

3.9 Factors apart from change of surface texture with age may influence calculated values of k_S and Manning's n, for example any effect of change in cross sectional shape not fully accounted for by the hydraulic radius R. The conclusion, however, is that any changes of roughness were minor and with no apparent direct association with age. Thus all test data may be regarded as a single set for a channel of constant roughness. Bearing in mind experimental tolerances, real change can not be identified with any confidence. Thus all test data were regarded as a single set for a channel of constant roughness.

3.10 Returning to the choice of a preferred resistance function, tests over a wide range of depths are best suited to this purpose. The 40 tests on channels 2 and 3 covered depths from 25-300mm, and a Reynolds number range from 20 000 to 900 000. Table A2.1 shows the order of performance to be:

1- Manning;

2- modified smooth-turbulent equation (S-T);

3- wide channel;

4- Colebrook-White equation (C-W).

The distinction is small, and does not by itself provide a rational basis of selection. All have a percentage discrepancy of between 1.7 and 2.0 percent. However, careful inspection of the detailed plots showed that the modified S-T equation had best followed the trend of data at shallow depths. Figs A2.2 and A2.3 show the discrepancy between computed velocity and measured velocity for channels 2 and 3 (1:2 side slopes) and for all results respectively. (Actual velocities were of the order of 0.5 m/s at minimum depth, 0.8 m/s at a depth of 0.15m, bank full when operating as a compound channel, and 1.2 m/s at maximum depth of 0.3 m.) Although shallow depths in the main channel are not important, they are significant in the analysis of compound channels: some of the most illuminating results were expected to be those with shallow flows over the flood plain. Thus the preferred equation was the generalised smooth- turbulent function with C = 2.02 and D = 1.38, i.e.

$$1/\sqrt{f} = 2.02 \log (Re\sqrt{f}) - 1.38 \qquad \qquad ...3.1$$

3.11 This is is remarkably close to the resistance law deduced from the velocity distribution by integration for the wide channel case with Clauser's (1954) parameter values (C = 2.027, D = 1.283). It is a little further removed from the classic smooth turbulent law of Nikuradse, in effect shifting several percent towards increased resistance. As already mentioned the classic Keulegan value for the second parameter for wide channels is 1.08, so equation 3.1 is a further shift of 0.3 in the $1/\sqrt{f}$ value. Reference to the more recent work by Clauser suggests that this might largely be explained without recourse to any significant increase in resistance over a smooth surface, although the Stanford consensus would still leave a change of 0.20 in the value of D to be explained as increased resistance.

3.12 Morris (1959) put forward some novel concepts on resistance functions, distinguishing between three types of flow:

- semi-smooth turbulent generated by isolated roughness elements
- hyper-turbulent, where there is interference between the wakes from roughness elements
- quasi-smooth, where there were additional localised sources of energy loss, such as flow skimming over grooves

The last of these provided a shift in the friction factor / Reynolds number plot whilst remaining parallel to the smooth- turbulent line.   Possibly the Wallingford facility is following this quasi-smooth function because of such localised additional energy losses, even if they cannot be identified. Whether the resistance law of equ 3.1 represents quasi-smooth or fully smooth flow with full allowance for channel shape is immaterial in terms of data analysis.   Because many readers will be unfamiliar with the term quasi-smooth, the latter explanation has been adopted in the main report.

3.13 There remains the question of why the Manning equation provides a good fit to data from a smooth channel.   The Manning equation is exponential rather than logarithmic, and a well-known exponential smooth-turbulent formula is that proposed by Blasius (1913):

$$f = 0.08 \ Re^{1/4} \qquad\qquad ...3.2$$

This was derived as a good fit to experimental data over a particular range of Reynolds number, but let us examine a more general form of the Blasius type of formula:

$$f = B \ Re^{-b} \qquad\qquad ...3.3$$

which can be expressed in detail as:

$$8 \ gRS/V = B \ (4VR/\upsilon)^{-b} \qquad\qquad ...3.4$$

This in turn yields:

$$V = R^{(1+b)/(2-b)} \ S^{1/(2-b)} \ [8g \ 4^{b}/B\upsilon^{b}]^{1/(2-b)} \qquad\qquad ...3.5$$

3.14 For R to appear to the 2/3 power as in the Manning equation, b must equal 0.2, not very different from the Blasius value of 0.25. Inserting this value then gives a Manning "look alike":

$$V = R^{2/3} \, S^{1/2} \, (8g/B)^{5/9} \, (4/\upsilon)^{1/9} \, S^{1/18} \qquad \qquad ...3.6$$

Thus one could consider the application of Manning in the present context to be for quasi-smooth conditions with the coefficient n depending on viscosity, gravity and hydraulic gradient as opposed to its usual role as a descriptor of surface texture:

$$n = [(8g/B)^{5/9} \, (4/\upsilon)^{1/9} \, S^{1/18}]_{-1} \qquad \qquad ...3.7$$

Because slope remained constant and water temperature approximately so in the Wallingford tests, the Manning equation provided a good fit: n as defined by equation 3.7 remained constant. If the Blasius value of b had been retained, namely 0.25, then the hydraulic mean depth would be raised to power 0.714 rather than 0.667, but conceivably would have also given a good fit.

3.15 For the best fit value of n = 0.010 to apply, with S = 1.027x10-3 and υ = 1.14x10-6m/s, then it can be shown that B = 0.20, and hence the Blasius/ Manning smooth equation becomes:

$$f = 0.20 \, Re^{-0.20} \qquad \qquad ...3.8$$

This would be a more appropriate expression of the Manning-like resistance of the Wallingford channel. It would plot on fig A2.1 virtually identical with the Manning line shown, passing through f = 0.02, Re = 0.1x10⁶.

4.Rod roughness

4.1 Some of the experiments on the Flood Channel Facility at Wallingford have been carried out with the flood plains roughened by vertical rods extending through the full depth of water. In order to establish the basic resistance function for this type of roughening, data is available from a set of seven tests carried out with the main channel roughened with the same pattern of rods used under compound channel conditions. These basic single channel tests covered depths of flow from 44mm to 119mm, a large part of the range of flood plain depths observed in the roughened flood plain tests.

4.2 The pattern of rods used consisted of a triangular distribution, of angle 60°. This was designed to have a density of 12 rods per m^2, and so the sides of the equilateral triangles forming the grid was 0.310m. This was the spacing between the rods transverse to the flow, and the longitudinal spacing of rows was therefore 268.5mm. See fig A2.4.

4.3 Under these conditions the resistance to flow is made up of the drag of the rods and the shear force at the channel boundaries. It is assumed that these may be treated separately as if the presence of the rods does not influence the boundary drag of the channel surface, except through the increase of velocity imposed by the blockage effect. Also it is assumed that any influence of the vertical velocity distribution on the drag on each rod can be accommodated by incorporating a suitable distribution coefficient into an equation that utilises the mean channel velocity calculated allowing for the blockage effect of the rods, by using the net cross sectional area in the plane of the row of rods.

4.4 The equation for the drag at the solid surface was derived earlier and is given by equ 3.1, applied in this case with subscript s denoting that part of the total friction factor arising from shear at the solid surface:

$$1/\sqrt{f_s} = 2.02 \log (Re\sqrt{f_s}) - 1.38 \qquad \qquad ...4.1$$

where:

f_s = the friction factor arising from the drag on the channel perimeter
Re = the Reynolds number of the flow as a whole

4.5 The drag of the rods arises from three sources: internal vortex sheet drag due to flow separation behind the rods; free surface drag arising from induced waves; and skin friction on the rods themselves. These effects might be affected by wake interference, i.e. each rod may provide some sheltering of the rod next downstream. The first of these components is the dominent one: the so-called form drag.

$$F_{ROD} = C_D N \, d \, z \, \rho \, \alpha U^2 / 2 \qquad \qquad \ldots 4.2$$

where

F_{ROD} = the form drag of the rods per unit length of channel

C_D = the drag coefficient

N = number of rods per unit channel length

d = dia of rods

z = flow depth

ρ = specific mass of fluid

α = velocity distribution coefficient

U = the mean velocity over the flow depth

The velocity distribution coefficient allows for the variation of velocity over the length of the rod, i.e. the depth of flow. The depth mean velocity U is calculated allowing for the blockage of the transverse rows of rods:

$$U = Q/(A - n \, z \, d) \qquad \qquad \ldots 4.3$$

where

Q = discharge

A = channel cross-section

n = number of rods in each row

On this basis, a blockage coefficient, β, may be defined:

$$\beta = (U/V)^2 = (1 - n \, z \, d/A)^{-2} \qquad \qquad \ldots 4.4$$

4.6 The total drag per unit length of channel is then given by:

$$F_{TOT} = \beta\rho\ V^2(\alpha N\ d\ z\ C_D/2 + f_S\ P/8) \qquad\qquad ...4.5$$

where

P = wetted perimeter of channel

4.7 The drag equation can be converted into a conventional form of resistance equation using the force balance equation:

$$F_{TOT} = \rho g\ A\ S = \rho g R S P \qquad\qquad ...4.6$$

where

g = acceleration due to gravity
A = cross sectional area of flow
S = channel gradient
R = hydraulic mean depth, A/P

$$f_{TOT} = 8gRS/V = \beta[4(N\ d\ z/P)\ \alpha C_D + f_S] \qquad\qquad ...4.7$$

where

f_{TOT} = overall friction factor

4.8 Equation 4.7 with the value of f_S obtained from equ. 4.1 formed the basis of analysing the test data. Note that the Reynolds Number, Re, for calculating the surface resistance incorporates U rather than V. For the main channel calibration tests, N was given by 10/0.2685 = 18.62 per unit length. Taking C_D as the unknown, all other parameters in equ. 4.7 were known, so that C_D could be calculated. (When using equation 4.7 in the reverse direction with f_{TOT} or V as unknown, iteration is required because f_S depends on the overall Reynolds Number, which in turn depends on the unknown mean channel velocity.)

4.9 The fact that resistance is generated over the full depth of flow by the rod roughness, with a minor part generated by the surface drag at the solid boundaries gives a more-than-usually uniform velocity distribution in the vertical. Thus the role of α is probably small compared with the blockage coefficient, in this case approximately $[310/(310-25)] = 1.18$, though varying with flow depth because the cross section is trapezoidal.

4.10 The basic assumption that the surface drag can be assessed by ignoring the presence of the rods (except, of course, in respect of the blockage and the reduction in channel Reynolds Number because the extra drag reduces mean velocity) was open to question. It might be argued that the surface drag would be reduced because in the wake of the rods the velocity close to the boundary would be less than average, and could even be reversed over some area behind each rod. On the other hand, the effect of the rods will produce irregularity of the transverse distribution of velocity and this would increase the average surface drag. Furthermore, the disruption to the boundary layer might modify the basic smooth law. There was no way of knowing which direction any change would be, let alone quantifying it from previous knowledge. The major effect is almost certainly due to blockage, which was taken into account through β. Some preliminary analyses with this calculated surface drag modified by factors either above or below unity did not provide any improvement in the correlations.

4.11 Figure A2.5 shows the variation of C_D calculated as above with the channel Reynolds Number. Figure A2.6 shows essentially the same information, but plotted against the ratio of flow depth to rod diameter: Figure A2.6 also shows the calculated values of the blockage coefficient. The experimental results display smooth trends with very little scatter. C_D varies from a minimum of about 0.97 at the shallowest flow tested (minimum Re) through a maximum approaching 1.22 at intermediate depths, dropping again at the deepest flow (maximum Re) to 1.16. These values may be compared with values for the drag coefficient of isolated cylinders in the

literature: see for example Rouse 1950. The Reynolds number of the rods themselves varies over a very narrow range, 4100 to 4600, because the mean channel velocity varies only from 0.19 to 0.22 m/s. This is a range where the drag coefficient is not expected to show any rapid change with the rod Reynolds Number, so it is most unlikely that the variation of drag coefficient is a Reynolds number effect.

4.12 The drag coefficient to be expected will depend on whether the rods are effectively smooth or rough. The former would give about 0.95 according to previously available information: the latter would be expected to be higher though data at this range of Reynolds Number are lacking. A further possible influence is the effect of the wake from the rods on those downstream from them. However, the actual longitudinal spacing between rods in this case was over 20 diameters, so although undoubtedly there would be some residual effect, it was probably very small. It would, moreover, remain the same in all tests so would not cause variation in the drag coefficient.

4.13 The above analysis takes no account of wave drag that could arise because the rods are "surface piercing" elements. It might be anticipated that if wave drag were significant, following the work of Froude on ship resistance, it would be expected to depend on channel Froude Number, $V/\sqrt{(gz)}$. This would also affect any surface interference between the rods as the pattern of waves would be angled to the channel axis as a function of Froude number. Although the channel Froude Number varies over quite a narrow range, from 0.3 at the shallowest flow to 0.2 at the deepest, it is conceivable that the surface wave pattern could pass through some sensitive zone within the range of these tests. Indeed Froude found that the wave drag showed a peak value at modest Froude numbers, falling before increasing again at high Froude numbers. The variation of overall drag coefficient may therefore arise from the free surface effects. The conclusion was that the drag coefficient is best expressed as a function of relative depth, i.e. flow depth/rod diameter.

4.14 A curve fitting exercise gave the following formula for the drag coefficient:

For $1.75 < Z_* < 6.6$.......

$$\alpha C_D = 1.184 - 0.277 \ Z_* + \sqrt{(0.529 \ Z_* - 0.843)} \qquad\qquad ...4.8$$

where

Z_* = flow depth/rod diameter

This is shown also on Figure A2.6 and provides a good fit over the range of data for the Wallingford tests.

4.15 There remains the problem of extrapolation outside the range of test results. From the evidence of past research on the drag of cylinders, it seemed inappropriate to allow the value of C_D to drop below 0.95 at shallow depths, which was the value obtained at the shallowest flow considered. It might be argued that allowing for interaction between the rods (the influence of the wake from one on the rod in line downstream) might reduce the expected drag coefficient, there is no direct evidence of this. At higher depths in the Wallingford flume, up to the maximum Z_* value of 6, the empirical equation predicts a drop in C_D towards 1.05. It is not necessary to extrapolate beyond this for this series of tests, but work at Glasgow by Ervine and Jasim (private-communication) suggests that higher values of Z_* would give a continuing downward trend towards a value of perhaps 0.8 or 0.85 as a limiting value for $Z_* > 10$.

4.16 When applying the functions to the tests on compound channels, there was a minor complication, because the number of rods in alternate rows

differed. Thus the basic equations for the combination of drag on the rods and the surface drag were reformulated, as with different rod numbers in alternate rows, the blockage coefficients differed in alternate rows.

5 *Conclusions*

5.1 The SERC Flood Channel Facility at Wallingford is effectively smooth.

5.2 From the empirical and pragmatic point of view, there was little to choose between four resistance functions that were compared with the data from tests on simple channels. These were the Colebrook-White equation for transitional turbulent flow in pipes, the conversion of this to a wide-channel form, the Manning equation and a generalised logarithmic smooth turbulent function.

5.3 Most variation between the test data and any of these established equations for flow resistance was due to experimental scatter: tests in an open channel at fixed slope are not well conditioned to differentiate between resistance functions.

5.4 On theoretical grounds, the Manning equation should not be used for analysing flow in smooth channels. It is most appropriate for rough-turbulent flow, which is not the situation in any of the tests in the Wallingford flood channel facility.

5.5 However, the Manning equation provided a good fit to the experimental results. This was so because an exponential formula with the hydraulic mean depth raised to the power 2/3 can also be derived from a power-law smooth-turbulent function, with the coefficient n dependent on viscosity and gradient, rather than surface texture.

5.6 In the context of the Wallingford flood channel facility, a preferable exponential formula is a modification of the Blasius smooth turbulent equation to suit wide open-channel conditions:

$$f = 0.20 \, Re^{-0.20}$$

5.7 The wide range of depths covered in tests on the channel with 1:1 side slopes made these data the most suitable for selecting a preferred equation. Paying due weight to shallow depths of flow, which are of significance in the analysis of the tests on compound channels with flood plains, a special form of the smooth-turbulent equation was derived and recommended for all subsequent analyses of Wallingford test data:

$$1/\sqrt{f} = 2.02 \log (Re\sqrt{f}) - 1.38$$

5.8 Although there was an observable change in the surface character of some sections of the test facility due to a hard deposit, this appears to have had very little influence on the flow resistance, although experimental tolerances make any influence difficult to detect or quantify.

5.9 The use of other equations in earlier analyses of the Wallingford results, including some published papers, did not introduce significant errors, but was potentially confusing.

5.10 It is preferable to distinguish between roughness coefficients and resistance coefficients. The former will not change because of the flow cross section becoming compound as they define the physical roughness of the channel which will be unchanged. The extra resistance arising from the interference effects with flood plain flow is best expressed as an adjustment to the shear streses, friction factor, velocity or discharge, leaving the basic roughness coefficients unchanged.

5.11 The basic resistance of the Wallingford channel when roughened with full depth rods can be described by combining the specific form of smooth law for the channel surface with the additional drag due to the rods.

5.12 A form of drag coefficient is used which also incorporates a velocity distribution factor. The values obtained are within the range of expectation, bearing in mind the values of drag coefficients for cylinders given in the literature and the actual blockage ratio. The drag coefficient has been expressed as a function of the relative depth of flow.

5.13 Basic resistance calculations for rod roughness as in the Wallingford tests may be based upon the following set of formulae, which allow for different numbers of rods in alternate rows:

$$\beta_1 = (1-n_1 z\ d/A)^{-2}$$

$$\beta_2 = (1-n_2 z\ d/A)^{-2}$$

For $1.75 < Z_* < 6.6$:

$$\alpha C_D = 1.184 - 0.277\ Z_* + \sqrt{(0.529\ Z_* - 0.843)}$$

else $\alpha C_D = 0.95$

$$1/\sqrt{f_S} = 2.02\ \log(Re\sqrt{f_S}) - 1.38$$

$$f_{TOT} = 8gRS/V^2 = 4\alpha C_D(\beta_1 N_1 + \beta_2 N_2)\ d\ z/P + (\beta_1 + \beta_2)f_S/2$$

where

Re	=	Reynolds number of blocked channel $= 2\ V\ R\ (\sqrt{\beta_1}+\sqrt{\beta_2})/\nu$
$\beta_{1,2}$	=	blockage effect, i.e. square of area ratios for alterate rows
$n_{1,2}$	=	number of rods of dia d across channel/flood plain, rows 1 and 2
$N_{1,2}$	=	number of rods per unit length of main channel/flood plain, in ditto
z	=	depth of flow in main channel/on flood plain
A	=	gross cross sectional area of zone under consideration
f_S	=	friction factor due to smooth boundary
f_{TOT}	=	overall friction factor
V	=	nominal velocity given by component discharge/A
αC_D	=	effective drag coefficient of rods
Z_*	=	z/d
R	=	hydraulic mean depth A/P, for zone under consideration
S	=	hydraulic gradient (water surface slope)

TABLE A2.1. ANALYSIS OF RESISTANCE DATA

Channel	Side slope hor/vert	Range of depths mm	No. of tests	Colebrook-White ks mm	RMS error % of V (V,cm/s)	Wide channel trans ks mm	RMS error % of V (V,cm/s)	Manning equation n	RMS error % of V (V,cm/s)	Mod. smooth turb't A, D	RMS error % of V (V,cm/s)
1	2	45-150	14	0.028	1.66 (1.20)	0.014	1.84 (1.33)	0.0096	1.61 (1.19)	2.00, 0.96	1.64 (1.18)
2	1	25-149	28	0.085	4.77 (2.86)	0.050	4.64 (2.85)	0.0096	4.36 (2.58)	2.20, 2.12	4.27 (2.84)
2	1	25-149	27	0.096	3.96 (2.15)	0.059	3.82 (2.13)	0.0100	3.66 (1.96)	2.08, 1.67	3.49 (2.12)
3	1	150-296	13	0.065	1.17 (1.12)	0.041	1.11 (1.08)	0.0100	1.10 (1.05)	1.91, 0.88	1.06 (1.03)
4	0	40-150	11	0.075	3.86 (1.81)	0.041	3.62 (1.72)	0.0991	3.46 (1.65)	2.53, 3.56	2.22 (1.26)
2 & 3	1	25-296	40	0.081	3.51 (1.94)	0.050	3.31 (1.89)	0.0100	3.06 (1.72)	2.02, 1.38	2.97 (1.84)
1,2,3,4	0,1,2	25-296	65	0.072	3.57 (1.99)	0.041	3.44 (1.97)	0.0994	3.30 (1.90)	1.91, 0.84	3.38 (1.99)

The bracketted error figures are the root mean square errors in velocity for the series of experiments, comparing measurement with best-fit formula prediction. The unbracketted figures are the RMS percentage differences.
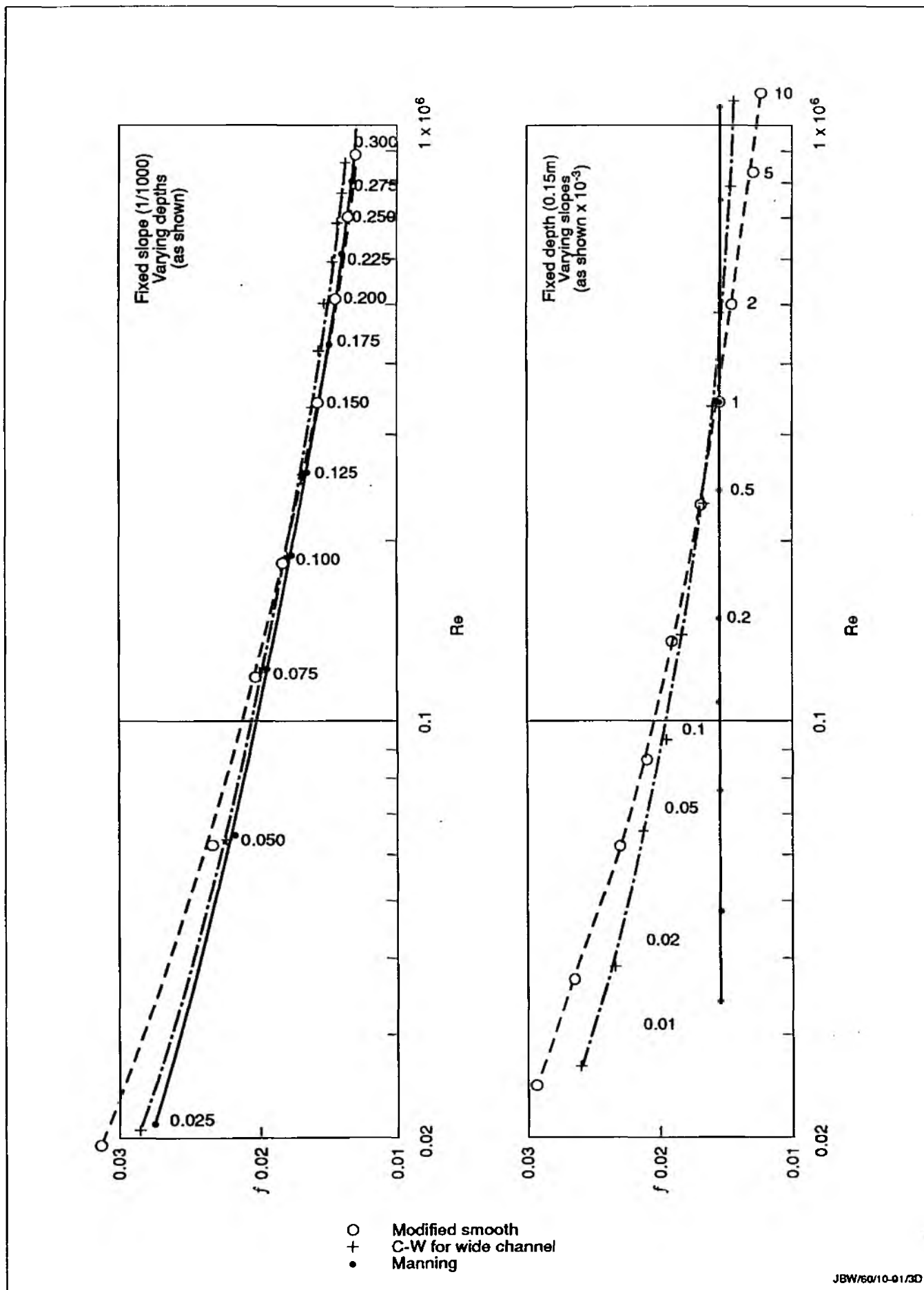
Fig A2.1 Comparison of friction formulae: (a) for fixed slope; (b) for fixed depth

Fig A2.2 Smooth channel calibration: 1/2 side slope

SERC-FCF data - generalised smooth turbulent results
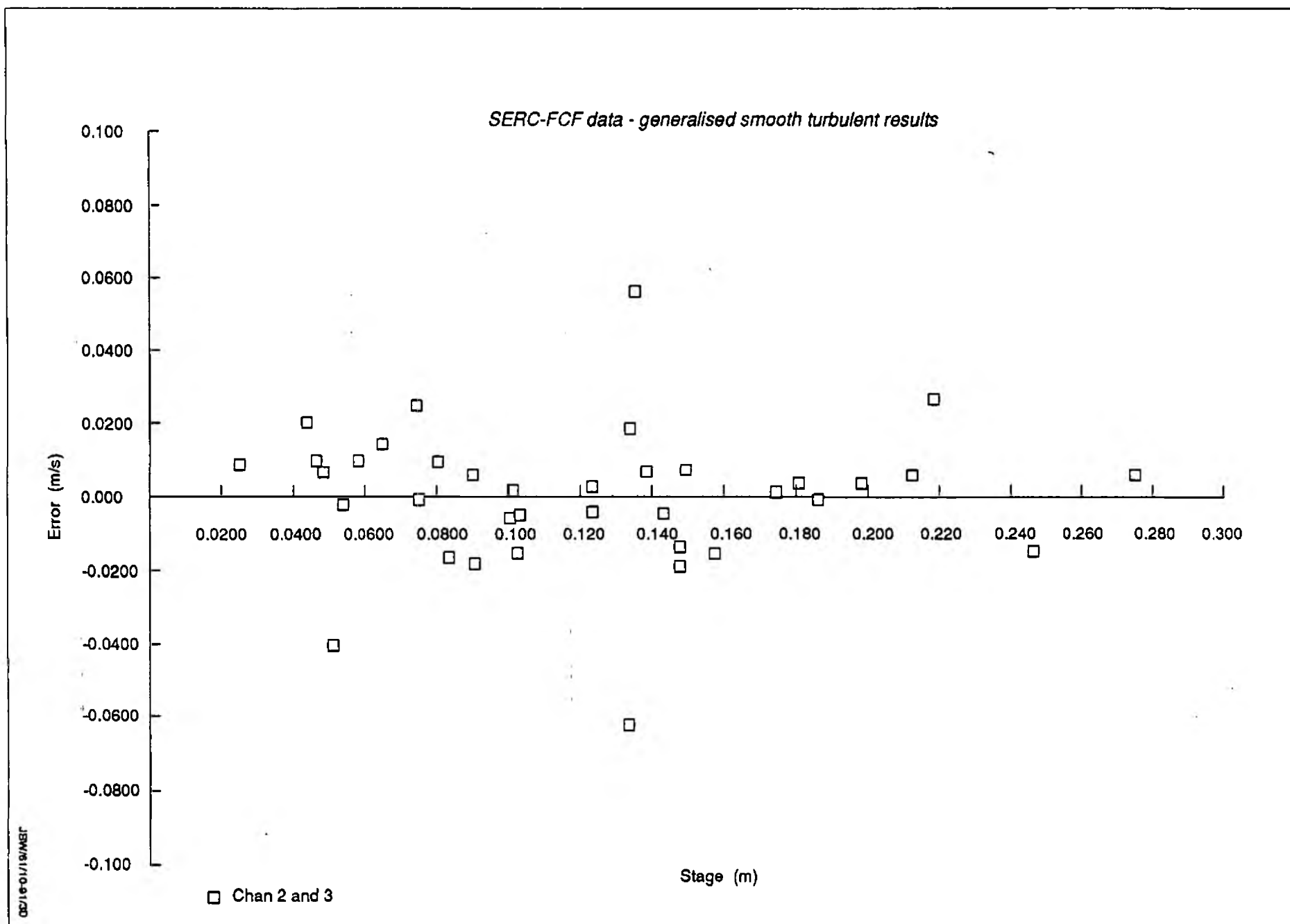
Fig A2.3 Smooth channel calibration: all results

SERC-FCF data - generalised smooth turbulent results - all data

Error (m/s)

Stage (m)

× All data

JBW/52/10-91/30
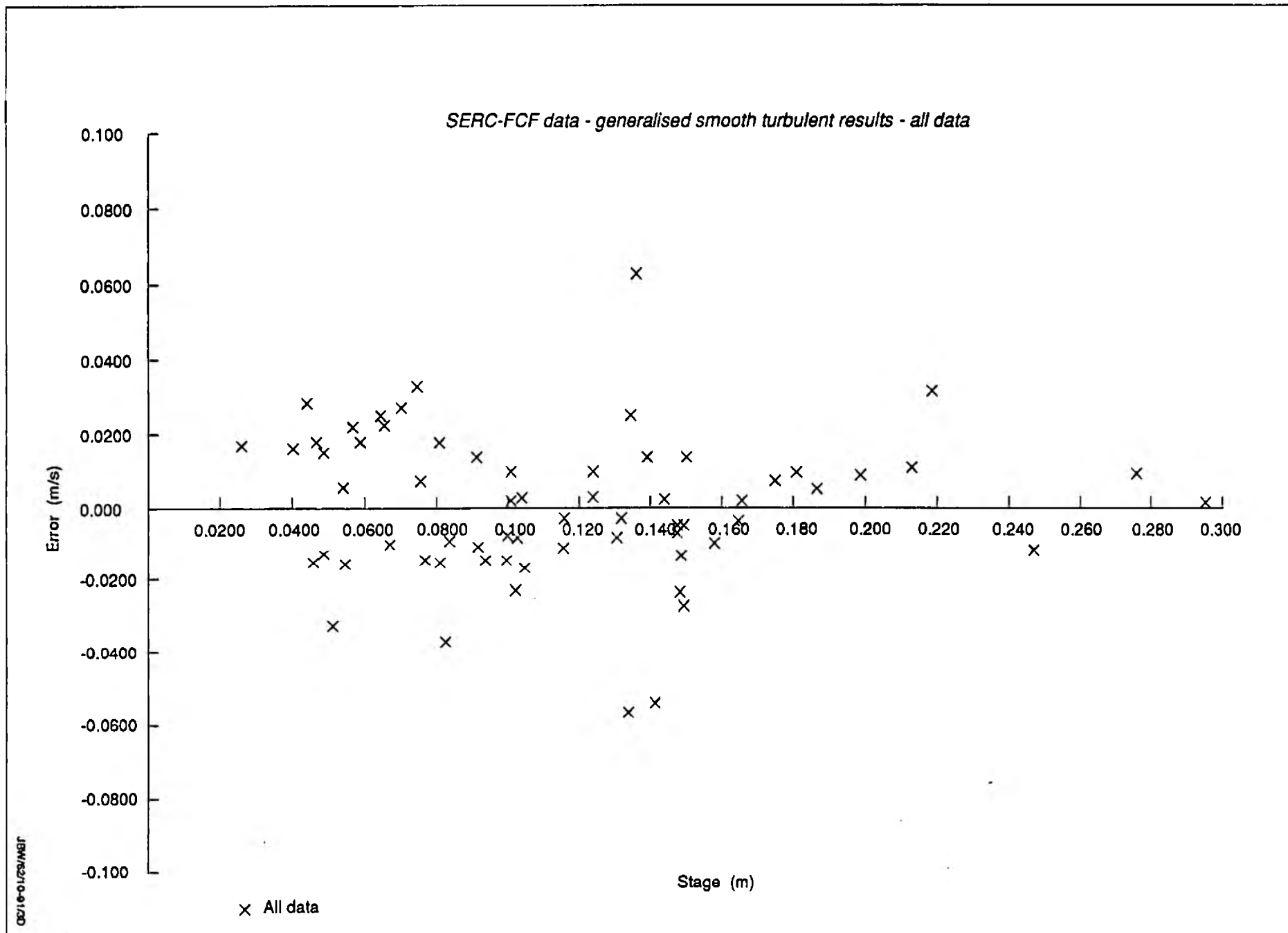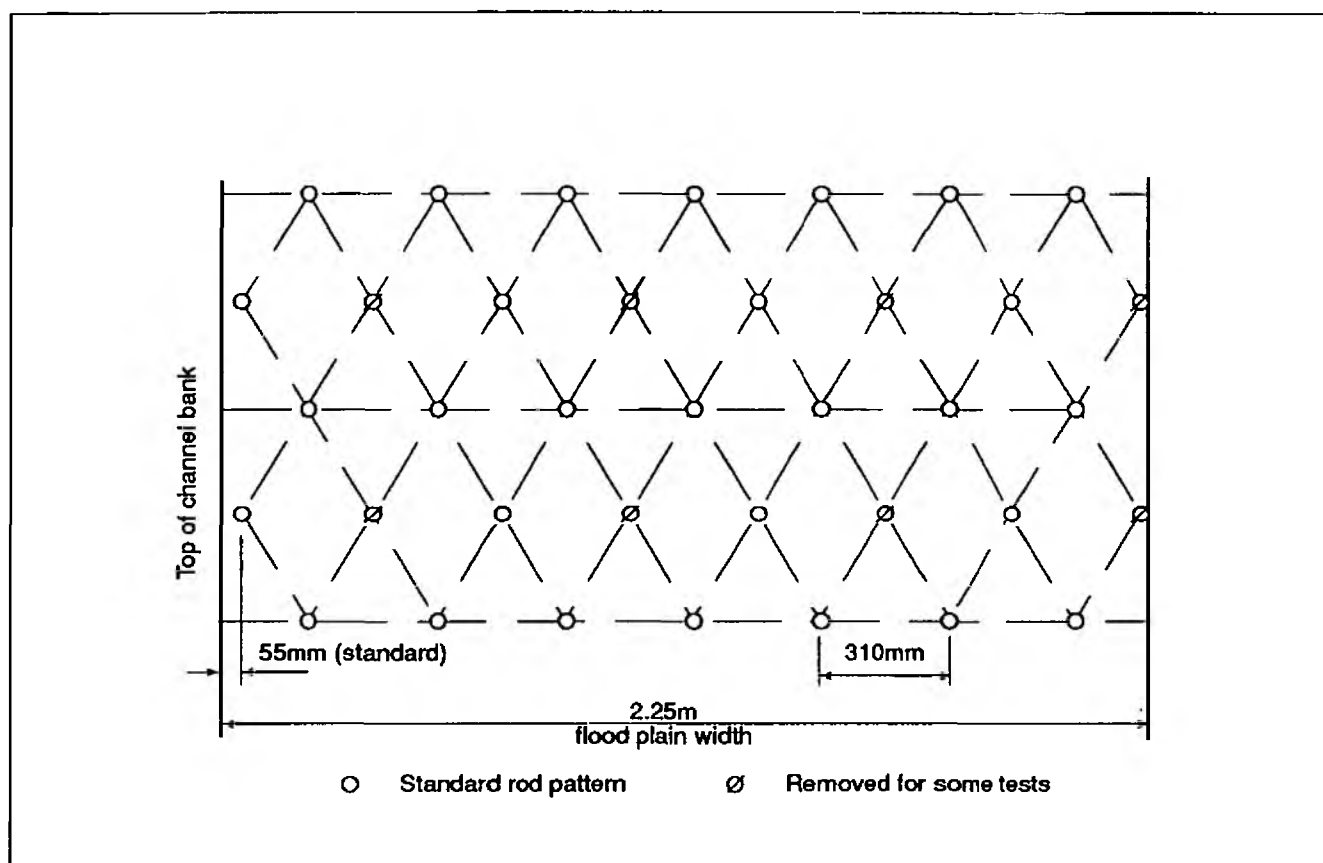
Fig A2.4   Pattern of roughness used on flood plains
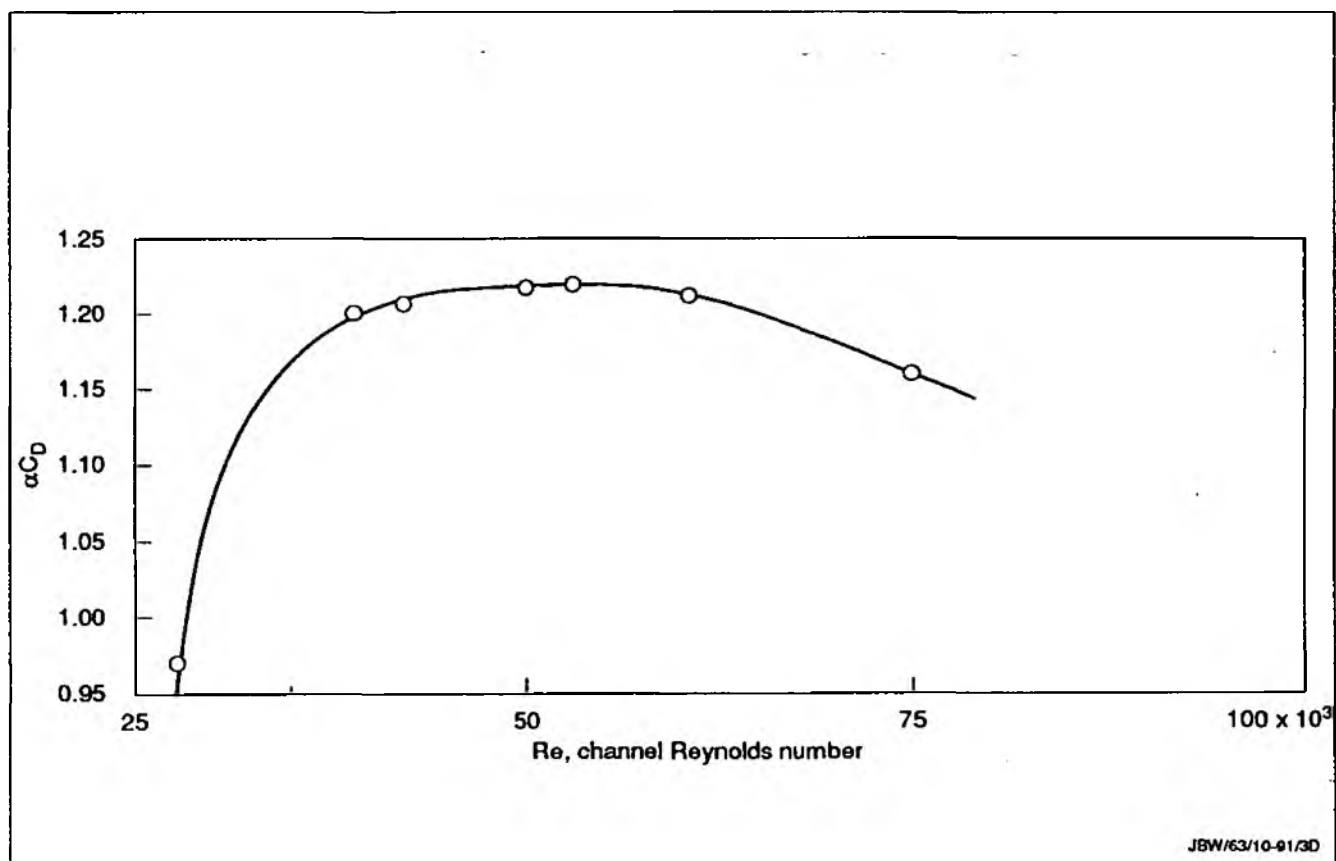
Fig A2.5   Drag coefficient as function of channel Reynolds Number
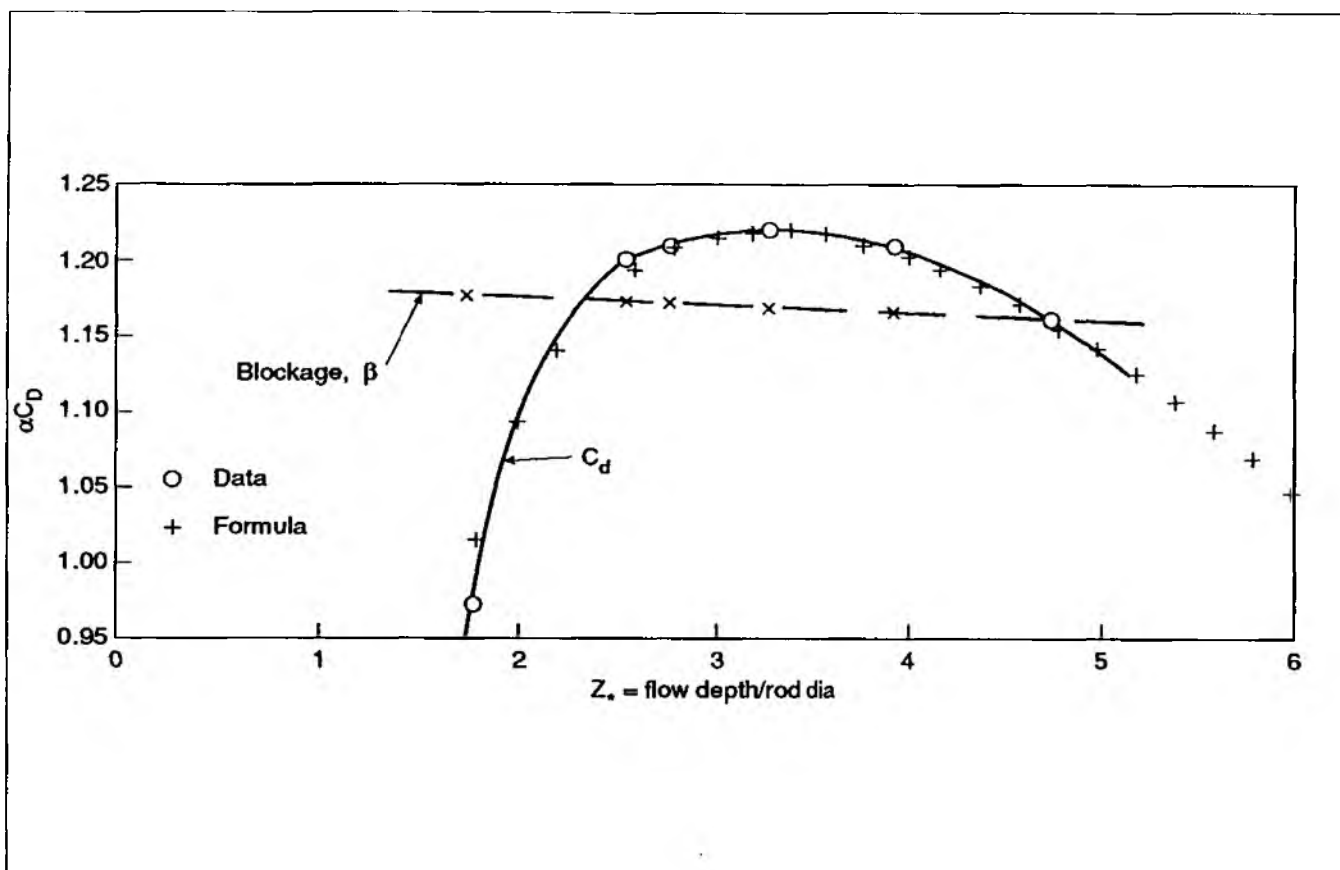
Fig A2.6   Drag coefficient and blockage coefficient as functions of ratio of flow depth to rod diameter, Z∗
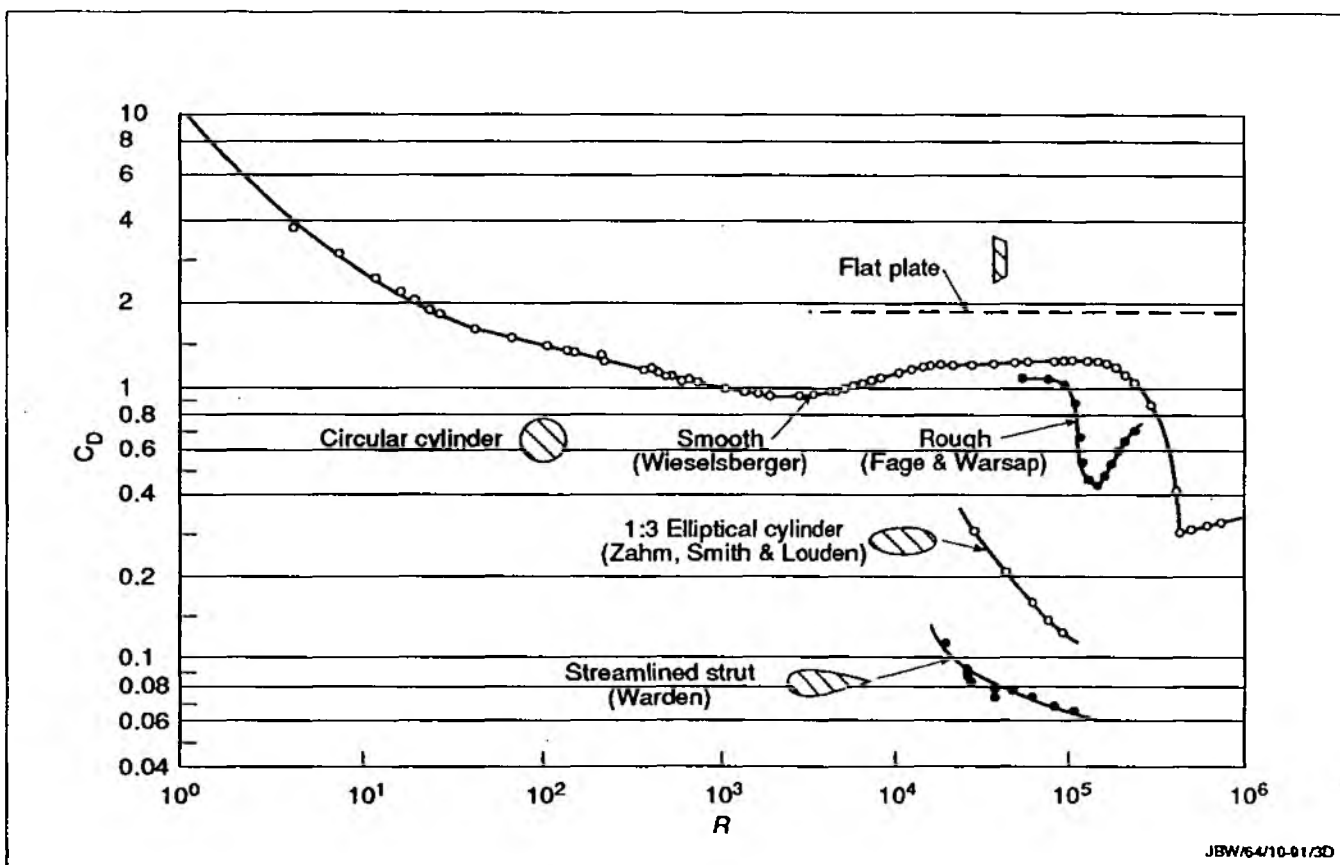
Fig A2.7   Coefficients of drag for two dimensional forms (Rouse, ed., 1950)

APPENDIX 3

CHANNEL COHERENCE

1.   The influence on the discharge of the interaction between main channel and flood plain flows depends on how comparable the hydraulic conditions in these zones are: if velocities and depths are very similar, then we can expect interaction effects to be small; if they are very dissimilar, then major effects are to be expected. The degree to which the different zones exhibit flow similarity will be referred to as their "coherence": the greater their coherence the more likely is the hydraulics of the section to approach simple channel (negligible interaction) conditions.

2.   Channel conveyance is a useful parameter in developing the concept of coherence. Conveyance, $K|V|$, was defined by Ven Te Chow (1959) as:

$$K_V = Q/\sqrt{S} \qquad \qquad \ldots A3.1$$

but it is preferable to redefine it to be consistent with dimensional analysis, as

$$K_D = Q/\sqrt{(8gS)} = A\sqrt{(A/fP)} \qquad \qquad \ldots A3.2$$

Thus the conveyance of a simple channel can be represented by the cross-section area, wetted perimeter and friction factor. For a compound section, the theoretical conveyance before allowing for any interaction effects is given by the sum of the conveyances of the main channel and flood plains:

$$K_D = A_C\sqrt{(A_C/f_C P_C)} + 2\,A_F\sqrt{(A_F/f_F P_F)} \qquad \qquad \ldots A3.3$$

for the situation of two symmetrical flood plains. If the Manning equation is appropriate, then this becomes

$$K_D = A_C(A_C/P_C)^{2/3}/n_C\sqrt{(8g)} + 2\,A_F(A_F/P_F)^{2/3}/n_F\sqrt{(8g)} \qquad \qquad \ldots A3.4$$

3.   This leads to a parameter for the coherence of the channel section, namely the ratio of the theoretical conveyance calculated by treating it as a single unit to that calculated by summing the conveyances of the separate zones. Ideally, the section coherence would be defined as:

$$COH_1 = \frac{\sum\limits_{i=1}^{i=n} A_i \sqrt{[\sum\limits_{i=1}^{i=n} A_i / \sum\limits_{i=1}^{i=n} A_i / f_o \sum P_i]}}{\sum\limits_{i=1}^{i=n} [A_i \sqrt{(A_i/f_i P_i)}]} \qquad \ldots A3.5$$

Note that f_i represents the friction factors for the separate zones, calculated from the appropriate zonal values of Manning's n, Re or relative roughness according to the resistance function being used. f_o, on the other hand, is a global value calculated on the basis of the summed section parameters.

4.   There is a problem with the above definition: in general f_o is not known, because in engineering practice it would depend on some whole-section compendium value of Manning's n. It is calculable if the flood plain and main channel follow identical resistance functions e.g. both smooth, or having the same Manning's n value. So equation 3.5 could be used as the definition of COH for the smooth laboratory case – but could not cover the rough flood plain condition or the general case when different roughnesses or resistance functions apply to different zones. A more useful definition for design purposes is obtained by replacing f_o by the perimeter weighted equivalent deduced from the separate (and calculable) values for the main channel and flood plains.

$$COH_3 = \frac{\sum\limits_{i=1}^{i=n} A_i \sqrt{[\sum\limits_{i=1}^{i=n} A_i / \sum\limits_{i=1}^{i=n}(f_i P_i)]}}{\sum\limits_{i=1}^{i=n} [A_i \sqrt{(A_i/f_i P_i)}]} \qquad \ldots A3.6$$

5.   This parameter, COH_3, varies with flow depth in a given channel, of course, and three cases are illustrated in fig A3.1: the Wallingford channel illustrated in Figure 2.3; the same but with flood plains reduced to 0.25m wide; and the Montford Bridge natural river section shown in Figure 2.2. For the smooth Wallingford channel, the appropriate friction factors were

using (varying with depth because Re varies with depth) and for the Montford Bridge section a constant value of Manning's n was applied for this illustration, with depths related to the lower edge of the flood plains. The artificial channel with horizontal flood plain and flood plain/main channel bed width ratio 1.5 (defined here as the ratio of width of each flood plain to bed width of main channel) has a very low COH value, below 0.3, when the flood plains are first inundated, increasing to 0.94 when the flood plain flow depth equals the depth of main channel. With narrow flood plains, width ratio 0.167, COH is less sensitive to depth and closer to unity, lying between about 0.5 and 0.94. The natural river section has wide flood plains with some cross fall (note that Figure 2.2 has considerable vertical exaggeration) with minimum COH value (0.52), not just above bank full but when the full width of flood plain is inundated. Above this the trend is very similar to the wide laboratory channel, whilst below the trend is towards unity because its sloping flood plains avoid the discontinuity in COH at bank full. (For these calculations the main channel zones 3,4 and 5 of Figure 2.2 were taken together, as were the remaining flood plain areas)

6. For a conventional compound cross-section geometry, the coherence of the section may be expressed in terms of the geometric ratios: let $A_* = N_F A_F / A_C$; $P_* = N_F P_F / P_C$; $H_* = (H-h)/H$; and $f_* = f_F / f_C$, where N_F is the number of flood plains. Then

$$COH_3 = \frac{(1 + A_*)\sqrt{[(1 + A_*)/(1 + f_* P_*)]}}{1 + A_*(A_*/f_* P_*)} \qquad \ldots A3.7$$

In this form it is obvious that as A_* becomes large (deep flow on flood plain) then COH_3 approaches unity, for equal roughness of main channel and flood plain (when f_* approaches unity as the depth increases). Also when A_* is very small (flood plains just inundated) COH_3 approaches $1/\sqrt{(1 + f_* P_*)}$. As A_* and P_* depend on H_*, then for a given geometry COH_3 also depends on H_*.

7. If the Manning equation applies, and perimeter weighting of the friction factor is applied, then the coherence equation becomes:

$$COH_2 = \frac{(1 + A_*)^{3/2}/\sqrt{(1 + P_*^{4/3} n_*^2 /A_*^{1/3})}}{1 + A_*^{5/3}/n_* P_*^{2/3}} \qquad \ldots A3.8$$

8.   Whether the most general form of these definitions of channel coherence (equation A3.7) provides a useful co-ordinating parameter in the analysis of the experimental results remains to be seen. Its potential benefit is that it brings together in one parameter most of the factors expected to influence the hydraulics of compound channels, and so might take the place of relative depth as an indicator of how like a single channel the performance might prove. An expected corollary is that the closer to unity COH approaches, the more likely it is that the channel can be treated as a single unit, using the overall geometry. As f_* is included in the general definition of COH_3 (see equ A3.7), there is some prospect too that dissimilar roughnesses will automatically be covered.

APPENDIX 4: TURBULENCE METHOD, SOLUTION FOR GENERAL CROSS-SECTION SHAPES

The following theory is given by Shiono and Knight (1991), whose assistance
is gratefully acknowledged. Some small corrections to equations 11 in the
published version have been provided by the Authors. The method uses the
depth averaged momentum equations and is general in the sense that it can be
applied to any cross-section which can be described by a series of zones
with linear cross-fall. The following text is a direct quotation from the
1991 paper:

This paper describes an improved analytical solution, developed from the earlier work of **Shiono &
Knight (1988)**, which now includes the effects of secondary flow. Data from the Science and
Engineering Research Council Flood Channel Facility (SERC-FCF) are used to quantify the apparent
shear stresses across a two stage channel arising from turbulence and secondary flow effects. These
apparent shear stresses are then depth averaged to give dimensionless depth averaged eddy viscosity
values. The analytical solution is thus capable of reproducing the lateral distributions of depth mean
velocity and boundary shear stress in compound or two stage channels. It has been applied to several
natural river channels in the Severn-Trent catchment in order to extend the stage discharge relationship
for overbank flow. See **Knight, Shiono & Pirt (1989)** and **Knight, Samuels & Shiono (1990)**.
A typical symmetric two stage channel in which there is no crossfall in regions 1 & 3 is shown in **Fig.2**.
For a sufficiently wide river channel (region 1) and flood plain (region 3), the depth averaged velocity, U_d,
and boundary shear stress, τ_b, will attain constant but different values in the two regions, thus creating a
shear layer in the vicinity of region 2. Due to the re-entrant and channel corners in this region the flow is
also strongly affected by secondary flows.

2. ANALYTICAL SOLUTION

In order to predict the lateral variation of depth mean velocity and boundary shear stress in
open channel flow, the depth mean momentum equation has to be solved for steady uniform turbulent
flow in the streamwise direction. The equation for the longitudinal streamwise component of momentum
on a fluid element may be combined with the continuity equation to give

$$\rho \left[\frac{\partial \overline{U}\overline{V}}{\partial y} + \frac{\partial \overline{U}\overline{W}}{\partial z} \right] = \rho g S_o + \frac{\partial}{\partial y}(-\rho\overline{uv}) + \frac{\partial}{\partial z}(-\rho\overline{uw}) \quad \cdots (1)$$

where
- x, y, z are streamwise, lateral and normal directions respectively
- $\overline{U},\overline{V},\overline{W}$ are temporal mean velocity components corresponding to x,y,z
- u,v,w are turbulent perturbations of velocity with respect to the mean
- ρ is the density of water
- g is the gravitational acceleration
- S_o is the bed slope gradient ($S_o = \sin\theta$)

The depth mean averaged momentum equation can be obtained by integrating **equation (1)** over
the water depth, H. Provided $\overline{W}(H) = \overline{W}(O) = 0$, then **Shiono and Knight (1988)** show that equation
(1) becomes

$$\frac{\partial H(\rho \overline{U}\overline{V})_d}{\partial y} = \rho g H S_o + \frac{\partial H \overline{\tau}_{yx}}{\partial y} - \tau_b \sqrt{1 + \frac{1}{s^2}} \quad \cdots (2)$$

where τ_b is the bed shear stress

          s   is the side slope (1:s, vertical:horizontal)

$$(\rho\bar{U}\bar{V})_d = \frac{1}{H}\int_0^H \rho\bar{U}\bar{V}dz \quad \text{and} \quad \bar{\tau}_{yx} = \frac{1}{H}\int_0^H (-\rho\overline{uv})dz$$

Analytical solutions have been obtained to equation (2) based on the eddy viscosity approach and by neglecting the secondary flow contribution i.e. $(\partial(H\rho\bar{U}\bar{V})_d/\partial y = 0)$. The eddy viscosity approach has been adopted because of its common usage by numerical modellers. In this model the depth averaged transverse shear stress, $\bar{\tau}_{yx}$, is expressed in terms of the lateral gradient of depth mean velocity

$$\bar{\tau}_{yx} = \rho\bar{\epsilon}_{yx}\frac{\partial U_d}{\partial y} \qquad \qquad \text{.... (3)}$$

Since the eddy viscosity has dimensions of m^2s^{-1}, it is often related to the local shear velocity, U_* and depth, H, by the dimensionless eddy viscosity coefficient, λ, defined by

$$\bar{\epsilon}_{yx} = \lambda U_* H \qquad \qquad \text{... (4)}$$

However as equation (2) shows, the local shear velocity, $U_* (= \sqrt{(\tau_b/\rho)})$ is affected by the free shear layer turbulence and the secondary flows. In regions of high lateral shear it might be argued that the U_* in equation (4) should be replaced by the primary or shear velocity difference between the two regions. However in the interests of simplicity and because of its common usage by hydraulic modellers the form of equation (4) is retained with λ being regarded as a 'catch all' parameter to describe various 3-D effects. In order to express equation (2) in terms of one variable only (U_d or τ_b), the Darcy-Weisbach friction, f $(=8\tau_b/(\rho U_d2))$ is used to link U_* and U_d, giving

$$U_* = \left[\frac{f}{8}\right]^{\frac{1}{2}} U_d \qquad \qquad \text{.... (5)}$$

The depth averaged eddy viscosity in equation (4) may then be expressed in the form

$$\bar{\epsilon}_{yx} = \lambda H \left[\frac{f}{8}\right]^{\frac{1}{2}} U_d$$

$$\text{... (6)}$$

Substituting equations (3) & (6) into equation (2) gives

$$\rho g H S_0 - \rho\frac{f}{8}U_d^2\sqrt{1+\frac{1}{s^2}} + \frac{\partial}{\partial y}\left\{\rho\lambda H^2\left[\frac{f}{8}\right]^{\frac{1}{2}}U_d\frac{\partial U_d}{\partial y}\right\} = \frac{\partial}{\partial y}\left\{H(\rho\bar{U}\bar{V})_d\right\} \qquad \text{.... (7)}$$

In an earlier paper, Shiono & Knight (1988) assumed that $\partial(H\rho\bar{U}\bar{V})_d/\partial y = 0$ and obtained analytical solutions to equation (7) for channels of various shape. The experimental results which are described in a later section of this paper suggest that for the particular cases considered the shear stress due to secondary flow, $(\rho\bar{U}\bar{V})_d$, decreases approximately linearly either side of a maximum value which

occurs at the edge of the flood plain and the main channel. Although this is a first order approximation to the data, as Fig.7 will later show, it does have the merit that it then allows equation (7) to be solved analytically. Further data from a wider range of channel geometries are clearly needed before this assumption may be generally accepted. However, if this is so, then the lateral gradient of the secondary flow force per unit length of the channel may be written as

$$\frac{\partial (H\rho \bar{U}\bar{V})_d}{\partial y} = \Gamma_{mc} \quad or \quad \Gamma_{fp} \qquad \qquad \cdots (8)$$

where the subscripts mc and fp refer to the main channel and flood plain respectively. The analytical solution to equation (7) may then be expressed for a constant depth H domain as

$$U_d = \left\{ A_1 e^{\gamma y} + A_2 e^{-\gamma y} + \frac{8gS_oH}{f}(1-\beta) \right\}^{\frac{1}{2}} \qquad \qquad \cdots (9)$$

and for a linear side slope domain as

$$U_d = \left\{ A_3\xi^{\alpha_1} + A_4\xi^{-\alpha_1-1} + \omega\xi + \eta \right\}^{\frac{1}{2}} \qquad \qquad \cdots (10)$$

where

$$\gamma = \left(\frac{2}{\lambda}\right)^{1/2} \left(\frac{f}{8}\right)^{1/4} \frac{1}{H} \quad , \qquad \beta = \frac{f\Gamma}{8gS_oH}$$

$$\alpha_1 = -\frac{1}{2} + \frac{1}{2} \left\{ 1 + \frac{s\sqrt{1+s^2}}{\lambda} \sqrt{8f} \right\}^{\frac{1}{2}}$$

$$\omega = \frac{gS_o}{\frac{\sqrt{1+s^2}}{s} \frac{f}{8} - \frac{\lambda}{s^2}\sqrt{\frac{f}{8}}}$$

$$\eta = -\frac{\Gamma}{s\sqrt{1+s^2} \frac{2}{\lambda}\sqrt{\frac{f}{8}}} \qquad \qquad \cdots (11)$$

and ξ = depth function on the side slope domain (e.g. ξ = H - ((y-b)/s) for the main channel side slope).

Equations (9)-(11) give the lateral variation of depth mean velocity and boundary shear stress (via equation (5)) in a channel of any shape provided its geometry can be described by a number of linear boundary elements. For a constant depth domain, equation (9) shows that as y $\rightarrow$ ∞ with γ > 0, since the flow must become two dimensional ($U_d = (8gS_oH/f)^{1/2}$) in the far field where no secondary flow exists (β = 0), therefore A_1 = 0. For a sloping side slope domain, equation (10) shows as s $\rightarrow$ ∞, A_3 must be zero in order that a solution might exist. Equations (9) and (10) also require boundary conditions of continuity of HU_d and $\partial(HU_d)/dy$ across joints of domains, together with the no slip condition, U_d = 0, at the remote boundaries. The sub division of the channel cross section into various sub areas with either constant depth domains or sloping side slope domains will therefore require sufficient computer capacity for the matrix inversion of the coefficients A_1 ... A_n. Examples of complex natural geometries modelled in this way are given in Knight, Shiono & Pirt (1989) and Knight, Samuels & Shiono (1990).

APPENDIX 5: DATA ON CHANNEL ROUGHNESS

The following information is extracted from Ven Te Chow (1959) and retains
his classification, with the omission of closed conduit data (class A).
Refer to Chapter 7 for additional information on channel roughness. The
following table is intended to provide some guidance where no other
information may be available, but wherever practicable the roughness
coefficients should be based on observations from the system under review,
or from similar systems for proposed channels. The information in Table
A5.1 here is in terms of Manning's n, but this is not to be taken as a
general recommendation for the best resistance function. In many
circumstances, and especially in lined channels, the Colebrook-White
function might be more appropriate. Some information on k_s values for use
in the Colebrook-White equation is given in a supplementary table, A5.2, at
the end of the Appendix.

TABLE A5.1. RECOMMENDED ROUGHNESS COEFFICIENTS FOR USE IN MANNING EQUATION AS GIVEN BY VEN TE CHOW. ("Normal" values are typically used).

Type of channel and description			Min	Normal	Max
B		Lined or built-up channels			
B-1		Metal			
	(a)	Smooth steel surface			
		1. Unpainted	0.011	0.012	0.014
		2. Painted	0.012	0.013	0.017
	(b)	Corrugated	0.021	0.025	0.030
B-2		Non-metal			
	(a)	Cement			
		1. Neat, surface	0.010	0.011	0.013
		2. Mortar	0.011	0.013	0.015
	(b)	Wood			
		1. Planted, untreated	0.010	0.012	0.014
		2. Planed, creosoted	0.011	0.012	0.015
		3. Unplained	0.011	0.013	0.015
		4. Plank with battens	0.012	0.015	0.018
		5. Lined with roofing paper	0.010	0.014	0.017
	(c)	Concrete			
		1. Trowel finish	0.011	0.013	0.015
		2. Float finish	0.013	0.015	0.016
		3. Finished, with gravel on bottom	0.015	0.017	0.020
		4. Unfinished	0.014	0.017	0.020
		5. Gunite, good section	0.016	0.019	0.023
		6. Gunite, wavy section	0.018	0.022	0.025
		7. On good excavated rock	0.017	0.020	
		8. On irregular excavated rock	0.022	0.027	
	(d)	Concrete bottom float finished with sides of:			
		1. Dressed stone in mortar	0.015	0.017	0.020
		2. Random stone in mortar	0.017	0.020	0.024
		3. Cement rubble masonry, plastered	0.016	0.020	0.024
		4. Cement rubble masonry	0.020	0.025	0.030
		5. Dry rubble or rip-rap	0.020	0.030	0.035
	(e)	Gravel bottom with sides of:			
		1. Formed concrete	0.017	0.020	0.025
		2. Random stone in mortar	0.020	0.023	0.026
		3. Dry rubble or rip-rap	0.023	0.033	0.036
	(f)	Brick			
		1. Glazed	0.011	0.013	0.015
		2. In cement mortar	0.012	0.015	0.018
	(g)	Masonry			
		1. Cemented rubble	0.017	0.025	0.030
		2. Dry rubble	0.023	0.032	0.035
	(h)	Dressed Ashlar	0.013	0.015	0.017
	(i)	Asphalt			
		1. Smooth	0.013	0.013	
		2. Rough	0.016	0.016	
	(j)	Vegetal lining	0.030	-	0.500

DATA ON CHANNEL ROUGHNESS (cont'd)

Type of channel and description	Min	Normal	Max
C. Excavated or dredged			
(a) Earth, straight and uniform			
1. Clean, recently completed	0.016	0.018	0.020
2. Clean, after weathering	0.018	0.022	0.025
3. Gravel, uniform section, clean	0.022	0.025	0.030
4. With short grass, few weeds	0.022	0.027	0.033
(b) Earth, winding and sluggish			
1. No vegetation	0.023	0.025	0.030
2. Grass, some weeds	0.025	0.030	0.033
3. Dense weeks or aquatic plants in deep channels	0.030	0.035	0.040
4. Earth bottom and rubble sides	0.028	0.030	0.035
5. Stony bottom and weedy banks	0.025	0.035	0.040
6. Cobble bottom and clean sides	0.030	0.040	0.050
(c) Dragline-excavated or dredged			
1. No vegetation	0.025	0.028	0.033
2. Light brush on banks	0.035	0.050	0.060
(d) Rock cuts			
1. Smooth and uniform	0.025	0.035	0.040
2. Jagged and irregular	0.035	0.040	0.050
(e) Channels not maintained, weeds and brush uncut			
1. Dense weeds, high as flow depth	0.050	0.080	0.120
2. Clean bottom, brush on sides	0.040	0.050	0.080
3. Same, highest stage of flow	0.045	0.070	0.110
4. Dense brush, high stage	0.080	0.100	0.140
D. Natural streams			
D-1 Minor streams (top width at flood stage <100 ft)			
(a) Streams on plain			
1. Clean, straight, full stage no rifts or deep pools	0.025	0.030	0.033
2. Same as above, but more stones and weeds	0.030	0.035	0.040
3. Clean, winding, some pools and shoals	0.033	0.040	0.045
4. Same as above, but some weeds and stones	0.035	0.045	0.050
5. Same as above, lower stages more ineffective slopes and sections	0.040	0.048	0.055
6. Same as 4, but more stones	0.045	0.050	0.060
7. Slugish reaches, weedy, deep pools	0.050	0.070	0.080

8. Very weedy reaches, deep pools, or floodways with heavy stand of timber and underbrush	0.075	0.100	0.150
(b) Mountain streams, no vegetation in channel, banks usually steep, trees and brush along banks submerged at high stages			
1. Bottom: gravels, cobbles, and few boulders	0.030	0.040	0.050
2. Bottom: cobbles with large boulders	0.040	0.050	0.070

D-2   Flood plains

(a) Pasture, no brush			
1. Short grass	0.025	0.030	0.035
2. High glass	0.030	0.035	0.050
(b) Cultivated areas			
1. No crop	0.020	0.030	0.040
2. Mature row crops	0.025	0.035	0.045
3. Mature field crops	0.030	0.040	0.050
(c) Brush			
1. Scattered brush, heavy weeds	0.035	0.050	0.070
2. Light brush and trees, in winter	0.035	0.050	0.060
3. Light brush and trees, in summer	0.040	0.060	0.080
4. Medium to dense brush, in winter	0.045	0.070	0.110
5. Medium to dense brush, in summer	0.070	0.100	0.160
(d) Trees			
1. Dense willows, summer, straight	0.110	0.150	0.200
2. Cleared land with tree stumps, no spouts	0.030	0.040	0.050
3. Same as above, but with heavy growth of sprouts	0.050	0.060	0.080
4. Heavy stand of timber, a few down trees, little undergrowth, flood stage below branches	0.080	0.100	0.120
5. Same as above, but with flood stage reaching branches	0.100	0.120	0.160

D-3   Major streams (top width at flood stage > 100 ft). The n value is less than that for minor streams of similar description, because banks offer less effective resistance.

(a) Regular section with no boulders or brush	0.025	–	0.060
(b) Irregular and rough section	0.035	–	0.100

TABLE A5.2. RECOMMENDED ROUGHNESS VALUES, k_S IN MM, FOR LINED CHANNELS, FOR USE IN COLEBROKE-WHITE EQUATION

	CONDITION		
CONCRETE:	Good	Normal	Poor
Class 4: Monolithic construction against oiled steel forms, with no surface irregularities.	0.06	0.15	–
Class 3: Monolithic construction against steel forms, but less perfect surface.	–	0.15	0.3
Class 2: Monolithic construction against rough forms; cement gun surface (for very coarse texture take k_S = aggregate size in evidence)	0.6	1.5	–
Class 1: Smooth trowelled surfaces	0.3	0.6	1.5
BRICKWORK:			
Well pointed brickwork	1.5	3	6
Old brickwork in need of pointing	–	15	30

APPENDIX 6: EXAMPLE OF CHANNEL GEOMETRY CONVERSION AND STAGE DISCHARGE COMPUTATION.

Channel geometry conversion

1. As natural channels, and also many man-made compound channels, do not have the "classical" shape of a symmetric two-stage trapezoidal cross-section, some method of working out an equivalent section is required, in order to define the various parameters that appear in the various formulae for predicting the discharge as a function of flow depth. The method was explained in Chapter 7, section 7.1, and examples from real rivers were illustrated in Figures 5.12 and 5.13. It should be appreciated, however, that the calculation of many of the basic geometric elements and discharges does not require any conversion or approximation: the full detail of the surveyed cross sections may be – and ideally should be – used for calculating the areas, wetted perimeters and hydraulic mean depths of the main channel and flood plain, once the vertical divisions at the top edge of the channel banks have been determined. An idealised section is, however, required to determine bank slopes, mean bed level, mean level of the bank tops (hence channel depth), channel top width, channel bed width and flood plain width. These geometric parameters of a somewhat idealised cross-section are required to solve the equations for Region 1 in particular.

2. The channel considered here is based on a real river which has been improved as part of a flood relief project. Thus realistic simulated flow data can be associated with it based on measured data, but the river section and flow data have been scaled and modified so that it becomes an anonymous case. The upper part of Figure A6.1 shows the section as it might have been surveyed, and crosses have been added to mark the eight points defining the idealised section in the lower part of the figure. The x-y co-ordinates of the idealised section are shown below. The vertical divisions between main channel and flood plains are now identified, as are bank slopes, mean bed level, bed width etc. In what follows, two depths of flow are considered in detail, corresponding to stages of 3.0m and 4.5m, to illustrate the detailed computation procedure. However, normally a computer program would be used for this, and so these two sample depths are set in the context of tabular summaries of the results of applying a program written in Basic. This

program was developed for analysing laboratory data so has some extra simplifications: it converts the idealised section of figure A6.1 into a completely symmetrical section before working out the geometry.

Using within bank data to assess main channel resistance coefficient

3. It is unnecessary to explain in detail how to work out Manning's n for within bank flows for a given set of stage discharge data: this is very conventional hydraulic computation. Similarly, if another friction equation such as the Colebrook-White formula was preferred, the calculations, though a shade more complex, are straight forward. Table A6.1 is computed output, showing:

- the geometric details
- the set of stage-discharge data available (z = stage relative to channel bed)
- the analysis of these data both in terms of Manning and Colebrook-White (wide channel version)
- check calculations for n_c = 0.025 to examine how good a fit to the data it is.

4. The stage-discharge data here assumes that the hydraulic gradient matched the channel slope in all cases. This is not necessarily so, and if reliable measurements of hydraulic gradient are available, they should be used, of course. The temperature is required in order to assess viscosity, though in practice in real rivers the viscous term in the Colebrook-white equation is small, and in some cases negligible. The analysis of the data shows n_c (Man in the table) to vary in the range 0.022 to 0.026, with perhaps a marginal trend to increase with depth. The results approaching bank full (z = 2.0m) suggest using n_c = 0.025, hence the final part of table A6.1. Here Qex/Qt shows the ratio of observed discharge to calculated discharge, with average 1.026 and standard deviation 5.56 %. Much of the positive discrepancy comes from one result at depth 1.58m, so the conclusion is that a Manning's n value for the main channel of 0.025 is appropriate for the computations under compound flow. The variability of around 5%, or 10% at 95% confidence, is fairly typical of field observations. As there are ten results, the accuracy of determination of the roughness coefficient is

about 3% (2 x s.d./√no. of observations, at 95%). It would have been equally valid to proceed using the Colebrook-White function, with k_S having an average value of 64mm.

Detailed calculations: sample for two flow depths

5. *Geometry*: Refer to figure A6.1 for co-ordinates, hence dimensions. Areas 1 to 7 proceed from left to right.

Side slopes: $s_{FL} = 0.30/1.47 = 0.204$, $\quad s_{CL} = 1.66/1.86 = 0.892$

$\qquad\qquad\quad s_{FR} = 2.10/1.68 = 1.25$, $\quad s_{CR} = 2.20/2.14 = 1.028$

$\qquad\qquad\quad s_{Fav} = \qquad\qquad 0.727 \quad s_{Cav} = \qquad\qquad 0.960$

Areas: Stage 3.0m: Stage 4.5m:

	Stage 3.0m		Stage 4.5m	
1.	0.42 x 0.204/2	0.018	1.92 x 0.204/2	0.376 m
2.	(0.42 + 1.07) 13.26/2	9.879	(1.92 + 2.57) 13.26/2	29.769
3.	(1.07 + 2.93) 1.66/2	3.320	(2.57 + 4.43) 1.66/2	5.810
4.	(2.93 + 3.07) 22.03/2	66.090	(4.43 + 4.57) 22.03/2	99.135
5.	(3.07 + 0.93) 2.20/2	4.400	(4.57 + 2.43) 2.20/2	7.700
6.	(0.93 + 0.36) 13.05/2	8.417	(2.43 + 1.86) 13.05/2	27.992
7.	0.36 x 1.25/2	0.081	1.86 x 1.25/2	2.162

$\qquad\qquad\qquad A_C \quad$ 73.810 $\qquad\qquad\qquad\qquad\qquad$ 112.645 m²

$\qquad\qquad 2 \times A_F \quad$ 18.395 $\qquad\qquad\qquad\qquad\qquad$ 60.299 m²

$\qquad\qquad\qquad A_T \quad$ 92.205 $\qquad\qquad\qquad\qquad\qquad$ 172.944 m²

Wetted perimeters: $\sqrt{(1 + s_{FL})} = 1.021$; $\sqrt{(1 + s_{CL})} = 1.340$

$\qquad\qquad\qquad\qquad\quad \sqrt{(1 + s_{FR})} = 1.601$; $\sqrt{(1 + s_{CR})} = 1.434$

Stage 3.0m: Stage 4.5m:

1.	1.021 x 0.42	0.429	1.021 x 1.92		1.960 m
2.	(13.26 + 0.65)	13.276			13.276 m
3.	1.340 x 1.860	2.492			2.492 m
4.	(22.03 + 0.14)	22.030			22.030 m
5.	1.434 x 2.14	3.067			3.067 m
6.	(13.05 + 0.57)	13.062			13.062 m
7.	1.601 x 0.36	0.576	1.601 x 1.86		2.978 m

$$P_C \quad 27.592 \qquad\qquad 27.592 \text{ m}$$
$$2 \times P_F \quad 27.343 \qquad\qquad 31.276 \text{ m}$$
$$P_T \quad 54.935 \qquad\qquad 58.868 \text{ m}$$

Hydraulic mean depths:

Stage 3.0m   Stage 4.5m

R_C = 73.810/27.592   2.675   112.645/27.592   4.083 m
R_F = 18.395/27.343   0.672   60.299/31.276   1.928 m

Ratios:

A_* = 18.395/73.810   0.249   60.299/112.645   0.535
P_* = 27.343/27.592   0.991   31.277/27.592   1.134
R_* = 0.672/2.675   0.251   1.928/4.083   0.472

6. *Basic resistance calculation:* The best value of the Manning
coefficient for the main channel was established at 0.025 by utilising
stage-discharge observations at high within-bank flows. There is no direct
way of establishing the appropriate flood plain value, so there is an
element of trial and error involved. Of course through experience and other
sources of information, a reasonable first guess may be made. The flood
plains here are grass berms, usually well maintained. Table A5.1 of
Appendix 5 suggests that the flood plain roughness might be in the range
0.025 to 0.035 (Pasture, no brush, short grass) so the first assumption is
that n_F = 0.030.

S = 0.470/1000 so s = 0.02168.

Stage 3.0m   **Stage 4.5m**

V_C = $2.675^{2/3}$ x 0.02168/0.025   1.671 $4.083^{2/3}$ x 0.02168/0.025   2.215 m/s
Q_C = 1.671 x 73.810   123.34   2.275 x 112.645   249.55 m³/s
V_F = $0.672^{2/3}$ x 0.02168/0.030   0.554 $1.928^{2/3}$ x 0.02168/0.030   1.119 m/s
2 Q_F (sum of flood plain flows) =
0.0554 x 18.395   10.20   1.119 x 60.299   67.50 m³/s

Q_{Tbasic} <u>133.54</u>   <u>317.05 m³/s</u>

Friction factors: f = 8gRS/V²; 8gS = 8 x 9.81 x 0.470/1000 = 0.03689

Stage 3.0m   **Stage 4.5m**

f_C = 0.03689 x 2.675/1.671   0.03535   0.03689 x 4.083/2.215   0.03068
f_F = 0.03689 x 0.672/0.554   0.08050   0.03689 x 1.928/1.119   0.05682
f_* = f_F/f_C 2.277   1.852

Coherence: all necessary parameters are now available to calculate
coherence, COH, using eq 13 of the Summary and Design Method.

Stage 3.0m   **Stage 4.5m** -

COH =

$$\frac{(1+0.249)\sqrt{[(1+0.249)/(1+2.277 \times 0.991)]}}{1 + 0.249\sqrt{(0.249/2.777 \times 0.991)}} \qquad \frac{(1+0.535)\sqrt{[(1+0.535)/(1+1.852 \times 1.134}}{1 + 0.0535\sqrt{(0.535/1.852 \times 1.134}}$$
= 0.7144   = 0.8506

7. In effect, the calculations for stages of 3.0m and 4.5m are examples of
what would normally be a sequential set of calculations for a full range of
stages, progressing in sufficiently small depth steps to provide all the
geometric information required to establish a close coverage of the
stage-discharge function. It is assumed that the actual range of depths for
this case goes up to 5m, to cover a rare flood, but when calculating for
Region 2 flows some geometric information is required for greater depths, as
values of coherence, COH, are needed as will be explained later. In
consequence, the computer version of the geometric calculation has been
taken up to 8m depth, in steps of 0.25m, as given in table A6.2. A

cross-check with the detailed calculation at depths, z = H of 3.0m and 4.5m shows close agreement, though as mentioned earlier the particular program used approximates the idealised section by a fully symmetric one, which marginally changes wetted perimeters. This feeds through the remaining computations to yield small differences to the values of COH. Note that these coherence values are specific to the assumed roughness coefficients for main channel and flood plain: any change in those would require a recomputation of friction factors etc. With this body of basic information, we may proceed to calculate discharges for our sample stages, for the four Regions of flow in turn.

8. Region 1: Some further parameter values are required: For both sample depths, the full flood plain width is inundated, which therefore provides the value of 2B. At shallower depths, 2B would be defined by the variable water surface width, as shown in Table A6.2.

$2B$ = 52.50 - 0.30 = 52.20m
$2b$ = 37.25 - 15.22 = 22.03m; b = 11.015m
$2w_C$ = 39.45 - 13.56 = 25.89m
h_{av} = (1.93 + 2.07)/2 - (0.07 + (-0.07))/2 = 2.00m
Aspect ratio = 22.03/2.00 = 11.015

As this is below 20 (see para 10.1.7), ARF = aspect ratio/10 = 1.10. Region 1 flows are calculated from the equations 2 to 9 of the Summary and Design Method. As s_C < 1, equ. 7 applies:

Stage 3.0m: H_* = 0.3333   Stage 4.5m: H_* = 0.5556

Eq 7; G = 10.42 +   10.42 +
0.17x0.960x1.852 + 0.34(1-0.960)   0.17x0.960x2.277 + 0.34(1-0.960)
= 10.42 + 0.3716 + 0.0136 = 10.805   = 10.42 + 0.3022 + 0.0136 = 10.736
Eq 2;
Q_{*2F} = -1.0x0.3333/2.277 = -0.146   -1.00x0.5556/1.852 =   -0.300
Eq 3;
Q_{*2C} = -1.240 + 0.395x52.20/25.89   -1.240 + 0.395x52.20/25.89
+ 10.805x0.3333   + 10.736x0.5556
= -1.240 + 0.7964 + 3.6017 = 3.158   = -1.240 + 0.7964 + 5.9649 = 5.521

Eq 8; DISDEF =

$$(3.158-2\times0.146)(1.671-0.554)x \qquad (5.521-2\times0.300)(2.215-1.119) \; x$$

$$3.00 \times 2.00 \times 1.10 = \quad 21.13 \; \text{m}^3/\text{s} \quad 4.50 \times 2.00 \times 1.10 = \quad 53.39 \; \text{m}^3/\text{s}$$

Eq 9;

$$Q_{R1} = 133.54 - 21.13 \quad \underline{112.41 \; \text{m}^3/\text{s}} \quad 317.05 - 53.39 = \quad \underline{263.66 \quad \text{m}^3/\text{s}}$$

9. Region 2: This depends on coherence calculated with a shift in H_*. As $s_C < 1$, eq 12 applies:

shift $= -0.01 + 0.05 \times 2 + 0.06 \; s_C = 0.09 + 0.06 \times 0.960 = 0.1476$

Stage 3.0m; $H_* = 0.3333$ Stage 4.5m: $H_* = 0.5556$

$H_* +$ shift $= \qquad 0.4809 \qquad\qquad\qquad\qquad\qquad 0.7032$

From the definition of H_*, $H_* = (H-h)/H$ and so $H = h/(1 - H_*)$

Shifted value of H =

$$2.00/(1 - 0.4809) = \quad 3.853 \quad 2.00/(1-0.7032) = \qquad 6.739$$

(Extending the depth beyond the real section raises some conceptual problems. but as it results from empirical analysis these need not cause concern. In practice, the flood plain back slopes should be extended upwards as necessary).

The detail for calculating COH at these values of H_* in essence repeats the calculations in paragraphs 1 to 6 above, but with the "shifted" hypothetical depths of flow. In practice a computer program would be used, as mentioned earlier leading to Table A6.2. The easy option of interpolating between the values in this table will be taken: and this also explains why that table was continued beyond the flow depth of 5m which the stage/discharge function is to cover.

Stage 3.0m   Stage 4.5m

Eq 10: DISADF

= COH for shifted $H_* = 0.819$ 0.894

Hence $Q_{R2} =$

0.819×133.54 $\underline{109.37\text{m}^3/\text{s}}$ 0.894×317.05 $\underline{283.44\text{m}^3/\text{s}}$

10.   <u>Region 3</u>: This depends on the value of COH (without H_* shift)

<u>Stage 3.0m</u>   <u>Stage 4.5m</u>

Eq 16: DISADF
= 1.567 - 0.667 x 0.7144   1.090   1.567 - 0.667 x 0.8506   0.9996
Q_{R3} = 1.090 x 133.54 =   <u>145.62</u> m³/s 0.9996 x 317.05 =   <u>316.94</u> m³/s

11.   <u>Region 4</u>:

Eq 18: DISADF = COH
Q_{R4} = 0.7144 x 133.54   <u>95.40</u> m³/s 0.8506 x 317.05   <u>269.68</u> m³/s

12.   <u>Logic for selection of region of flow</u>: Equations 20, and if necessary
in turn 21 and 22, are applied to determine which region the flow is in:

<u>Stage 3.0m</u>   <u>Stage 4.5m</u>

From eq 20,
Q_{R1} = 112.41, Q_{R2} = 109.37, Q_{R1} = 263.66, Q_{R2} = 283.44,
Q_{R1} > Q_{R2}, hence: Q_{R1} < Q_{R2}, so region 1 is eliminated

REGION 1: Q_{PRED} = 112.41 m³/s

                                              From eq 21: Q_{R3} = 316.94, hence
                                              Q_{R1} < Q_{R2} AND Q_{R2} < Q_{R3} so

                                              REGION 2: Q_{PRED} = 316.94 m³/s

                                              (Eq 22 only becomes relevant if the test
                                              of eq 21 fails).

<u>Continuation of stage/discharge assessment</u>

13.   The above assumed that a Manning's n value of 0.030 was appropriate for
the flood plains. However, the hydraulic engineer should have access to
some above- bank data when carrying out this project, so should compare the
results obtained with this value of n_F with the available observations. If
no computer program were available, he/she would have to go through the
above procedure for each of the observed flow depths, and then compare the

predicted discharges with the measured values. This is illustrated in Table A6.3, the nine assumed observations being listed at the top of the table. These go up to a depth of about 1.5m on the flood plains, though the stage/discharge function requires extending to some 3m depth on the flood plains.

14. With the benefit of a computer program, it is only a matter of a few minutes work at the PC to test a range of assumptions about flood plain roughness. Table A6.3 looks at n_F = 0.030, 0.025 and 0.0275 in turn, the column headed Qex/Qpr being the ratio of observed discharge to predicted flow. The comparison is summarised in terms of the average and standard deviation of these ratios, so indicating the goodness of fit. The first assumption of n_F = 0.030 under-predicts by about 3.3 percent on average, with a variability of about 5%. This led to trying n_F = 0.025, which over-predicts by about half a percent, but reduces the variability. So the third attempt was with n_F = 0.0275, giving agreement to within 1.6% on average, with some 3.6% variability. This may well be the preferred assumption with this data set: at high stages n_F = 0.0275 tends to be a conservative assumption. Note that a Q_{*zc} limit of 0.5 was applied and affected stages below 2.2m only.

15. Having decided upon the best roughness coefficients in this way, the stage/ discharge function over the full range required may be calculated. Obviously this would be considered tedious if all calculations were manual, but with the benefit of suitable PC software, is quickly accomplished. Table A6.4 provides the extended stage/discharge functions for the three alternative flood plain roughnesses considered, the final one being the preferred prediction. Note the transition from Region 1 to Region 2 at a depth of 3.25m, and the trend of the discharge adjustment factor, DISADF. This drops to about 0.85 at the limit of region 1, but rises through Region 2 to 0.93. It is also interesting to note that with equal roughness on flood plain as in main channel, the second case, the flow reaches Region 3, with DISADF approx. 0.95 at maximum depth. This illustrates how the progress through the regions depends on the ratio of the roughnesses: high flood plain roughness will delay that progression, and perhaps result in only Region 1 applying.

Table A6.1 Use of within-bank field observations to assess roughness of main channel: channel geometry; stage/discharge observations; analysis of individual observations to determine Manning's n and k_S in Colebrook-White equation (wide channel version); tabular assessment of goodness of fit of Manning equation with selected n_c value

geono	g	bed w	FP w	No FP	chdepth	ac,H/V	hfp	af,H/V	afp,V/H	S/1000	Aspect
99.000	9.810	22.030	13.155	2.000	2.000	0.965	2.610	0.727	0.046	0.470	11.015

Experimental data: sampwb.obs Test numbered 1

z exp	Q exp	S/1000	Temp
1.060	21.780	0.470	15.000
1.200	25.560	0.470	15.000
1.280	29.690	0.470	15.000
1.360	33.180	0.470	15.000
1.580	47.050	0.470	15.000
1.720	45.470	0.470	15.000
1.770	48.900	0.470	15.000
1.780	48.170	0.470	15.000
1.900	58.610	0.470	15.000
1.920	54.290	0.470	15.000

Analysis of experiments as single channel

z	z/h	Q	A	P	R	V	ReE6	FF	V*	V/V*	Man	Kse
1.060	0.530	21.780	24.436	24.976	0.978	0.891	3.060	0.045	0.067	13.271	0.024	54.205
1.200	0.600	25.560	27.826	25.365	1.097	0.919	3.536	0.048	0.071	12.916	0.025	70.231
1.280	0.640	29.690	29.779	25.588	1.164	0.997	4.071	0.043	0.073	13.610	0.024	56.159
1.360	0.680	33.180	31.746	25.810	1.230	1.045	4.511	0.042	0.075	13.879	0.024	53.199
1.580	0.790	47.050	37.216	26.421	1.409	1.264	6.248	0.033	0.081	15.687	0.022	29.162
1.720	0.860	45.470	40.746	26.811	1.520	1.116	5.951	0.045	0.084	13.331	0.026	82.198
1.770	0.885	48.900	42.016	26.949	1.559	1.164	6.367	0.042	0.085	13.727	0.025	71.764
1.780	0.890	48.170	42.271	26.977	1.567	1.140	6.265	0.045	0.085	13.407	0.026	82.164
1.900	0.950	58.610	45.341	27.311	1.660	1.293	7.530	0.037	0.087	14.775	0.024	49.869
1.920	0.960	54.290	45.855	27.366	1.676	1.184	6.961	0.044	0.088	13.470	0.026	85.642

MAIN CHANNEL EQUATION
Manning calculation
Main channel Man = 0.025
Bank full discharge at 15 degC 60.0457605
FLOOD PLAIN EQUATION
Manning calculation
Flood plain Mannings n = 0.03

z	Qex	Vm	Qm	Vfp	Qfp	Qt	FmE2	FfpE2	FtE2	Qex/Qt
1.060	21.780	0.855	20.884	0.000	0.000	20.884	4.941	0.000	4.941	1.043
1.200	25.560	0.922	25.666	0.000	0.000	25.666	4.756	0.000	4.756	0.996
1.280	29.690	0.959	28.573	0.000	0.000	28.573	4.663	0.000	4.663	1.039
1.360	33.180	0.995	31.603	0.000	0.000	31.603	4.578	0.000	4.578	1.050
1.580	47.050	1.090	40.554	0.000	0.000	40.554	4.376	0.000	4.376	1.160
1.720	45.470	1.146	46.708	0.000	0.000	46.708	4.266	0.000	4.266	0.974
1.770	48.900	1.166	48.990	0.000	0.000	48.990	4.230	0.000	4.230	0.998
1.780	48.170	1.170	49.451	0.000	0.000	49.451	4.223	0.000	4.223	0.974
1.900	58.610	1.216	55.127	0.000	0.000	55.127	4.142	0.000	4.142	1.063
1.920	54.290	1.223	56.097	0.000	0.000	56.097	4.130	0.000	4.130	0.968

Average Qratio = 1.02647054   Standard deviation = 5.56235E-02

Table A6.2 Geometric calculations: x-y coordinates; summary of idealised geometry (assumed symmetric); geometric parameters and channel coherence

```
COMPOUND TRAPEZOIDAL CHANNELS: FIELD DATA, version TRAPEZ21, june 91
X coord Y coord
 0.000   4.050
 0.300   2.580
13.500   1.930
15.220   0.070
37.250  -0.070
39.450   2.070
52.500   2.640
54.600   4.320
```

geono	g	bed w	FP w	No FP	chdepth	sc,H/V	hfp	sf,H/V	sfp,V/H	S/1000	Aspect
99.000	9.810	22.030	13.155	2.000	2.000	0.965	2.610	0.727	0.046	0.470	11.015

MAIN CHANNEL EQUATION
Manning calculation
Main channel Man = 0.025
Bank full discharge at 15 degC 60.0457605
FLOOD PLAIN EQUATION
Manning calculation
Flood plain Mannings n = 0.03
Geometry of compound channel

z	H*	Am	Pm	Rm	Afp	Pfp	Rfp	At	Pt	Rt	P*	A*	f*	2 Beff	COH3
0.250	-7.000	5.568	22.725	0.245	0.000	0.000	0.000	5.568	22.725	0.245	0.000	0.000	0.000	25.890	
0.500	-3.000	11.256	23.420	0.481	0.000	0.000	0.000	11.256	23.420	0.481	0.000	0.000	0.000	25.890	
0.750	-1.667	17.065	24.115	0.708	0.000	0.000	0.000	17.065	24.115	0.708	0.000	0.000	0.000	25.890	
1.000	-1.000	22.995	24.809	0.927	0.000	0.000	0.000	22.995	24.809	0.927	0.000	0.000	0.000	25.890	
1.250	-0.600	29.045	25.504	1.139	0.000	0.000	0.000	29.045	25.504	1.139	0.000	0.000	0.000	25.890	
1.500	-0.333	35.216	26.199	1.344	0.000	0.000	0.000	35.216	26.199	1.344	0.000	0.000	0.000	25.890	
1.750	-0.143	41.508	26.894	1.543	0.000	0.000	0.000	41.508	26.894	1.543	0.000	0.000	0.000	25.890	
2.000	0.000	47.920	27.589	1.737	0.000	-0.000	0.000	47.920	27.589	1.737	0.000	0.000	0.000	25.890	
2.250	0.111	54.393	27.589	1.972	0.674	5.397	0.125	55.740	38.383	1.452	0.391	0.025	3.613	36.673	0.666
2.500	0.200	60.865	27.589	2.206	2.696	10.794	0.250	66.256	49.177	1.347	0.783	0.089	2.977	47.456	0.612
2.750	0.273	67.338	27.589	2.441	5.861	13.342	0.439	79.060	54.273	1.457	0.967	0.174	2.550	52.200	0.653
3.000	0.333	73.810	27.589	2.675	9.198	13.651	0.674	92.206	54.891	1.680	0:990	0.249	2.280	52.200	0.715
3.250	0.385	80.283	27.589	2.910	12.580	13.960	0.901	105.443	55.510	1.900	1.012	0.313	2.128	52.200	0.757
3.500	0.429	86.755	27.589	3.145	16.008	14.269	1.122	118.771	56.128	2.116	1.034	0.369	2.030	52.200	0.788
3.750	0.467	93.228	27.589	3.379	19.481	14.579	1.336	132.190	56.746	2.330	1.057	0.418	1.962	52.200	0.811
4.000	0.500	99.700	27.589	3.614	23.000	14.888	1.545	145.700	57.364	2.540	1.079	0.461	1.912	52.200	0.829
4.250	0.529	106.173	27.589	3.848	26.564	15.197	1.748	159.301	57.982	2.747	1.102	0.500	1.873	52.200	0.842
4.500	0.556	112.645	27.589	4.083	30.174	15.506	1.946	172.993	58.600	2.952	1.124	0.536	1.844	52.200	0.853
4.750	0.579	119.118	27.589	4.318	33.829	15.815	2.139	186.775	59.219	3.154	1.146	0.568	1.820	52.200	0.862
5.000	0.600	125.590	27.589	4.552	37.529	16.124	2.328	200.648	59.837	3.353	1.169	0.598	1.801	52.200	0.869
5.250	0.619	132.063	27.589	4.787	41.275	16.433	2.512	214.613	60.455	3.550	1.191	0.625	1.785	52.200	0.875
5.500	0.636	138.535	27.589	5.021	45.066	16.742	2.692	228.668	61.073	3.744	1.214	0.651	1.773	52.200	0.880
5.750	0.652	145.008	27.589	5.256	48.903	17.051	2.868	242.814	61.691	3.936	1.236	0.674	1.762	52.200	0.884
6.000	0.667	151.480	27.589	5.491	52.785	17.360	3.041	257.051	62.310	4.125	1.259	0.697	1.754	52.200	0.887
6.250	0.680	157.953	27.589	5.725	56.713	17.669	3.210	271.378	62.928	4.313	1.281	0.718	1.746	52.200	0.890
6.500	0.692	164.425	27.589	5.960	60.686	17.979	3.375	285.797	63.546	4.497	1.303	0.738	1.740	52.200	0.892
6.750	0.704	170.898	27.589	6.194	64.705	18.288	3.538	300.307	64.164	4.680	1.326	0.757	1.736	52.200	0.894
7.000	0.714	177.370	27.589	6.429	68.769	18.597	3.698	314.907	64.782	4.861	1.348	0.775	1.732	52.200	0.895
7.250	0.724	183.843	27.589	6.664	72.878	18.906	3.855	329.598	65.400	5.040	1.371	0.793	1.728	52.200	0.897
7.500	0.733	190.315	27.589	6.898	77.033	19.215	4.009	344.381	66.019	5.216	1.393	0.810	1.726	52.200	0.898
7.750	0.742	196.788	27.589	7.133	81.233	19.524	4.161	359.254	66.637	5.391	1.415	0.826	1.723	52.200	0.899
8.000	0.750	203.260	27.589	7.367	85.479	19.833	4.310	374.218	67.255	5.564	1.438	0.841	1.722	52.200	0.899

Table A6.3 Comparison of observations of stage/discharge with predicted flows: list of observations; calculations for three assumed values of n_F. (subscript m = main channel; fp = flood plain; Qpred is the predicted discharge)

Experimental data: sampab.obs Test numbered 2

z exp	Q exp	S/1000	Temp
2.050	60.750	0.470	15.000
2.080	63.470	0.470	15.000
2.140	63.820	0.470	15.000
2.400	79.490	0.470	15.000
2.540	84.960	0.470	15.000
2.770	91.460	0.470	15.000
3.000	117.900	0.470	15.000
3.160	140.910	0.470	15.000
3.570	183.670	0.470	15.000

MAIN CHANNEL EQUATION
Manning calculation
Main channel Man = 0.025
Bank full discharge at 15 degC 60.0457605
FLOOD PLAIN EQUATION
Manning calculation
flood plain Mannings n = 0.03
following uses full predictive functions. Region 1 incorporates an aspect ratio factor for both Q*2F and Q*2C:
 aspect ratio of this geometry is 11.015
Aspect ratio used in following = 1.1

z	H*	Qex	Vm	Qm	Vfp	Qfp	F*	Qpred	Qex/Qpr	Region	QtR1	QtR2	QtR3	QtR4
2.050	0.024	60.750	1.276	62.773	0.062	0.002	5.975	60.040	1.012	1.000	60.040	39.079	63.752	51.903
2.080	0.038	63.470	1.289	64.433	0.084	0.006	5.135	61.689	1.029	1.000	61.689	39.733	67.317	50.477
2.140	0.065	63.820	1.315	67.805	0.123	0.026	4.305	65.049	0.981	1.000	65.049	41.279	73.488	49.240
2.400	0.167	79.490	1.428	83.196	0.247	0.426	3.161	76.955	1.033	1.000	76.955	58.578	96.653	52.550
2.540	0.213	84.960	1.486	91.998	0.302	0.949	2.918	82.747	1.027	1.000	82.747	69.295	109.025	57.135
2.770	0.278	91.460	1.580	107.216	0.430	2.632	2.521	95.999	0.953	1.000	95.999	88.423	126.818	74.119
3.000	0.333	117.900	1.671	123.352	0.555	5.109	2.280	112.463	1.048	1.000	112.463	109.386	145.645	95.440
3.160	0.367	140.910	1.733	135.105	0.633	7.191	2.175	125.173	1.126	1.000	125.173	124.948	160.126	111.123
3.570	0.440	183.670	1.887	167.139	0.808	13.718	2.009	168.336	1.091	2.000	161.937	168.336	201.724	154.686

Average Qratio = 1.03326263   Standard deviation = 4.92698E-02

Main channel Man = 0.025
flood plain Mannings n = 0.025
following uses full predictive functions. Region 1 incorporates an aspect ratio factor for both Q*2F and Q*2C:
 aspect ratio of this geometry is 11.015
Aspect ratio used in following = 1.1

z	H*	Qex	Vm	Qm	Vfp	Qfp	F*	Qpred	Qex/Qpr	Region	QtR1	QtR2	QtR3	QtR4
2.050	0.024	60.750	1.276	62.773	0.074	0.002	4.149	60.068	1.011	1.000	60.068	43.730	61.934	54.630
2.080	0.038	63.470	1.289	64.433	0.101	0.007	3.566	61.730	1.028	1.000	61.730	44.569	65.107	53.796
2.140	0.065	63.820	1.315	67.805	0.147	0.031	2.990	65.117	0.980	1.000	65.117	46.485	70.759	53.355
2.400	0.167	79.490	1.428	83.196	0.296	0.511	2.195	77.857	1.021	1.000	77.857	65.311	92.710	58.862
2.540	0.213	84.960	1.486	91.998	0.362	1.138	2.026	84.292	1.008	1.000	84.292	76.857	104.650	64.585
2.770	0.278	91.460	1.580	107.216	0.515	3.158	1.751	99.140	0.923	1.000	99.140	97.646	122.042	83.753
3.000	0.333	117.900	1.671	123.352	0.666	6.130	1.584	120.598	0.978	2.000	117.713	120.598	140.805	107.496
3.160	0.367	140.910	1.733	135.105	0.760	8.629	1.510	137.707	1.023	2.000	132.125	137.707	155.384	124.989
3.570	0.440	183.670	1.887	167.139	0.970	16.462	1.395	185.651	0.989	2.000	174.020	185.651	197.659	173.672

Average Qratio = 0.995695525   Standard deviation = 3.12895E-02

Main channel Man = 0.025
flood plain Mannings n = 0.0275
following uses full predictive functions. Region 1 incorporates an aspect ratio factor for both Q*2F and Q*2C:
 aspect ratio of this geometry is 11.015
Aspect ratio used in following = 1.1

z	H*	Qex	Vm	Qm	Vfp	Qfp	F*	Qpred	Qex/Qpr	Region	QtR1	QtR2	QtR3	QtR4
2.050	0.024	60.750	1.276	62.773	0.067	0.002	5.021	60.053	1.012	1.000	60.053	41.315	62.836	53.276
2.080	0.038	63.470	1.289	64.433	0.092	0.006	4.315	61.708	1.029	1.000	61.708	42.054	66.214	52.133
2.140	0.065	63.820	1.315	67.805	0.134	0.028	3.617	65.080	0.981	1.000	65.080	43.770	72.143	51.267
2.400	0.167	79.490	1.428	83.196	0.269	0.465	2.656	77.375	1.027	1.000	77.375	61.829	94.752	55.581
2.540	0.213	84.960	1.486	91.998	0.329	1.035	2.452	83.462	1.018	1.000	83.462	72.965	106.926	60.687
2.770	0.278	91.460	1.580	107.216	0.469	2.871	2.118	97.445	0.939	1.000	97.445	92.917	124.503	78.714
3.000	0.333	117.900	1.671	123.352	0.606	5.573	1.916	114.877	1.026	1.000	114.877	114.855	143.255	101.205
3.160	0.367	140.910	1.733	135.105	0.691	7.845	1.828	131.172	1.074	2.000	128.370	131.172	157.748	117.760
3.570	0.440	183.670	1.887	167.139	0.882	14.965	1.688	176.770	1.039	2.000	167.494	176.770	199.562	163.787

Average Qratio = 1.01602969   Standard deviation = 3.58727E-02

Table A6.4 Calculated stage discharge functions up to stage of 5.0m: three assumed values of n_F in turn

Main channel Man = 0.025
Flood plain Mannings n = 0.03
Following uses full predictive functions. Region 1 incorporates an aspect ratio factor for both Q*2F and Q*2C: aspect ratio of geometry is 11.015
Aspect ratio factor used in following, ARF = 1.1

z	H*	Vm	Qm	Vfp	Qfp	F*	Qt	Qpred	Region	QtR1	QtR2	QtR3	QtR4	DISADF
2.000	0.000	1.253	60.046	0.000	0.000	0.000	60.046	60.046	0.000	60.046	38.188	94.092	0.000	1.000
2.250	0.111	1.363	74.163	0.181	0.122	3.613	74.406	71.578	1.000	71.578	47.396	83.562	49.524	0.962
2.500	0.200	1.470	89.447	0.287	0.773	2.977	90.992	81.013	1.000	81.013	66.187	105.449	55.677	0.890
2.750	0.273	1.572	105.856	0.418	2.448	2.550	110.751	94.676	1.000	94.676	86.680	125.306	72.326	0.855
3.000	0.333	1.671	123.352	0.555	5.109	2.280	133.569	112.463	1.000	112.463	109.386	145.645	95.440	0.842
3.250	0.385	1.768	141.902	0.674	8.482	2.128	158.866	134.047	2.000	132.744	134.047	168.724	120.268	0.844
3.500	0.429	1.861	161.477	0.780	12.490	2.030	186.457	160.582	2.000	155.259	160.582	194.193	146.905	0.861
3.750	0.467	1.953	182.052	0.877	17.080	1.962	216.211	188.906	2.000	179.822	188.906	221.854	175.335	0.874
4.000	0.500	2.042	203.601	0.966	22.212	1.912	248.025	218.935	2.000	206.291	218.935	251.575	205.518	0.883
4.250	0.529	2.130	226.104	1.049	27.856	1.873	281.816	250.589	2.000	234.550	250.589	283.256	237.405	0.889
4.500	0.556	2.215	249.540	1.126	33.987	1.844	317.514	283.793	2.000	264.506	283.793	316.822	270.949	0.894
4.750	0.579	2.299	273.893	1.200	40.584	1.820	355.061	318.476	2.000	296.082	318.476	352.211	306.103	0.897
5.000	0.600	2.382	299.143	1.269	47.631	1.801	394.406	354.572	2.000	329.211	354.572	389.370	342.825	0.899

Main channel Man = 0.025
Flood plain Mannings n = 0.025
Following uses full predictive functions. Region 1 incorporates an aspect ratio factor for both Q*2F and Q*2C: aspect ratio of geometry is 11.015
Aspect ratio factor used in following, ARF = 1.1

z	H*	Vm	Qm	Vfp	Qfp	F*	Qt	Qpred	Region	QtR1	QtR2	QtR3	QtR4	DISADF
2.000	0.000	1.253	60.046	0.000	0.000	1.067	60.046	60.046	0.000	60.046	42.524	94.092	0.000	1.000
2.250	0.111	1.363	74.163	0.217	0.146	2.509	74.455	71.981	1.000	71.981	53.270	80.216	54.655	0.967
2.500	0.200	1.470	89.447	0.344	0.927	2.067	91.301	82.356	1.000	82.356	73.506	101.187	62.792	0.902
2.750	0.273	1.572	105.856	0.501	2.937	1.771	111.730	97.653	1.000	97.653	95.743	120.549	81.758	0.874
3.000	0.333	1.671	123.352	0.666	6.130	1.584	135.613	120.598	2.000	117.713	120.598	140.805	107.496	0.889
3.250	0.385	1.768	141.902	0.809	10.178	1.478	162.258	147.733	2.000	140.729	147.733	164.081	135.199	0.910
3.500	0.429	1.861	161.477	0.936	14.988	1.410	191.453	177.059	2.000	166.392	177.059	189.973	164.968	0.925
3.750	0.467	1.953	182.052	1.052	20.496	1.362	223.043	208.487	2.000	194.481	208.487	218.252	196.787	0.935
4.000	0.500	2.042	203.601	1.159	26.655	1.327	256.910	241.931	2.000	224.826	241.931	248.759	230.614	0.942
4.250	0.529	2.130	226.104	1.258	33.427	1.301	292.959	277.309	2.000	257.294	277.309	281.378	266.399	0.947
4.500	0.556	2.215	249.540	1.352	40.784	1.280	331.109	314.547	2.000	291.774	314.547	316.019	304.091	0.950
4.750	0.579	2.299	273.893	1.440	48.701	1.264	371.295	352.609	3.000	328.175	353.571	352.609	343.644	0.950
5.000	0.600	2.382	299.143	1.523	57.158	1.251	413.459	391.086	3.000	366.418	394.315	391.086	385.013	0.946

Main channel Man = 0.025
Flood plain Mannings n = 0.0275
Following uses full predictive functions. Region 1 incorporates an aspect ratio factor for both Q*2F and Q*2C: aspect ratio of geometry is 11.015
Aspect ratio factor used in following, ARF = 1.1

| z	H*	Vm	Qm	Vfp	Qfp	F*	Qt	Qpred	Region	QtR1	QtR2	QtR3	QtR4	DISADF
2.000	0.000	1.253	60.046	0.000	0.000	0.741	60.046	60.046	0.000	60.046	40.281	94.092	0.000	1.000
2.250	0.111	1.363	74.163	0.197	0.133	3.036	74.428	71.768	1.000	71.768	50.212	81.934	52.016	0.964
2.500	0.200	1.470	89.447	0.313	0.843	2.501	91.133	81.635	1.000	81.635	69.735	103.402	59.075	0.896
2.750	0.273	1.572	105.856	0.456	2.670	2.143	111.196	96.047	1.000	96.047	91.095	123.004	76.823	0.864
3.000	0.333	1.671	123.352	0.606	5.573	1.916	134.498	114.877	1.000	114.877	114.855	143.255	101.205	0.854
3.250	0.385	1.768	141.902	0.735	9.253	1.788	160.408	140.721	2.000	136.415	140.721	166.371	127.419	0.877
3.500	0.429	1.861	161.477	0.851	13.625	1.706	188.728	168.610	2.000	160.378	168.610	191.977	155.562	0.893
3.750	0.467	1.953	182.052	0.956	18.633	1.648	219.317	198.434	2.000	186.564	198.434	219.860	185.621	0.905
4.000	0.500	2.042	203.601	1.054	24.232	1.606	252.064	230.107	2.000	214.816	230.107	249.876	217.553	0.913
4.250	0.529	2.130	226.104	1.144	30.389	1.574	286.881	263.548	2.000	245.012	263.548	281.919	251.309	0.919
4.500	0.556	2.215	249.540	1.229	37.077	1.549	323.694	298.683	2.000	277.051	298.683	315.906	286.840	0.923
4.750	0.579	2.299	273.893	1.309	44.274	1.529	362.440	335.439	2.000	310.848	335.439	351.770	324.099	0.926
5.000	0.600	2.382	299.143	1.385	51.962	1.513	403.067	373.748	2.000	346.332	373.748	389.455	363.043	0.927
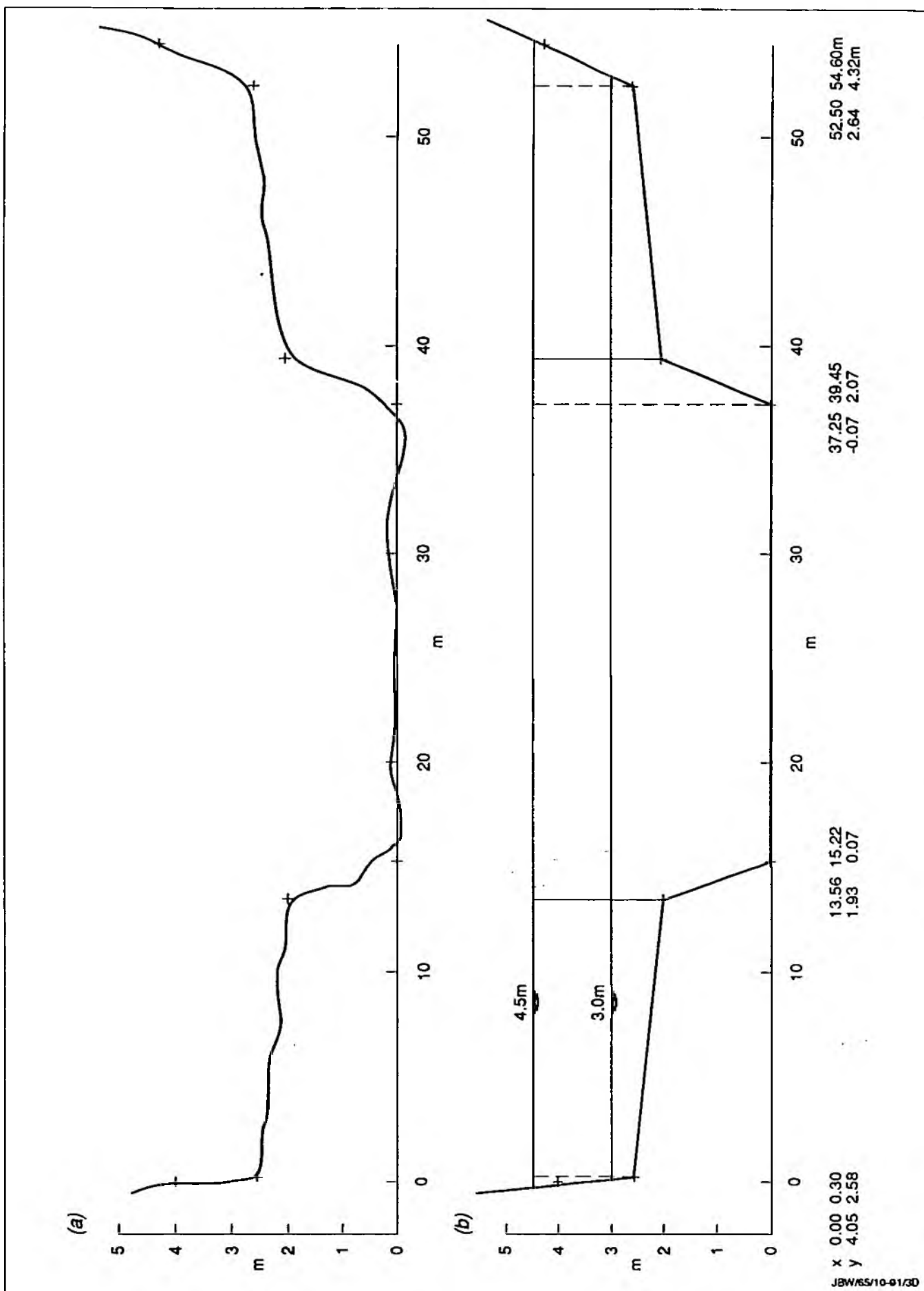
Fig A6.1 (a): river channel as surveyed.
(b): idealised form of cross-section, with co-ordinates defining its shape

APPENDIX 7 : ANALYSIS OF OTHER SOURCES OF LABORATORY DATA

1. Asano T, Hashimoto H and Fujita K. Characteristics of variation of Manning's roughness
    coefficient in a compound cross section. International association for Hydraulic
    Research, Proc. 21st Congress, Melbourne, Vol 6, August 1985, pp 30-34.

TABLE A7.1 : STATISTICAL ANALYSIS OF GOODNESS OF FIT BETWEEN VARIOUS PREDICTION ASSUMPTIONS
           AND ASANO et al RESULTS

Upper   Average ratio of experimental discharge to prediction.
Lower   Standard deviation expressed as percentage variation.

Series	B/h	B/b	Case 1	Case 2	Case 2a	Case 3	Case 4	Case 5	Case 6	Case 6a	Case 7	Case 8
5	10	2.50	0.998			0.913	0.955	0.997			0.913	0.913
			1.77			1.46	1.73	1.77			1.46	1.46
Values of ARF:			1	3	2	3	3	3	1	2	2	1
3	30	2.50	1.072	1.137	1.108	1.004	1.051	1.032	0.942	0.975	0.975	0.942
			5.27	4.80	4.54	3.06	4.39	2.81	4.02	3.25	3.25	4.02
9	30	3.33	1.031	1.082	1.058	1.011	1.029	1.030	0.968	0.991	0.991	0.968
			3.37	4.59	3.74	3.79	4.80	4.61	3.43	3.42	3.42	3.43
10	30	2.00	0.917	0.962	0.942	1.021	1.068	1.005	0.987	1.006	1.006	0.987
			1.48	3.81	2.81	2.51	4.20	3.39	0.79	1.49	1.49	0.79
11	30	1.67	1.029	1.074	1.056	1.032	1.060	1.039	1.000	1.019	1.019	1.000
			2.31	1.72	0.77	2.73	3.14	3.17	2.35	1.87	1.87	2.35
12	30	1.42	1.012	1.044	1.031	1.008	1.004	1.022	0.980	0.997	0.997	0.980
			1.55	3.44	2.15	3.05	3.46	3.52	1.54	1.89	1.89	1.54
13	30	1.25	0.945	0.980	0.983	0.992	1.032	0.994	0.967	0.984	0.982	0.967
			1.36	1.97	5.46	1.55	2.24	2.03	1.24	1.52	1.57	1.24
AVER	30 ONLY		1.001	1.046	1.030	1.011	1.047	1.020	0.974	0.995	0.995	0.974
			2.55	3.39	3.25	2.78	3.71	3.25	2.23	2.24	2.25	2.23

CASE 1. Chap 3 predictors with k_s = 0.15mm on both flood plains and in main channel, using wide channel transition function for the basic resistance

CASE 2. Q_{*2} for region 1 redefined to depend on main channel bed width rather rather than depth, ie aspect ratio factor, ARF = aspect ration/10, k_s = 0.15mm

CASE 2a Q_{*2} for region 1 redefined to depend on channel aspect ration, but using an intermediate value of ARF = 2 for aspect ratio 30, k_s = 0.15mm

CASE 3. Redefined Q_{*2}, ARF = aspect ratio/10, using Manning equation with the Authors' values for individual test series for main channel, flood plain constant at 0.0098

CASE 4. Redefined Q_{*2}, ARF = aspect ratio/10, but with wide-channel transition, k_s values for individual test series calculated from within bank tests in that series, and applied also to flood plain

CASE 5. As above but some massaging of channel values, coupled with k_s = 0.15mm on flood plain

CASE 6. Reverting to Authors' Mannings n values, original definition of Q_{*2} ie ARF = 1

CASE 6a Authors' Mannings n, redefined Q_{*2} but ARF at intermediate value of 2 for main channel aspect ratio of 30

CASE 7. As 6a but with the alternative Region 3 formula, DISADF = 0.95

CASE 8. Authors' Mannings n, ARF set at 1, Region 3 – DISADF = 0.95

2. US WES, Hydraulic capacity of meandering channels in straight floodways, Tech. Memo. 2.249, Waterways Experiment station,. Vicksburg, Mississippi, March 1956.

TABLE A7.2 : CALIBRATION DATA FOR THE WES EXPERIMENTAL FACILITY

Condition	WES value of Manning's n quoted; 10^{-3}			Calculated value of Manning's n; 10^{-3}			Calculated value of k ; mm$_s$		
Roughness case:	0	1	2	0	1	2	0	1	2
1ft bankfull	12			11.8			0.64		
2ft bankfull	12			12.0			0.72		
0.1ft on. FP	12	25	35	11.3	28.1	43.4	0.39	27.9	69.4
0.2ft on FP	12	25	35	11.7	22.9	33.0	0.56	21.1	62.2
0.3ft on FP	12	25	35	12.3	21.9	30.9	0.83	20.5	65.2

TABLE A7.3 : US WATERWAYS EXPERIMENT STATION RESEARCH:
COMPARISION OF PREDICTION WITH MEASUREMENT FOR VARIOUS ASSUMPTIONS

Case	Channel width	Roughness coefficients Channel	Flood plain for roughness 0, 1, 2	Av. error %	S E E (1) %
1. Manning, ARF = 1, original defn	1ft	0.012	as Table 7.2	6.3	9.4
of Q_{*2}	2ft	0.012	as Table 7.2	25.5	31.7
2. Manning,	1ft	0.012	as Table 7.2	6.3	9.4
Q_{*2} mod	2ft	0.012	as Table 7.1	2.4	5.2
3. Manning, ARF = aspect ratio/10					
Q_{*2c} & Q_{*2F}	1ft	0.012	as Table 7.2	6.3	9.4
modified	2ft	0.012	as Table 7.2	2.9	5.0
4. Wide-transition, ARF = 1, orig defn	1ft	0.68mm	0.60, 23.2, 65.6mm	3.6	5.1
of Q_{*2}	2ft	0.68mm	ditto	18.8	19.6
5. Wide-transition,	1ft	0.68mm	ditto	3.6	5.0
Q_{*2c} mod	2ft	0.68mm	ditto	4.6	5.1
6. Wide transition, ARF = aspect ratio/10					
Q_{*2c} & Q_{*2F}	1ft	0.68mm	ditto	3.6	5.0
modified	2ft	0.68mm	ditto	5.2	5.0
7. Wide transition, ARF = 0.8	2ft	0.68mm	ditto	16.9	15.0
0.6	2ft	0.68mm	ditto	11.9	7.9
8. Wide transition, ARF = 0.4	2ft	0.50mm	0.30, 30.0, 50.0mm	0.6	3.8
9. Wide transition, ARF = 0.4	2ft	0.50mm	0.30, 30.0, 50.0mm	0.7	3.7

Note (1). S E E, standard error of the estimate is the r.m.s of the variation about the mean error value, expressed here as percentage.

3. Myers W R C. Momentum transfer in a compound channel, Journal of Hydraulic Research, Col 16, 1978, No 2, 139-150
    Myers W R C. Frictional Resistance in channels with flood plains; Channels and channel control structures, 1st Int. Conf. Southampton, England, 1984, ed. K V H Smith, pub Springer-Verlag, 1984, p 4.73-4.87
    Myers W R C. Flow resistance in smooth compound channels, experimental data, University of Ulster, March 1985.

TABLE A7.4 : STATISTICAL ANALYSIS OF GOODNESS OF FIT BETWEEN VARIOUS PREDICTION ASSUMPTIONS AND MYERS RESULTS

Note: The following utilises the Region 3 function based on COH.

Geometry	B/b 2b/h	Using Colebrook-White, mean errors and SD's,%					Myer's equ.
		ARF = 0.13	0.20	0.40	0.60	1.00	0.60
1	4.68		+1.6 *	+1.6 *	+1.6 *	+1.6 *	+5.7 *
	1.99		2.9	2.9	2.9	2.9	3.1
2	3.21		-1.0	-0.6 *	-0.6 *	-0.6 *	+5.5 *
	1.98		5.7	5.2	5.2	5.2	5.3
3	4.74	+1.7	+1.8 *	+1.8 *	+1.8 *	+1.8 *	*7.3 *
	1.32	4.5	4.5	4.5	4.5	4.5	4.0

Note: * denotes no depths shallow enough to yield Region a.

TABLE A7.5 : COMPARISON OF ALTERNATIVE FORMULA FOR REGION 3

Note: Based on Colebrook-White function with $k_s = 0$

Formula number	Geometry number	Overall fit:			Region 3 only:		
		Number of tests	Mean error	SD %	Number in region	Mean error	SD %
1	1	42	+0.16	2.90	5	+2.28	3.84
	2	49	-0.58	5.20	5	-0.06	3.98
	3	34	+1.84	4.19	4	+2.93	5.48
	Average:		+0.47	4.19		+1.72	4.43
2	1	42	+0.19	2.89	9	+1.34	3.14
	2	49	-0.64	5.17	10	-0.07	3.16
	3	34	+1.91	4.38	15	+2.08	3.86
	Average:		+0.49	4.15		+1.12	3.39
3	1	42	-0.70	2.67	7	+0.54	2.16
	2	49	-1.04	5.00	6	+3.18	4.47
	3	34	+0.56	4.32	1 *	-2.73	
	Average:		-0.39	4.00		+1.86	3.32

* omitted from average

FORMULA 1 : DISADF = 1.567 - 0.667 COH_3
FORMULA 2 : DISADF = 0.95
FORMULA 3 : DISADF = 1.06 - 0.24 H*

4. Prinos P and Townsend R D. Estimating discharge in compound open channels, Canadian Soc. for Civil Engineering, 6th Canadian Hydrotechnical Conference, Ottawa, Ontario, June 1983, 120-146.
   Prinos P and Townsend R D. Comparison of methods for predicting discharge in compound open channels. Advances in Water Resources, 1984, Vol 7, Dec, CML Publications, 180-187..

TABLE A7.6 : STATISTICAL ANALYSIS OF FIT BETWEEN VARIOUS PREDICTION ASSUMPTIONS AND PRINOS AND TOWNSEND RESULTS

CHANNEL WIDTH,mm		203		305		406		508	
Manning's n used for FP	ARF	Mean	SD,%	Mean	SD,%	Mean	SD,%	Mean	SD,%
0.011	0	0.903	6.19	0.910	2.07	0.899	5.95	0.894	4.07
	0.2	0.960	6.49	0.954 *	2.78	0.933	6.88	0.921	4.51
	0.4	0.985 *	4.19	0.990 *	2.55	0.969	7.71	0.949 Φ	5.10
	0.6	0.997 *	2.58	1.008 *	1.76	0.990	6.95	0.974 Φ	5.21
	0.8	1.002 *	2.30	1.017 *	1.29	1.002 Φ	5.88	0.991 *	4.44
	1.0	1.002 *	2.30	1.024 *	1.82	1.010 *	5.04	1.003 *	3.56
0.014	0	0.841	5.76	0.857	6.17	0.869	6.09	0.865	5.09
	0.2	0.919	7.13	0.913	7.66	0.912	7.61	0.899	5.62
	0.4	0.983	6.54	0.978	9.59	0.961	9.43	0.963	6.45
	0.6	1.009 *	3.82	1.021	8.71	1.012	11.06	0.976	7.62
	0.8	1.024 *	1.63	1.042	6.42	1.043	10.46	1.013	8.20
	1.0	1.037 *	2.66	1.057 Φ	4.69	1.068	9.35	1.039	7.64
0.018	0	0.772	6.94	0.822	6.53	0.844	6.40	0.874	7.33
	0.2	0.865	9.49	0.890	8.89	0.896	8.47	0.874	7.33
	0.4	0.975	11.87	0.971	12.02	0.957	11.03	0.918	8.74
	0.6	1.027	8.72	1.059	14.82	1.027	14.24	0.968	10.65
	0.8	1.054 Φ	5.67	1.109	13.46	1.097	16.72	1.024	13.12
	1.0	1.074	3.39	1.137	11.24	1.139	16.17	1.076	14.71
0.022	0	0.721	8.03	0.783	6.25	0.808	7.88	0.798	6.56
	0.2	0.822	11.48	0.858	9.04	0.867	10.38	0.841	7.95
	0.4	0.961	16.88	0.950	12.91	0.934	13.57	0.890	9.86
	0.6	1.051	15.95	1.067	18.43	1.016	17.70	0.946	12.37
	0.8	1.097	11.81	1.149	18.89	1.116	23.19	1.010	15.64
	1.0	1.117	8.027	1.197	16.87	1.187	24.27	1.086	19.91

* These results are within 5% mean error and also 5% variability
Φ These come close to those limits

5. Knight D W, Demetriou J D and Hamed M E. Stage discharge relations for compound channels, Proc 1st Int. conf. Channels and Channel Control Structures. April 1984, ed Smith K V H, Springer Verlag, 1984, 4.21-4.36
   Knight D W and Demetriou J D. Flood plain and main channel interaction, ASCE, J Hudraulic Eng. Vol 109, No 8, Aug 1983, 1073-1092.

TABLE A7.7 : STATISTICAL ANALYSIS OF GOODNESS OF FIT BETWEEN VARIOUS PREDICTION ASSUMPTIONS AND KNIGHT AND DEMETRIOU RESULTS

Aspect ratio	B/b	ARF = 1.0 Mean	SD%	ARF = 0.6 Mean	SD%	ARF = 0.4 Mean	SD%	ARF = 0.2 Mean	SD%	ARF = 0.1 Mean	SD%	ARF = 0 Mean	SD%
2	2	1.105	3.85	1.100	2.92	1.092	1.82	1.077	1.84	1.047	1.97	1.003	1.33
2	3	1.043	3.81 ±	1.043	3.81 ±	1.043	3.81 ±	1.031	5.31	1.012	6.76	0.975	6.60
2	4	1.014	3.02 ±	1.014	3.02 ±	1.014	3.02 ±	1.000	2.07	0.986	2.96	0.951	2.95

* denotes no region 1 flows predicted with this value of ARF
The underlined values are those showing least variability

---

6. Kiely: unpublished thesis plus personal communication

TABLE A7.8 : STATISTICAL ANALYSIS OF GOODNESS OF FIT BETWEEN VARIOUS PREDICTION ASSUMPTIONS AND KIELY'S RESULTS

SMOOTH FLOOD PLAINS:

Roughness used: Main ch	Flood pl	ARF values:	0.20	0.34	0.37	0.5
0.011	0.010	Av disc%	-6.0		-5.1 *	-5.1 *
		S D %	3.0		2.5	2.5

ROUGH FLOOD PLAINS:

0.011	0.0157		-3.0	+1.8		+5.2
			2.5	1.0		4.7

Note: * denotes no Region 1 results remained

---

7. Wormleaton P R, Allen J and Hadjipanos P, Proceedings ASCE, J Hy Div, Vol 108, No HY9, Sept 1982, pp 975-994

TABLE A7.9 : STATISTICAL ANALYSIS OF GOODNESS OF FIT BETWEEN VARIOUS PREDICTION ASSUMPTIONS AND WORMLEATON et al RESULTS

Upper figure: mean discrepancy %

Lower figure: variability %

Nominal n value	Assumed value of ARF:						
	1.0	0.8	0.6	0.4	0.24	0.20	0
0.011	+3.5 *	+3.5 *	+3.5 *	+2.6	+0.9	-2.0	-9.5
	6.0	6.0	6.0	6.1	5.7	5.9	6.0
0.014	+0.3 *	+0.3 *	+0.3 *	+0.3 *	-2.5	-3.8	-13.6
	2.1	2.1	2.1	2.1	4.5	5.2	5.2
0.017	+5.3 *	+5.3 *	+4.5	+1.7	-4.4	-7.3	-19.8
	2.2	2.2	2.6	6.6	9.9	9.5	7.3
0.021	+2.0 *	+2.0 *	-1.5	-7.2	-18.2	-21.3	-34.0
	6.7	6.7	11.8	16.8	16.4	15.3	11.5

Note: * indicates Region 1 is eliminated under these conditions at minimum depth tested